Hamilton's Hidden Hazard:

The Characterisation and Mapping of Zones of Tectonic Deformation within the Hamilton Basin

A thesis

submitted in partial fulfilment

of the requirements for the degree

of

Master of Science

at

The University of Waikato

by

Benjamin Ross Campbell

THE UNIVERSITY OF
WAIKATO
Te Whare Wānanga o Waikato

2017

Abstract

The Hamilton Basin has long been thought of as an area of simple geologic structure with two major faults recognised to the west and east of the Basin; the Waipa and Kerepehi Faults. However, recent identification of deformation signatures within the Basin suggests that the geological structure of the Hamilton Basins may be far more complex than previously recognised. At the time of this study, 26 potential zones of interest associated with tectonic deformation had been identified within the Hamilton Basin. This study investigates two of these identified areas.

The first zone of interest runs through a hill section on Kay Road, near Horsham Downs in northern Hamilton (Kay Road field site). The field area was created during construction of the Waikato Expressway, through excavation of a hillslope. Consequent exposure of geology showed extensive deformation of the Walton Sub-group (Puketoka & Karapiro Formations) and the Kauroa Ash Formation, through uplift, offset and displacement of bedding. This deformation varied within the field area, with displacement of beds ranging in size from a few millimetres in the Walton Sub-group, to > 7 m of displacement within the Kauroa Ash Formation. The total throw of the Kay Road field area was calculated at 7.41, with the field area appearing down-thrown towards the south. This down-throw was associated with extensive, steeply dipping normal faulting, and associated displacement of geologic units.

Geological investigation of this field site along with detailed unit descriptions and structural information measurements were used to generate geologic models using Leapfrog® Geologic Modelling software. Geologic Models of the Kay Road field area confirmed initial field observations; that normal faulting was extensive within at the Kay Road field site, and that deformation at Kay Road is confined to a time period older than the Rangitawa Tephra (0.35 Ma). This was illustrated by the irregular distribution of strata within the Kay Road field site, extensive intrusion structures present in the field area, and the undisturbed nature of the Rangitawa Tephra unit.

The second field site studied an inferred fault running parallel to Osborne Road in the northern boundary of Hamilton City (Osborne Road field site). Initially, this was discovered through observation of a ridgeline in study of LiDAR information of the Hamilton Basin. The presence of this ridgeline then led to study of field geomorphology, soil distribution and soil electrical resistivity properties within the Osborne Road field area. Study of these phenomenon is thought to corroborate a hypothesis that reverse faulting is present within the Hinuera Formation (c. 16 ka). This is evidenced by a 2 m concave slope break running through the field site parallel to Osborne Road, alongside irregular soil distribution within the field area. This irregular distribution shows an extensive presence of coarser, sandy units in the east of the slope break, with finer grained silty-sand and silty-clay units found to the west of the slope break. A zone of mixed sand and silts was found between these two units, that is thought to have been created in the reverse fault roll over zone, a phenomenon commonly associated with reverse faulting. Due to the non-invasive investigation approach that was undertaken at Osborne Road, faulting cannot be definitively confirmed; however significant evidence was found within the field area, suggesting it is highly likely that recent deformation is present.

Evidence suggesting deformation is present within the Hamilton Basin is extensive, with this investigation detailing evidence of both normal and reverse faulting. These discoveries were found in close proximity to one another, suggesting that deformation within the Hamilton Basin has been far more extensive and complex then previously recognised. Through detailing of offset bedding, alongside extensive study of geomorphic and deformation structures within the Hamilton Basin, this study corroborates hypotheses first presented by Kleyburg (2015) and Moon and de Lange (2017), that suggest tectonic deformation is present within the Hamilton Basin.

These discoveries contradict widely accepted literature, that suggests that evidence of deformation and faulting has been limited to the outer extents of the Hamilton Basin, and that the Hamilton Basin is an area that has been subject to very little to no tectonic deformation (McCraw, 1967; Kamp & Lowe, 1981; de Lange & Lowe, 1990; Stirling *et al.*, 2002; McCraw, 2011; Stirling *et al.*, 2012). The presence of such extensive tectonic deformation in the Hamilton Basin is thought

to contradict the low national seismic hazard rating that Hamilton City currently holds (Stirling *et al.*, 2002; Stirling *et al.*, 2012). For this claim to be validated however, further study and definitive evidence is required.

Acknowledgements

Thank you to my chief supervisor Dr Vicki Moon. Not only have you offered unwavering support throughout this journey, you have done so in a way that has been challenging but reassuring, and serious yet comical.

Thank you to both the Hamilton City Council, alongside the University of Waikato for assisting with funding of this investigation.

Dr Beth Fox, Dr David Lowe and Dr Peter Kamp, thank you for the insight you provided. The foundational knowledge you established regarding the Hamilton Basin, alongside your commitment to answer any question big or small has been much appreciated. Similarly, thank you to Cheryl Ward, Chris Morcom and Ben Andrews for your assistance in both field and lab environments.

Islay Laird, without your assistance this project would not have been possible. Sincere thanks to both yourself and Coffey for assisting with site access.

The support offered by my classmates throughout all aspects of this course has been second to none. Not only have you helped with academic pursuits, you have made this experience an enjoyable one. Tom Robertson, Francesca Spinardi and Aleesha McKay, for this I thank you dearly. Similarly, Rebecca Yeates, Shannon Hunter, Jamie Millar and Caitlin Murphy, thank you all for the various forms of support you have offered.

So many of my dear friends have helped me through this portion of my life. From pushing me to work harder, to reminding me to relax; Encouraging me with both support and wisdom, alongside providing me with much needed distractions, I am incredibly grateful.

My dearest sister Rachael, you have supported and encouraged me from day one. Your relentless encouragement has been a crucial to my post-graduate studies, and I don't know where I would be without you. I am truly blessed that you are a part of my life, and I cannot wait to try repay the support you have provided.

My parents, Ross and Sandra, I could not have done this without you. I am eternally grateful for the support you have offered me throughout not only this, but all of my academic pursuits. I cannot begin to imagine this journey without the support you have offered me. Thank you.

Table of Contents

List of Figures

List of Tables

Chapter 1

Introduction

1.1 Background of research

The Hamilton Basin is a fault bound, oval shaped depression of Late Tertiary to Pleistocene age. The basin occupies a large area of land within the central North Island, New Zealand, and has long been thought of as an area of simple geology in a country plagued by tectonic deformation. Currently, the Hamilton Basin holds a low National Seismic Hazard Rating due to the lack of known active tectonic features within the Basin. Recent discovery of an injectite in the recent Hinuera Formation (c. 16 ka) by Kleyburg (2015) however, was the first discovery of many that suggests that the Hamilton Basin is far more complex than previously recognised.

Consequently, substantial research into the structure of the Hamilton Basin has been commissioned. Although preliminary, research regarding the Hamilton Basin has already found extensive evidence indicative of tectonic deformation within the basin. Thus far, the study of LiDAR data and geomorphic signatures within the Hamilton Basin, alongside observation of sidescan and multibeam data within the Waikato River, and study of seismic profiling and resistivity survey has identified over 26 zones of interest (Moon & de Lange, 2017). These zones of interest all show potential signatures associated with tectonic deformation.

Two sites of particular significance within the Hamilton Basin were identified; Kay Road and Osborne Road. Both of these field sites are located in northern Hamilton, near Horsham Downs. The Kay Road field site was first discovered during construction of the Waikato Expressway, which unearthed a number of extensive fault systems and paleoliquefaction structures, indicating tectonic deformation. Conversely, the Osborne Rd field site was found after study of LiDAR data, alongside observation of a concave slope break running through the extent of the field area. To the east of this slope break, elevation averages 39 m above sea level (asl), with elevation on the west of the break averaging 37 m asl. As both sites

were hypothesized to be regions of potential faulting, this project focussed on the investigation of the two field sites.

1.2 Aims and objectives

This study set out with the aim to characterise two regions of inferred faulting, detailing any evidence of deformation within the identified sites. This was completed through study of exposed faces at Kay Road, alongside the use of soil auger sampling and soil electrical resistivity surveys at Osborne Road. Through the compilation and evaluation of evidence, this study aims to establish the most likely methods of deformation responsible for said faulting, alongside characterising any deformation present.

Key objectives of the study are as follows:

1. to use geomorphic mapping, soil auger sampling and soil electrical resistivity surveys to identify whether or not displacement is present at Osborne Road;
2. to describe the fault zone at Kay Road, including description of geological units, and evidence of deformation
3. to construct 3D geologic models of the Kay Road fault zone using LeapFrog geological modelling software.

1.3 Research benefits

The Hamilton Basin is an area that is somewhat understudied, with limited information regarding deformation within the basin in existence. This research project aims to improve the understanding of the Hamilton Basin through documentation of tectonic deformation; thus contributing to foundational research regarding deformation within the Hamilton Basin. Although this investigation will not exclusively establish the validity of the National Seismic Hazard Model (NSHM) for Hamilton City, it will contribute to the overall improvement of knowledge regarding the Hamilton Basin.

1.4 Thesis layout

Chapter 2 presents a literature review, assessing and summarising information regarding the formation of the Hamilton Basin, known tectonic deformation, and

typical units found within the Hamilton Basin, This chapter will also address current knowledge regarding the Hamilton Basin. Chapter 2 also addresses typical forms of faulting and structures associated with tectonic deformation.

Methodology used in this investigation is outlined in Chapter 3. This includes all of field, laboratory and processing methods used.

Results of this investigation are presented in Chapters 4 and 5, with Chapter 4 addressing results found in the Kay Road field site. Results of investigation undertaken at Osborne Road site are addressed in Chapter 5.

Discussion of results and subsequent evaluation are outlined in Chapter 6. Chapter 6 also conducts an assessment of the validity of findings, alongside making comparisons with literature.

Chapter 7 summarises this investigation, and draws conclusions regarding the implications of this investigation. Recommendations are also made that address both this investigation, and potential future research.

Chapter 2

Literature Review

2.1 Hamilton Basin overview

The Hamilton Basin is a fault bound, oval shaped depression of Late Tertiary to Pleistocene age. The basin occupies an area in the Central North Island, New Zealand, and is between Taupiri in the north and Te Awamutu in the south (McCraw, 1967; Kamp & Lowe, 1981; Selby & Lowe, 1992; Edbrooke, 2005; McCraw, 2011; Kleyburg, 2015). An image illustrating the Hamilton Basin is shown below in Figure 2.1.

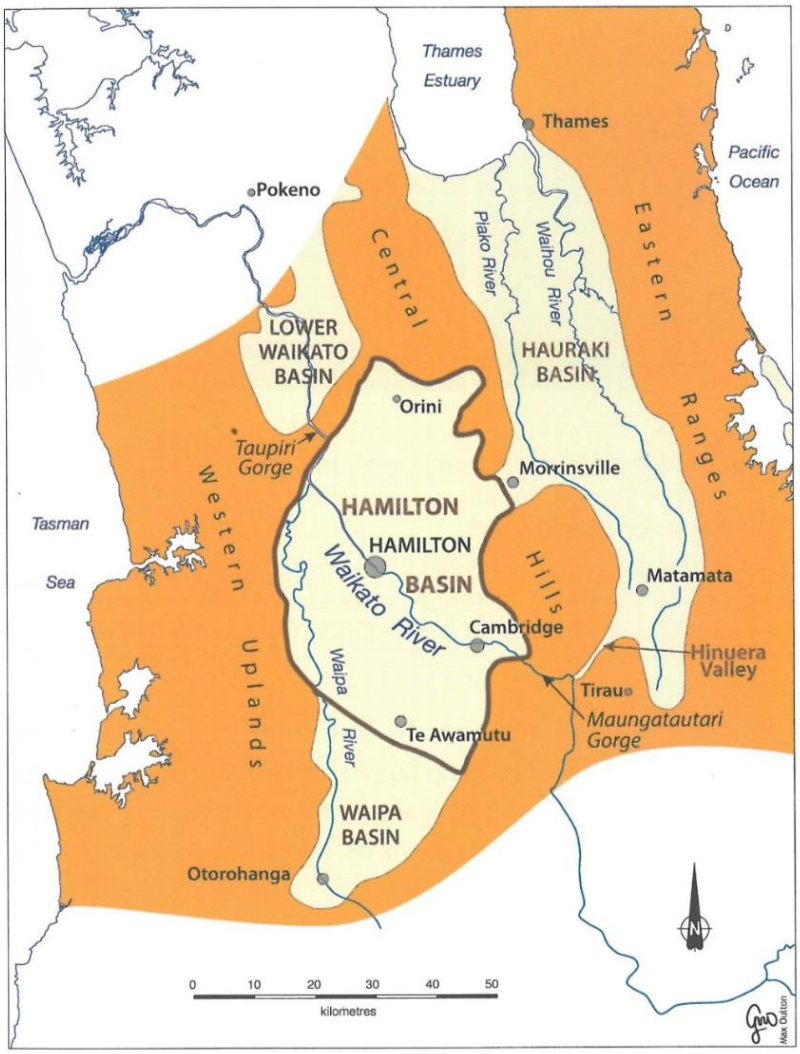

Figure 2.1 - Map illustrating the Hamilton Basin, alongside surrounding Waipa, Lower Waikato and Hauraki Basins (McCraw, 2011).

2.2 Geology of the Hamilton Basin

Structurally, the Hamilton Basin is viewed as relatively simple, with a major fault (Waipa Fault) recognised to the west of the basin. Other nearby faults bound and bisect the neighbouring Hauraki Basin, and several faults are inferred in the Lower Waikato Valley to the north of the Hamilton Basin (Figure 2.2)

Figure 2.2 - Image illustrating recognised faults in and around the Hamilton Basin

The Hamilton Basin is surrounded by dissected mountain ranges up to 300 m high to the north, west and east. The basin rises gently and merges with the dissected plateaux of the King Country basin to the south (Selby & Lowe, 1992). To the west, surrounding ranges are primarily composed of sandstone, siltstones and conglomerates, alongside Tertiary coal measures, and limestones which overlie Triassic and Jurassic material. To the east, Tertiary rocks bordering the basin once overlay expansive greywacke deposits, however these Tertiary deposits have since been uplifted and eroded (Kear, 1967).

Ultimately, rocks forming the Hamilton Basin can be can be divided into four major units. Basement rocks are hard, Mesozoic, broadly-folded wacke-type rocks, all of which originated during the New Zealand Geosyncline (Kear, 1967). Overlying these basement rocks, are softer, gently dipping Tertiary strata, exposed in the western hills of the Hamilton Basin, alongside the early Quaternary terrestrial formations that occur in many parts of the area (Walton Sub-group). The Walton Sub-group forms prominent low hills within the basin, which rise above alluvial planes. Materials that overlie Tertiary strata within the central lowlands of the basin are predominantly comprised of near-horizontal, upper Cenozoic alluvial sediments known as the Hinuera Formation. The Hinuera formation was largely deposited by the ancestral Waikato River and is one of the most expansive and recognisable deposits within the Hamilton Basin (Lowe, 2010).

2.3 Hamilton Basin formation

The Hamilton Basin began to adopt aspects of its present form during the Kaikoura Orogeny in Early Pliocene times. Throughout this orogeny, faulting and differential uplift caused the basin to remain a relatively depressed graben, whilst the Raglan Hill blocks to the west, and the Hapuakohe-Hangawera-Pakaroa-Maungakawa hills to the east were uplifted and gently tilted as horsts (Selby & Lowe, 1992; McCraw, 2011).

Erosion within the area presently recognised as the Hamilton Basin then occurred, continuing until the region was a surface of low relief. Deformation occurred during the early Tertiary period, which caused peat to accumulate thickly in the wet depressions of the landscape. As the sea transgressed, these peat deposits were covered with marine sediments which would become sandstone, siltstone and limestone. Ultimately, the added weight of this strata enabled the transition of peat to coal to occur. These formations are now largely recognised as the Waikato Coal Measures, which are distributed sporadically throughout the Hamilton Basin (Lowe, 2010; McCraw, 2011).

Separation of blocks by sub-parallel and north-south faulting then occurred, resulting in the formation of ranges within the lowlands of the Basin. Volcanic activity then broke out, forming many of the Western Uplands and Eastern ranges

recognised within the Hamilton and Hauraki Basins. A long period of erosion then occurred, stripping much of the vegetation within the basin. Ultimately, these newly eroded depressions then became receptacles of terrestrial sediment (Selby & Lowe, 1992; McCraw, 2011). Figure 2.3 below illustrates the processes involved in the formation of the Hamilton Basin.

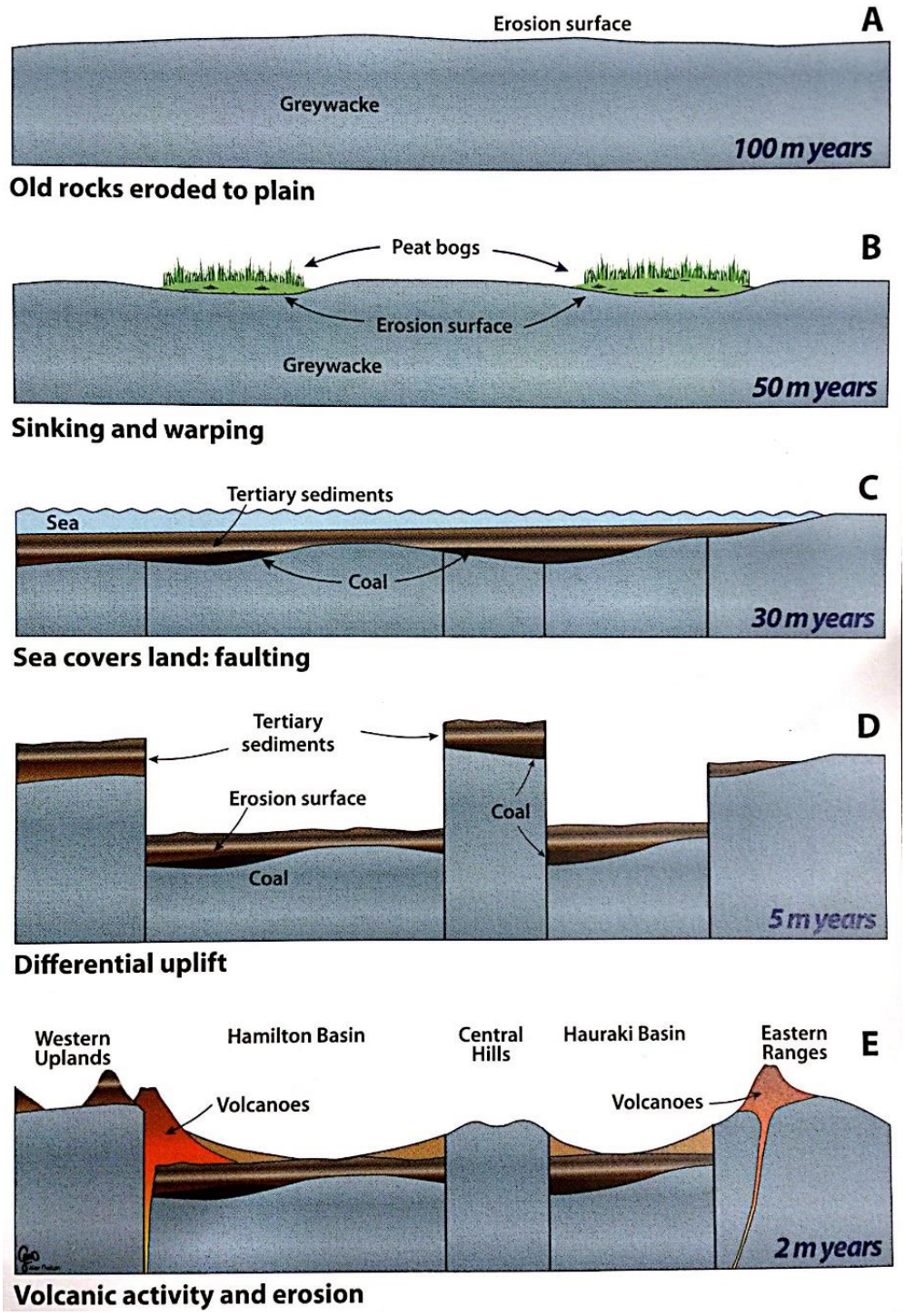

Figure 2.3 - A series of diagrams illustrating a simplified version of events which lead to the formation of the Hamilton Basin (McCraw, 2011).

Volcanic processes around the margin of the Hamilton Basin have contributed to the infill of the Hamilton Basin. Discussion on the alluvial infilling of sediments derived from these margins, and rhyolitic eruptions from the Central North Island is discussed in section 2.5.

2.4 Geology of the Hamilton Basin and general landscape patterns

Four main landscape features are present within the Hamilton Basin, including low rolling hills, flattish alluvial plains, low terraces and gullies (Lowe, 2010). An image depicting these landscape features alongside typical soil types found within the Hamilton Basin is shown in Figure 2.4.

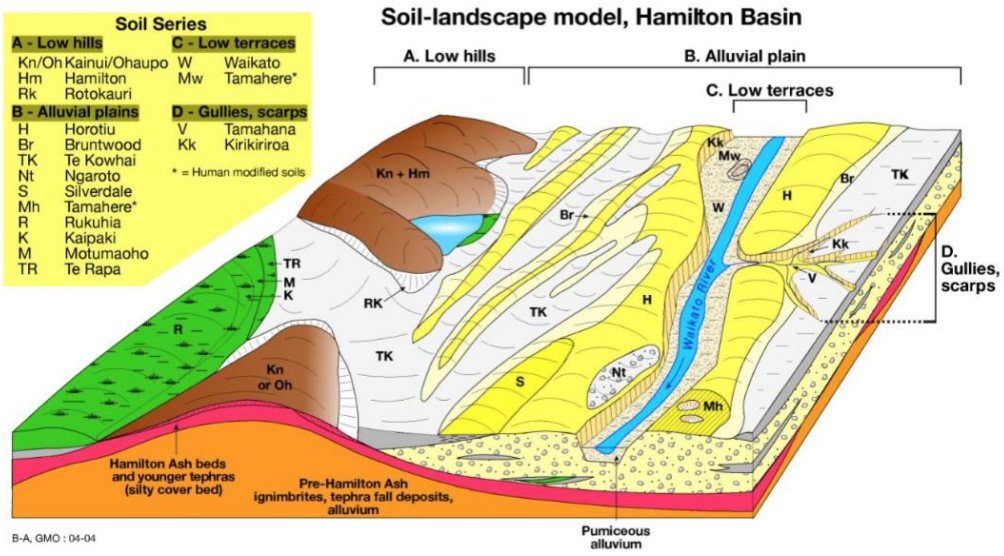

Figure 2.4 – Model of typical units found within the Hamilton Basin. Figure taken from Lowe (2010).

Lithologies of units that generally comprise these landscape formations are detailed below.

2.5 Lithologies of the Hamilton Basin

Many sediments infill the Hamilton Basin, including those derived from fluvial, alluvial and volcanic sources. These are described in various sub-sections below.

2.5.1 The Walton Sub-group:

Within the Hamilton Basin are a number of early Quaternary terrestrial formations. These units form many of the prominent hills within the Hamilton Basin, and protrude through alluvial plains of the Hamilton Basin. An example of

these hills is shown in Figure 2.4. Collectively, these units are recognised as the Walton Sub-Group, which incorporates the Puketoka Formation and Karapiro Formation (Selby & Lowe, 1992).

The Puketoka Formation is the oldest member of the Walton Sub-group; and contains well sorted, pale grey pumiceous clays, sands and breccias, alongside unsorted beds which are distal portions of rhyolitic ignimbrite sheets (Selby & Lowe, 1992). The Waerenga Gravels are then younger than the Puketoka Formation, and consist of weathered greywacke debris which were most likely deposited in fans extending throughout the surrounding ranges (Selby & Lowe, 1992).

Younger than the Puketoka Formation is the Karapiro Formation, which is comprised of current-bedded rhyolitic sands and gravels. Often these gravels are strongly weathered and clayey, and show dark reddish to orange colouring (Selby & Lowe, 1992).

Primarily, the Walton Sub-group was laid down by both braided and meandering streams from the south and the surrounding ranges, or as lacustrine deposits. It is thought that multiple low angle fan surfaces with little relative relief occupied the floor of the Hamilton Basin. Once deposition of these units stopped, it has been suggested that streams began dissecting and cutting down the landscape with hills some tens of metres high. It is thought that this landscape existed with only slight changes for thousands of years, as shown by the intense weathering exhibited by the Karapiro Formation and other Walton Sub-group materials (Ward, 1967; Kamp & Lowe, 1981; Selby & Lowe, 1992; Lowe *et al.*, 2001).

2.5.2 Tephra deposits

Following infilling of the Hamilton Basin during the Quaternary period through fluvial, lacustrine, and ignimbrite deposits, significant erosion occurred. This resulted in the formation of a hilly landscape, which was then influenced by deposition of a series of air fall tephra layers. Primarily, these tephras stemmed from large rhyolitic calderas of the Taupo Volcanic Zone, however some tephras from the andesitic stratovolcanoes of both Tongariro and Egmont Volcanic

Centres, and offshore volcano of Mayor Island (Tuhua Volcanic Centre), have also been found within the Hamilton Basin (Selby & Lowe, 1992).

2.5.2.1 Kauroa Ash Formation

The oldest sequence of tephra deposits within the Hamilton Basin is a series of strongly weathered, clay-rich rhyolitic beds collectively known as the Kauroa Ash Formation. Much of this formation has been eroded, with the unit seldom thicker than 1 – 2 m within the Hamilton Basin (Selby & Lowe, 1992). Typically, the unit comprises up to 15 beds that vary in age, ranging from the oldest at 2.3 Ma, to more recent deposits of 1.5 Ma. Where preserved, the most recent bed of the Kauroa Ash Formation has an extremely prominent dark reddish-brown colour with a strongly developed blocky or prismatic structure. Older units often display a golden brown-colour. Although exposure of the Kauroa Ash Formation within the Hamilton Basin is limited, where exposed interfingering with the Puketoka and Karapiro formations has been observed (Selby & Lowe, 1992; Lowe *et al.*, 2001).

2.5.3 Karapiro Formation

The Karapiro Formation overlies older tephra units within the Hamilton Basin, and is composed of current-bedded rhyolitic clays, sands and gravels, which are often strongly weathered. Fragments of volcanic rocks and greywacke are also present within the material. Often presenting as a clayey bed, the Karapiro formation often has distinctive red colouring. This red colouring is associated with weathering of old sediments during a warmer period (McCraw, 1967; Selby & Lowe, 1992).

2.5.4 Hamilton Ash Series and Rangitawa Tephra

After an extended period, much of the Kauroa Ash Formation and weathered sediments below were eroded. Another tephra mantle between 3-5 m thick (Hamilton Ashes), thick was then deposited. The oldest bed within the Hamilton Ash Beds is the Rangitawa Tephra, dated at 0.35 Ma (Kohn *et al.*, 1992; Lowe *et al.*, 2001). Previously, the Rangitawa Tephra has been called H1, or the Ohinewai Ash, dependant on location (Selby & Lowe, 1992; Pillans *et al.*, 2005). Hereon however, the formation is referred to as the Rangitawa Tephra.

The Rangitawa Tephra is a pale greyish-brown, and has a sharp lower boundary marked by a coarse, yellow, sandy layer. Micaceous flakes are also present within

the Rangitawa Tephra (Lowe *et al.*, 2001). This layer forms a prominent marker bed. Overlying Hamilton Ash Beds are typically strongly-weathered, clay textured, and friable to firm with reddish-yellow to strong brown colours. The ages of these beds are unknown, but characteristics of some of these units suggest that eruptions responsible for the formation of many of these beds were separated over many thousands of years, including long periods without eruptions.

Younger than the Hamilton Ash Beds still is an air fall cover bed that ranges between 0.5 and 1.5 m thick. This unit is comprised of multiple tephra layers that have accumulated over the previous 50 000 years. These Quaternary cover beds cap many of the low hills (Lowe, 2000; Lowe *et al.*, 2001; Lowe, 2010).

2.5.5 The Hinuera Formation

The Hinuera Formation is defined as part of the Piako Supergroup, which is within the greater Tauranga Group, and is a terrestrial formation underlying the extensive fertile plains of the Hamilton lowland and southern half of the Hauraki lowlands (Kear *et al.*, 1978; Edbrooke, 2005; Kleyburg, 2015). Comprising mass emplaced volcanoclastic alluvium, and deposited by large, low angle fans by a high energy braided ancestral river, the Hinuera Formation is found throughout the greater Hamilton Basin. Earliest known deposition of the Hinuera Formation sediments has been dated between 140 000 and 50 000 years (Houghton & Cuthbertson, 1989; Selby & Lowe, 1992).

An unconsolidated alluvial deposit, quartz, feldspar, rounded rhyolitic rock fragments, pumice and heavy minerals comprise the Hinuera Formation. Up to 90 m thick in some areas, the Hinuera Formation underlies some 2000 km^2 of the plains of the Hamilton Basin and southern half of the Hauraki lowlands (Selby & Lowe, 1992). Typically, the formation is dominated by gravelly or slightly gravelly sands, sandy gravels and silts; with some peat beds having developed locally within the formation. Internally, gravel-sized material is dominated by rhyolitic breccia, rhyolite, pumice and ignimbrite, with sand and silt fractions dominated by volcanic quartz, plagioclase, pumice and glass shards. Some heavy minerals are present within the formation, including hypersthene, magnetite, hornblende, augite, epidote and biotite. Minor clay minerals are also present, including

halloysite, kaolinite, illite and chlorite (Hume *et al.*, 1975; McGlone *et al.*, 1978; Selby & Lowe, 1992). Within the Hinuera Formation, reported grain size parameters are largely variable. Complex grain size distribution is observed within the Hinuera Formation, with textural data indicating that the bulk of the Hinuera Formation was deposited rapidly in an environment of fluctuating high turbulent energy (Hume *et al.*, 1975; McGlone *et al.*, 1978; Selby & Lowe, 1992).

From the composition, texture, and sedimentary structures observed in a study conducted by Hume *et al.* (1975) we can deduce that the Hinuera Formation formed in a variety of sub environments in a braided river system of the ancestral Waikato River. Geomorphology of the Hinuera Formation within the Hamilton Basin is that of a large, very low angle alluvial fan. This fan formed from transport of sediment through the narrow Maungatautiri Gorge out into the current day Basin (Hume *et al.*, 1975; McGlone *et al.*, 1978). Aggradation then occurred in two phases, initiated by volcanism from the Central Volcanic Region. This aggradation was sustained by erosion of the Upper Waikato Basin (Figure 2.5) under a cold, seasonally wet climate (Hume, 1972 & Hume *et al.*, 1975).

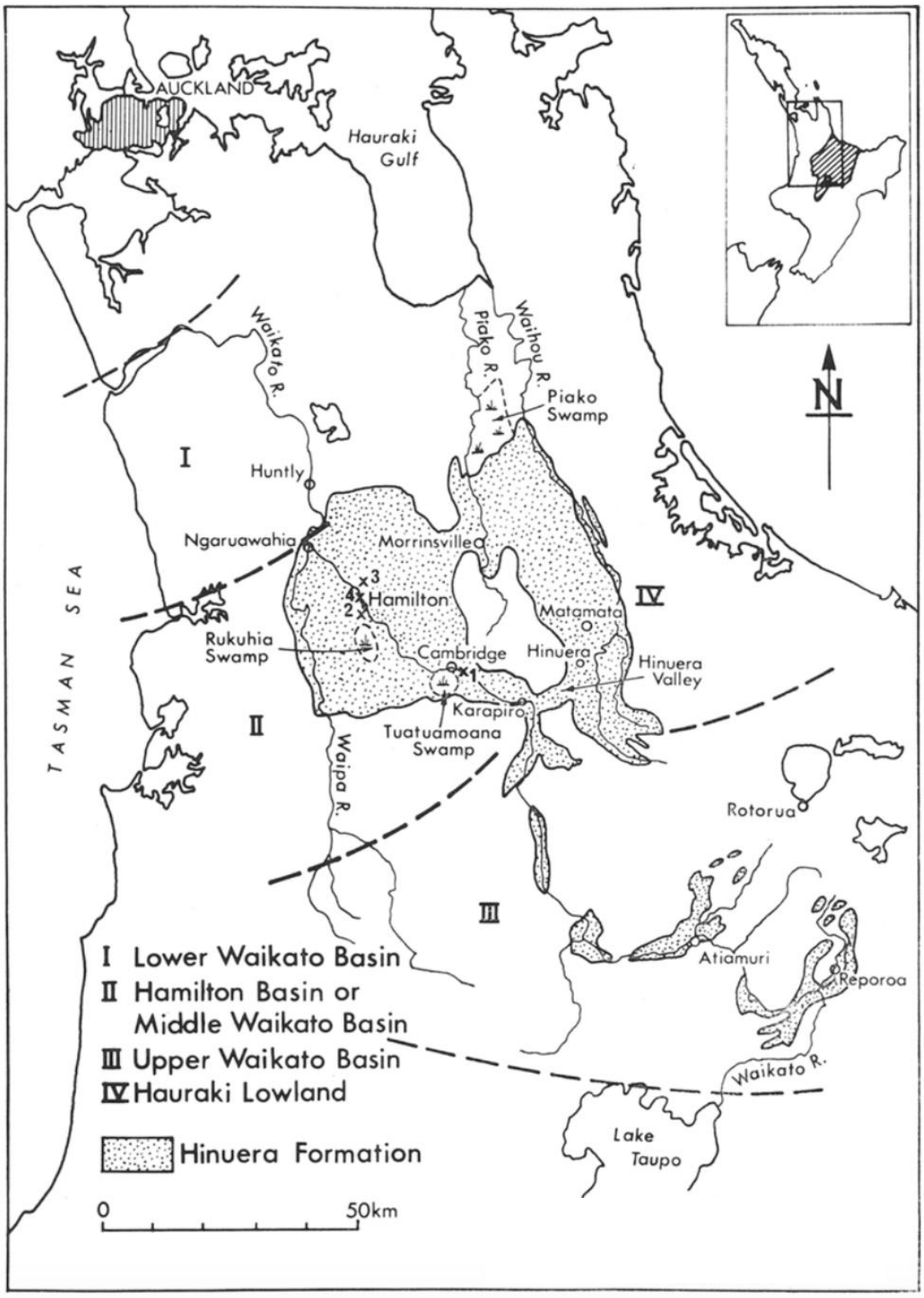

Figure 2.5 - Image of the Hamilton Basin, showing the distribution of the Hinuera Formation in the Hamilton and Hauraki Basin. Image taken from McGlone *et al.* (1978).

The reported age of the Hinuera Formation varies due to the diverse characteristics of the formation, however most recent deposition of the Hinuera Formation is reported to have occurred between 22,000 and 16,000 cal. years ago (Selby & Lowe, 1992; Manville & Wilson, 2004; Lowe, 2010).

2.5.6 Taupo Pumice Alluvium

It is thought that approximately 1850 years ago, the Waikato River carried and deposited huge quantities of pumice sands, silts and gravels from the Taupo Eruption, depositing what is recognised as the Taupo Pumice Alluvium. Up to 30 m thick, it is now thought that much of the Taupo Pumice Alluvium has since been eroded (Hume, 1972; Hume *et al.*, 1975; Selby & Lowe, 1992).

2.6 Tectonic deformation and associated landscape features

2.6.1 Introduction

Tectonic deformation is a change in the mode of bedding, volume, internal structure or relative position of a body of rock due to extensional, compressional or displacement forces (Yeats *et al.*, 1997; Ferrari & Guiseppi, 2009; Marshak, 2011).

To understand processes associated with tectonic deformation, it is necessary to have an identifiable feature that has been displaced (Burbank & Anderson, 2011). As tectonic processes have a significant influence on characteristics observed within a landscape, geomorphic signatures within landscapes are recognised as evidence of deformation. Best geomorphic markers indicative of tectonic deformation are usually recognizable landforms, surfaces or linear trends which display three characteristics: (i) a known consistent undeformed geometry: (ii) a known age and: (iii) high preservation potential (Burbank & Anderson, 2011).

This section outlines tectonic deformation, presenting a literature review of methods of deformation, associated geomorphic signatures and current knowledge of deformation within the Hamilton Basin.

2.6.2 Faulting

When rocks are subjected to stress that exceeds their strength, they rupture, fold or flow. Different varieties of faults (strike-slip, normal, thrust) characterize contrasting tectonic stress regimes in the upper crust. When faults break the Earth's surface (either in a single earthquake, or during seismic events) they commonly create geomorphic features which can be associated with different types of faulting. Sometimes, in faults that do not reach the Earth's surface, no

ground deformation is associated with a fault trace. Nonetheless, the Earth's surface will deform by folding in response to these stresses.

Because of the rigidity of rocks, and constant pressures generated by plate tectonics, stress builds up in rocks. Once this exceeds the strain threshold, the accumulated potential energy dissipates by the release of strain. This is focussed into a plane along which motion occurs; more commonly known as a fault.

In reality, fault geometries are often far more varied than might be expected from simple models related to regional stress fields (Burbank & Anderson, 2011). This is due to inhomogeneities in rocks including variable strengths and bedding characteristics. The orientation of weaknesses within rocks that are subjected to stresses can exert a strong control on how they deform. Due to the characteristics of different materials, various different types of faulting can arise. These are discussed below, and a simple diagram comparing normal and reverse faults is shown in Figure 2.6.

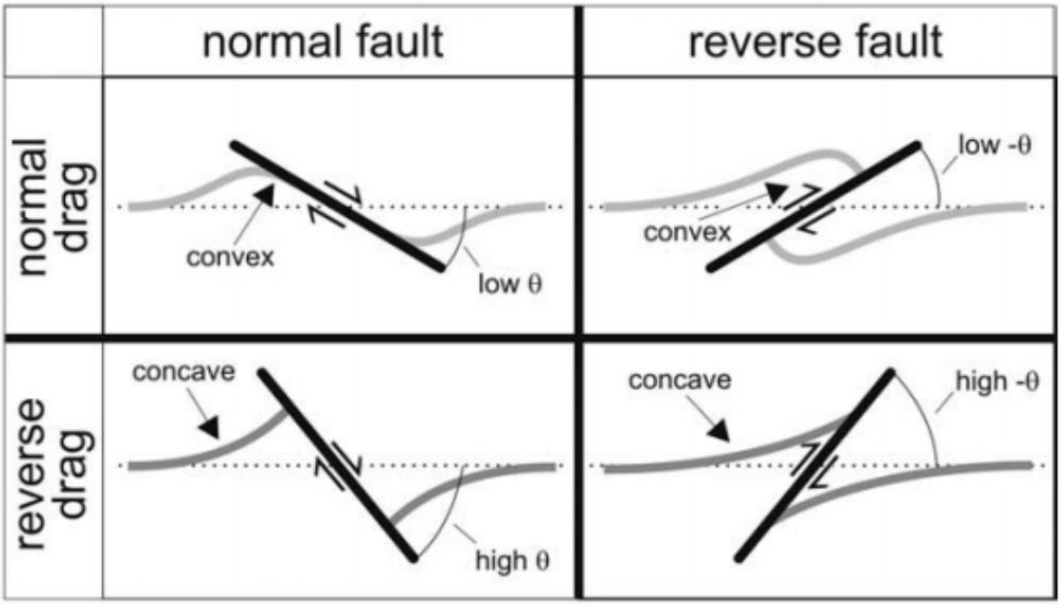

Figure 2.6 – Simple diagrams illustrating normal and reverse faulting, two common methods of tectonic deformation. Image taken from Grasemann *et al.* (2005).

2.6.3 Normal Faulting

Discussed by Burbank and Anderson (2011), normal faults (also known as a dip-slip faults) form in settings where maximum compressive stress (σ_1) is vertical and a deviatoric tensile stress in a horizontal orientation is present. Typically, these

faults cut a face at high angles between ~50-70°, and are a consequence of crustal extension. In normal faulting, the hanging wall moves downward relative to the footwall.

A down-thrown block between two normal faults dipping together is known as a graben; conversely two normal faults dipping away from each other form a horst. Normal faulting can often create half-grabens or fault-angle depressions. Grabens, half grabens and fault angle depressions can also create basins in which sediments accumulate (Barnett *et al.*, 1987).

2.6.4 Listric faults

Listric faults are similar to normal faults, however a curve is observed in the fault plane. Dip is also steeper near the surface of a listric fault, and will often shallow with increasing depth (Allaby, 2013).

2.6.5 Reverse faulting

Reverse faulting is characterised by rock fractures where the hanging side of the fault is uplift compared to the footwall (Gorse *et al.*, 2012). Typically, the dip of a reverse fault is relatively steep, often greater than 45°.

2.6.6 Thrust faults

Similar to a reverse fault, a thrust fault has a similar sense of motion however the dip of the fault plane is less than 45°. Typically, thrust faults generate ramps, flats and fault bending, and are often the result of crustal compression (Gorse *et al.*, 2012).

2.6.7 Strike-slip faults

Strike-slip faults are vertical or nearly vertical fractures where blocks move mostly horizontal (USGS, 2017a). Strike slip faults are sometimes known as lateral faults, transcurrent faults or wrench faults (Encyclopaedia Britannica, 2017).

2.6.8 Oblique-slip faults

Faults that have a component of a strike slip and a dip-slip fault are categorised as oblique-slip faults. As many faults have some component of strike and dip slip, defining oblique-slip faults requires components to be both significant, and measureable. Oblique-slip faults are most commonly associated with

transtensional and transgressional regimes that involve the direction of extension shortening or changing (Allaby, 2013).

2.6.9 Other faults

A number of other less common faults occur, including ring faults which are associated with the collapse of volcanic calderas, and synthetic/antithetic faults which are terms used to describe minor faults associated with major faults (Huggett, 2007; Ferrari & Guiseppi, 2009; Burbank & Anderson, 2011).

2.7 Deformation Signatures

Tectonic faulting has a definite influence on the landscape. Common signatures associated with tectonic deformation include linear valleys, scarps, springs, benches, offset drainage channels, sag ponds, beheaded streams, shutter ridges and linear valleys or troughs.

Transfer zones are a common feature within basins where tectonic deformation is present. Simplified geometries of structures that are associated with normal faults (both overlapping and non-overlapping) are shown in Figure 2.7. Shown in Figure 2.7A is an antithetic interbasin ridge, Figure 2.7B is an antithetic interference zone, Figure 2.7C is a transfer fault zone, and Figure 2.7D is a synthetic relay ramp.

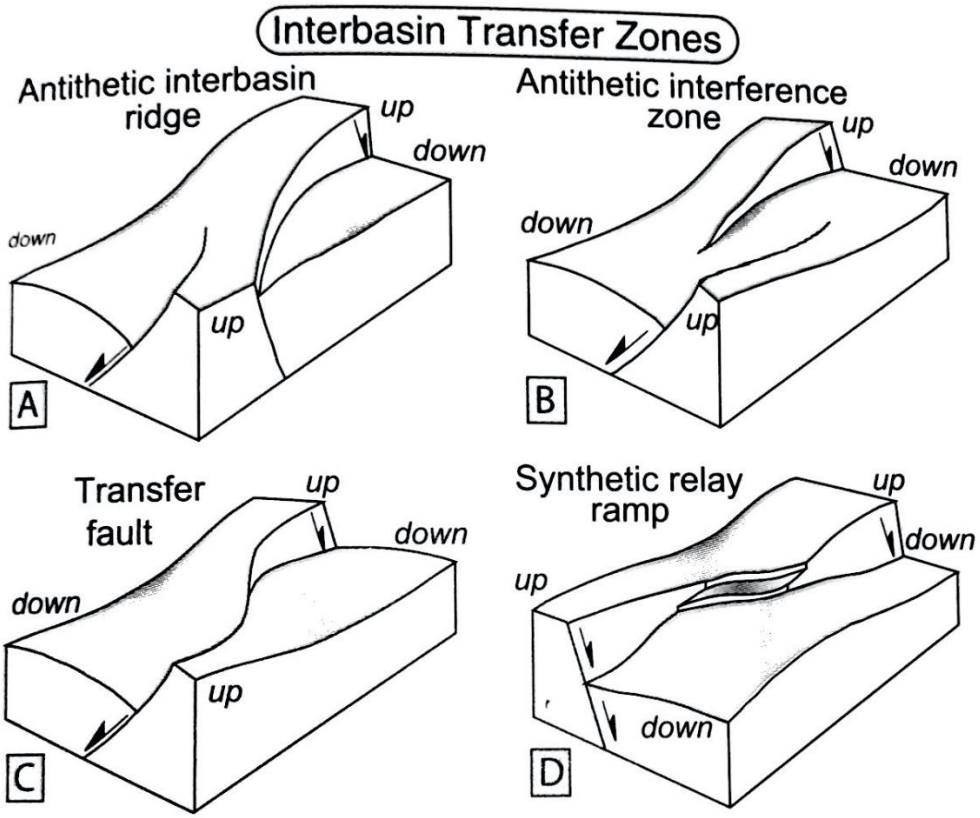

Figure 2.7 – Schematics showing a number of simplified interbasin transfer zones and associated landscapes. Image taken from Burbank & Anderson (2011).

Landscape features associated with zones of extensional tectonic deformation are often complex. Crustal extension is a phenomenon often associated with normal faulting, and can result in a number of distinctive landscape features. This can include, but is not limited to the presence of horsts, grabens, hanging-wall roll-over, antithetic faults, synthetic faults, half grabens and back tilting. These phenomenon are shown in Figure 2.8.

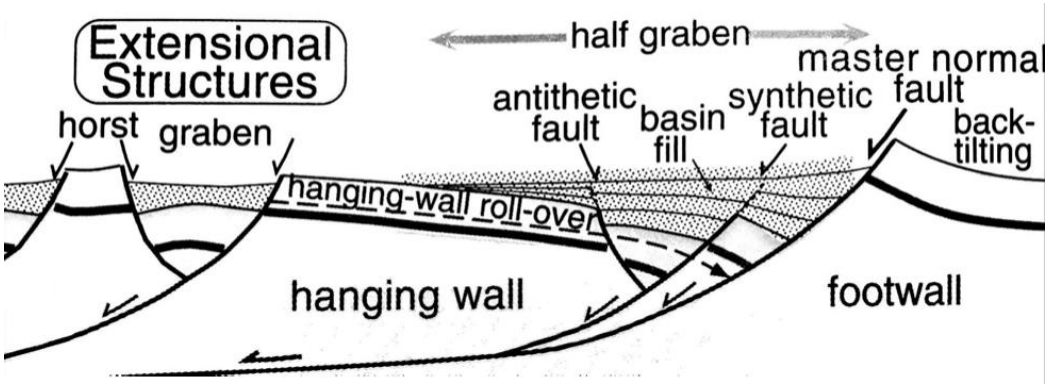

Figure 2.8 –Landscape formations associated with crustal stretching. Image taken from Burbank & Anderson (2011). Shown in this image is listric like faulting in the right of the image.

As shown above, tectonic faulting and consequent deformation has distinctive geomorphic signatures within a landscape. Many of these phenomenon have been recognised within the Hamilton Basin, supporting the idea that tectonic deformation is present within the Basin.

2.7.1 Intrusion structures, injection structures and seismites

Injection structures are a phenomenon commonly associated with tectonic deformation, and can vary significantly in both size and structure. Most commonly, injection structures can be ductile deformation structures including ball and pillow structures, plastic intrusions or disturbed lamination. Irregular convolute stratification and fractured layers, alongside recumbently folded laminations or brittle structures such as sand dyke, or autoclastic breccias are also common injection structures and seismites (Berra & Felletti, 2011).

Seismites is a term that is less specific than the previously mentioned injection structures, that refers to any structures generated by seismic shaking, or earthquake deformed layers. Commonly, the term is applied to both sedimentary layers and sediment deformation structures induced by shaking. Emphasis on correct use of the term when classifying these features is stressed in literature, as similar looking features may be products of non-seismic perturbation. As of the time of this investigation however, no formal classification system exists, so the term is rather loose (Sims, 1975; Owen & Moretti, 2011). Hereon, injection structures (sand dike, liquefaction structures), and seismites are referred to generically as intrusion structures.

2.8 Known faults around the Hamilton Basin

The Hamilton Basin is regarded as an area of low to moderate seismicity, however both the Hamilton Basin and wider regions appear to have previously been influenced by tectonic processes. Kamp and Lowe (1981) suggest 200 – 300 m of vertical displacement along the western margin of the basin on the Waipa Fault. Multiple north/northeast trending normal faults appear within the basin, with an estimated 400 m of vertical movement observed on the Hauraki Fault (Selby & Lowe, 1992). This marks the eastern margin of the Hauraki Plains, and resulted in uplift of the Kaimai Ranges between 0.84 and 0.14 My BP.

A number of other major active faults are known extrinsic to the Hamilton Basin. Running NNW through the centre of the Hauraki Plains and as far south as Okoroire, the Kerepehi Fault is one of the most widely recognised faults in the greater Waikato region. With 1.6 m of displacement over the last 10 700 years, it is thought that the Hauraki Plains lie in a zone of active continental rifting (de Lange & Lowe, 1990; Selby & Lowe, 1992). An image illustrating known faults within the wider Hamilton basin is shown below in Figure 2.2.

A study undertaken by Persaud *et al.* (2016) investigated the general Hauraki Basin area. Key findings from this paper is that the Kerepehi Fault is an active normal fault, which stretches for approximately 80 km within the Hauraki Basin. This study observed an average slip rate of 0.08-0.4 mm a^{-1}. It was noted that within the Hinuera Surface, single event displacements (SED's) along the Kerepehi fault were found to vary between 1m and 1.8 m. Subsequently an annual vertical slip rate between 0.08 and 0.4 mm a^{-1} was calculated. Primarily, it is thought that earthquakes in the range of M_w 6.3 – 7.0 have occurred in the past, and are to be considered a future hazard within the region.

2.9 Current knowledge of Hamilton Basin deformation

Recent research has been conducted within the Hamilton Basin which suggests significant tectonic deformation had occurred within the Hamilton Basin. These discoveries were first reported by Moon and de Lange (2017), and included recognition of a previously unknown fault line running through Hamilton City.

The idea that deformation was present in the basin was first brought to attention when discoveries of historic liquefaction in a construction site in northeast Hamilton were first made. Further research was conducted, and several possible faults were identified, with confidence the highest in a fault line that runs from Templeview, through the Waikato River and Days Park, out to Gordonton; an area predominantly affecting the northwest of the city.

An investigation by Kleyburg (2015) showed that definitive evidence of paleoliquefaction features were present. These were earthquake induced injection structures (sand dikes). It is thought that a seismic event causing liquefaction occurred sometime after c. 20,749 ± 204 calendar years ago (95% probability range) at Aspin Road near Cambridge and after c. 19,964 ± 222 calendar years ago (95% probability range) at Endeavour Primary School in northern Hamilton.

Consequently, research by Moon and de Lange (2017) continued. Updated research showed that 5 known and potential fault zones are found in the Basin; these include the previously mapped Taupiri Fault, and inferred Horotiu Fault, Kukutaruhe Fault, Te Kourahi Fault and the Te Tatua O Wairere Fault. Figure 2.8 below illustrates the relationship between these faults , and Hamilton City.

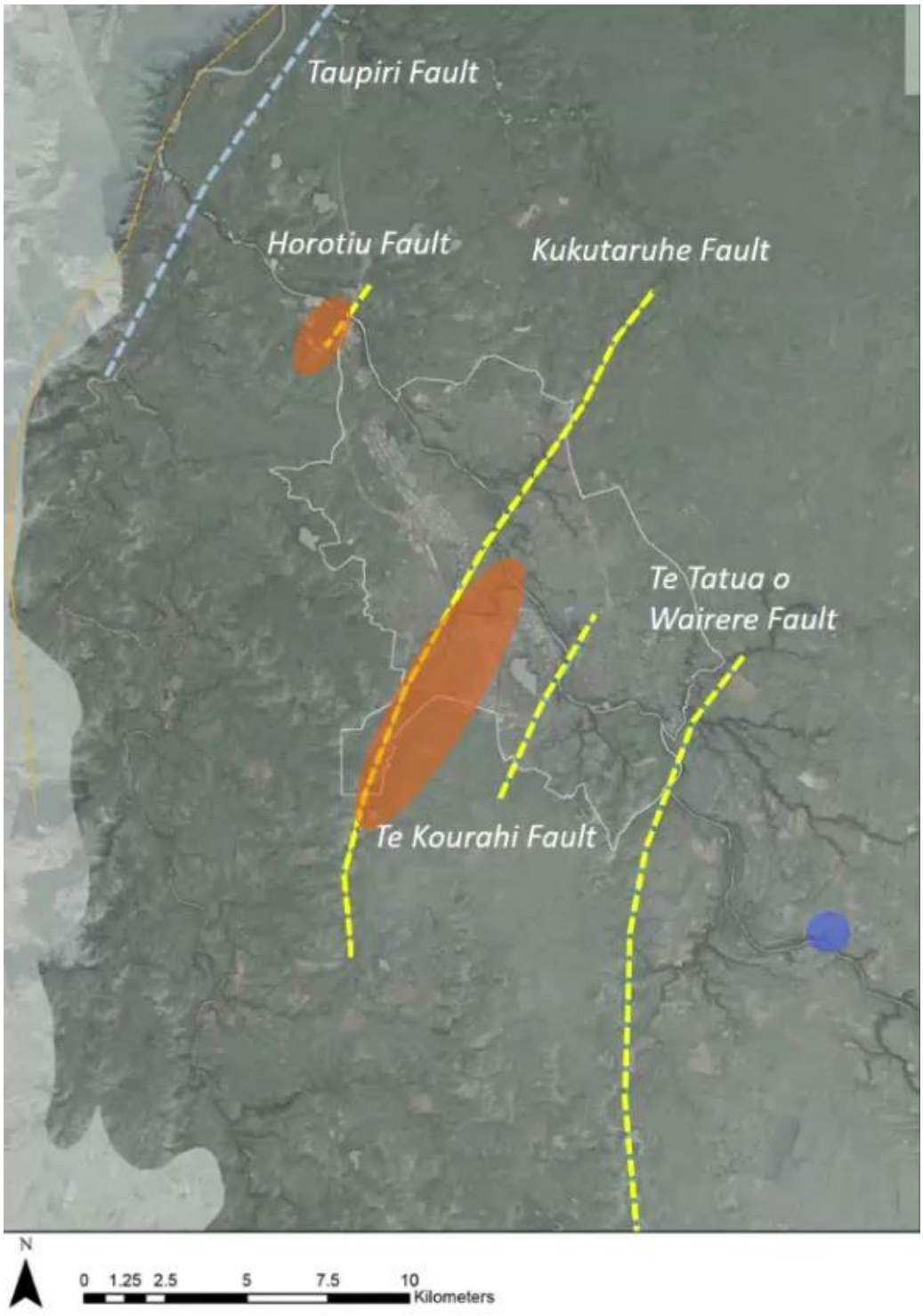

Figure 2.9 - Image of known and inferred fault lines running through the Hamilton Basin. Shown in a faint white outline is the Hamilton City boundary, and shown in dashed yellow are inferred fault lines. Image taken from Moon and de Lange (2017).

The presence of these inferred fault lines encouraged research within the Hamilton Basin. Further review of existing research data (such as gravity, seismic and drill oil, gas and coal surveys) has continued, alongside CHIRP seismic reflection and mapping within the Waikato River, and coring of peat lakes with CT

scanning of recovered cores. The following section reviews some of this information, alongside other evidence which supports the idea of tectonic deformation.

Found within the Hamilton Basin is a significant gravity anomaly. This gravity anomaly shows a deeper basin towards Ngaruawahia to the northwest of the Hamilton Basin, with the deepest area recorded in Te Rapa. This anomaly is shown in Figure 2.10. In this image is a stark change in gravity properties alongside the area that aligns with an inferred fault zone at Osborne Road, northern Hamilton.

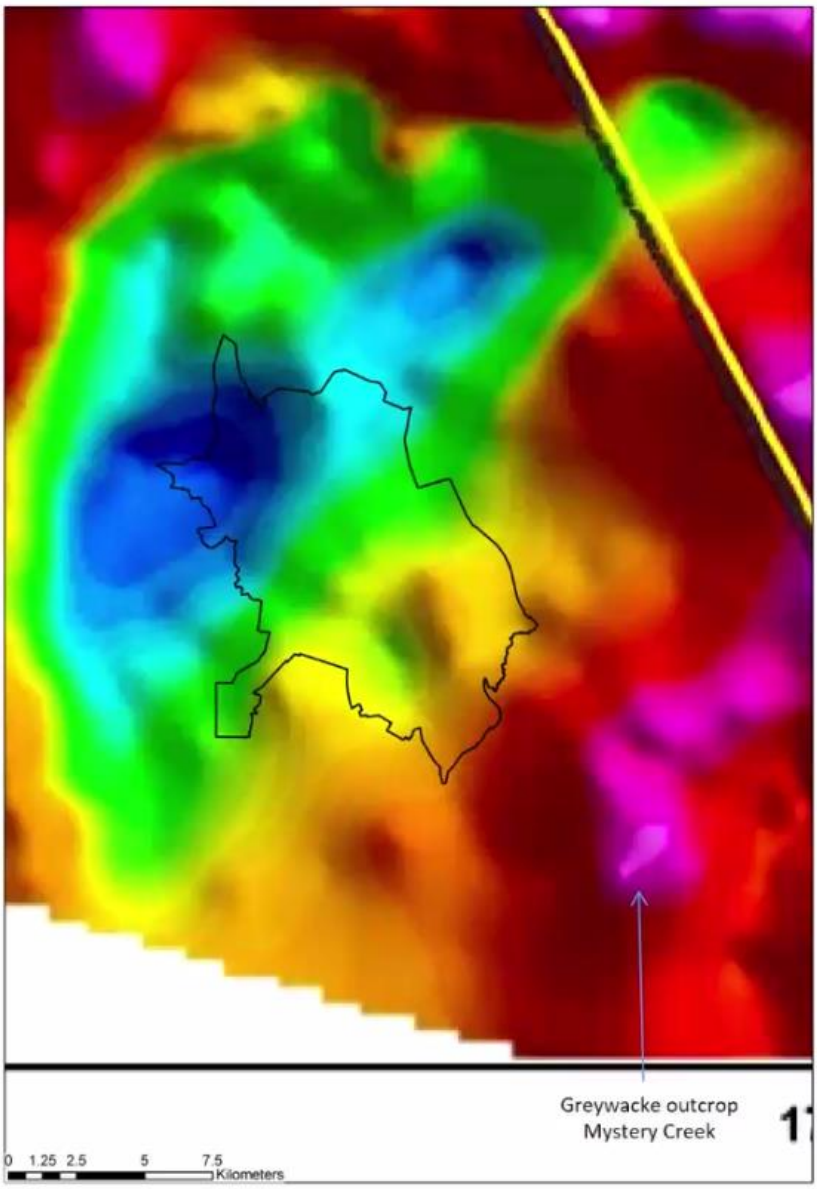

Figure 2.10 - Gravity anomaly map illustrating various depths within the Hamilton Basin. Shown in this image is areas of depression (cooler colours) in the NW of the Hamilton Basin, alongside an outline of the Hamilton City boundary (black). Image from Moon and de Lange (2017).

Seismic reflection was undertaken along the profile of the Waikato River, identifying some ~26 zones of interest. These zones of interest are thought to be faults or fault zones, due to distinctive deformation signatures. An image showing zones of interest is shown below in Figure 2.11.

Figure 2.11 - Zones of interest associated with tectonic deformation within the Waikato River. Image from Moon and de Lange (2017).

All of this information was then compiled to generate a map illustrating various fault zones, alongside the confidence of said faults. This map, shown in Figure 2.12, shows known faults in orange, inferred faults in white, and possible faults in yellow.

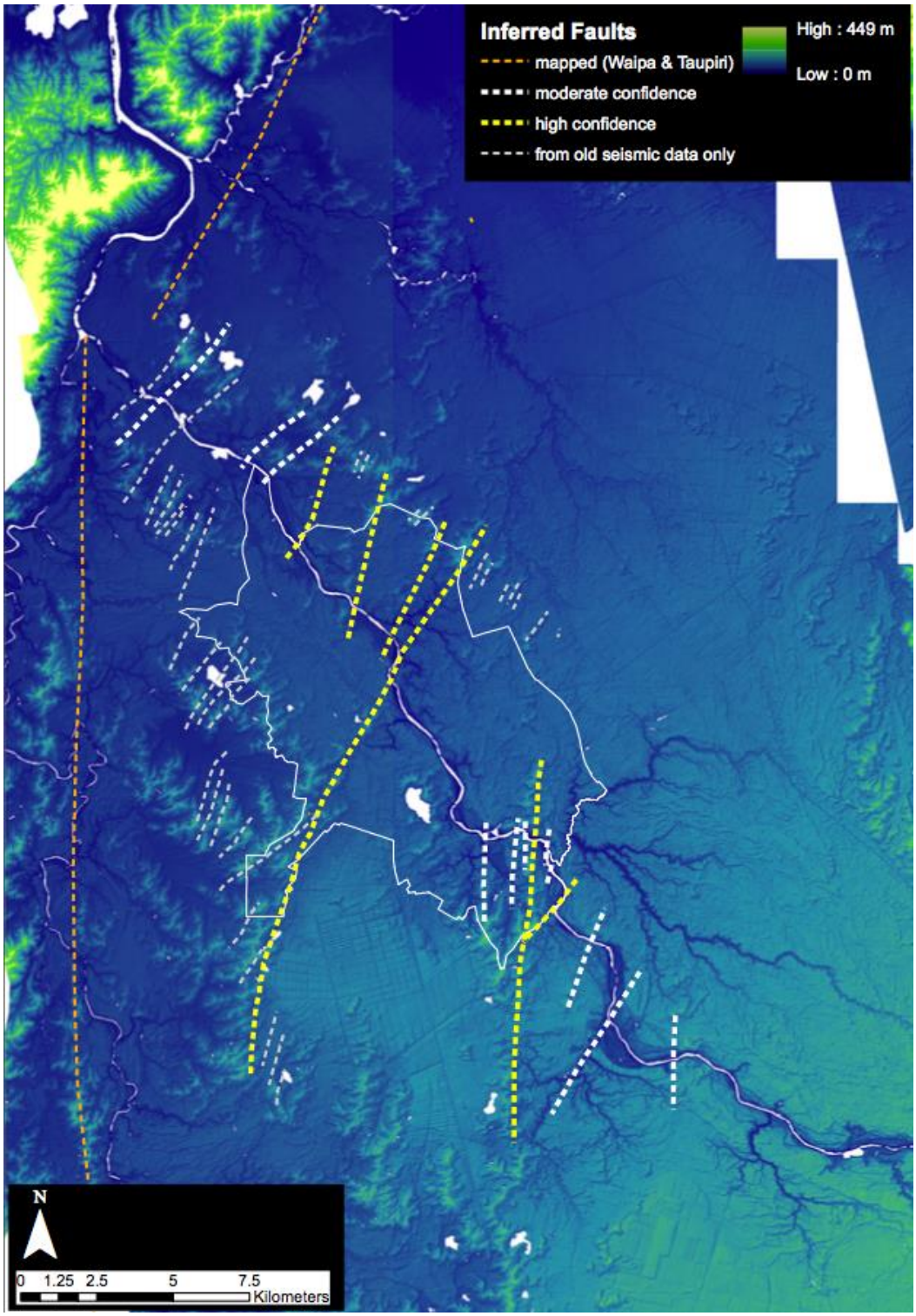

Figure 2.12 - Map summarizing current knowledge of the Hamilton Basin. Shown in this image are known, inferred and possible faults. Image taken from de Lange & Moon, 2017.

A recent influx of information regarding the Hamilton Basin has been observed since initial discoveries in 2015. Consequently, multiple theses investigating the Hamilton Basin are being prepared. Although unpublished at the time of this

investigation, work by McKay (2017) and Spinardi (2017) discussing deformation within the Hamilton Basin is currently being produced.

2.10 National Seismic Hazard Model

Currently the seismic hazard within the Hamilton Basin is considered minor, with no active faults recognised within the basin (Stirling *et al.*, 2012). Current faults known near the Hamilton Basin are illustrated in Figure 2.13.

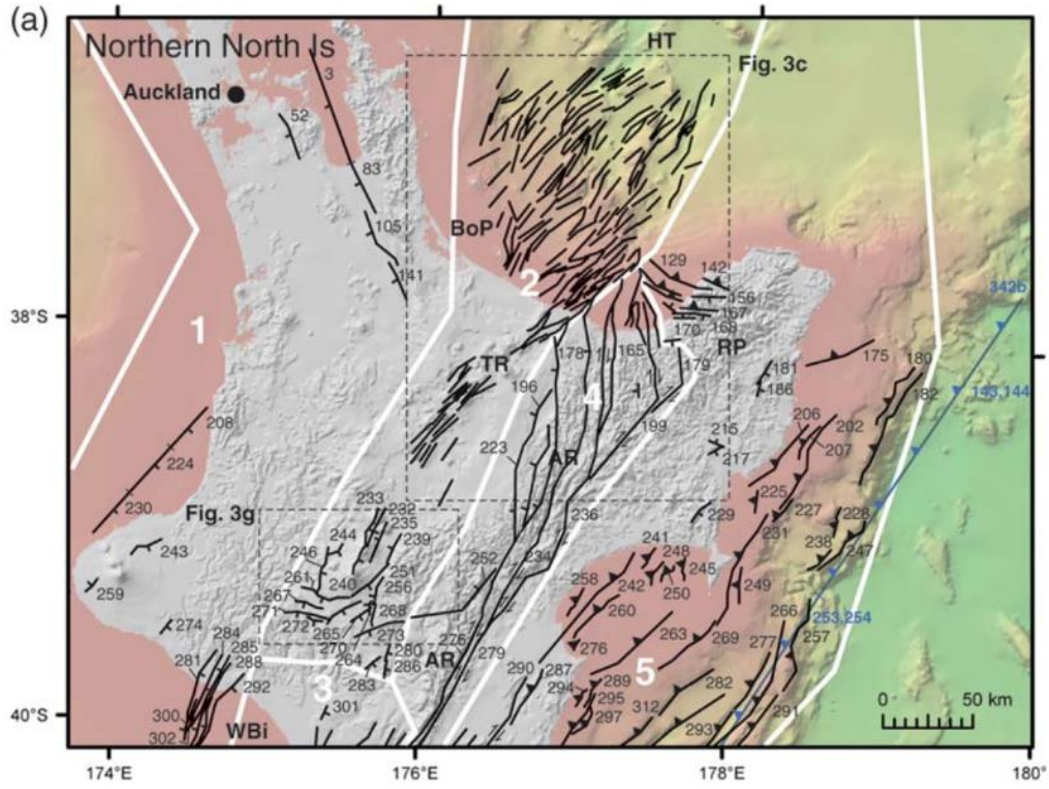

Figure 2.13 - showing known faults within the North Island, New Zealand. Image taken from Stirling *et al.* (2012).

Claims that the Hamilton Basin is an area of low seismicity are somewhat un-justified as aforementioned evidence by Kleyburg (2015), and Moon and de Lange (2017), alongside an investigation by Spindardi *et al.* (2017 (In Press)) that indicates faulting has occurred within the previous 125, 000 years. More evidence is needed to define the seismic hazard present however, as huge areas of the Hamilton Basin remain undescribed in terms of tectonics. The extent of the current knowledge gap is shown in Figure 2.14, which illustrates where paleoseismic investigations have occurred within New Zealand. As shown in this image, vast areas of the Hamilton Basin are largely unexplored.

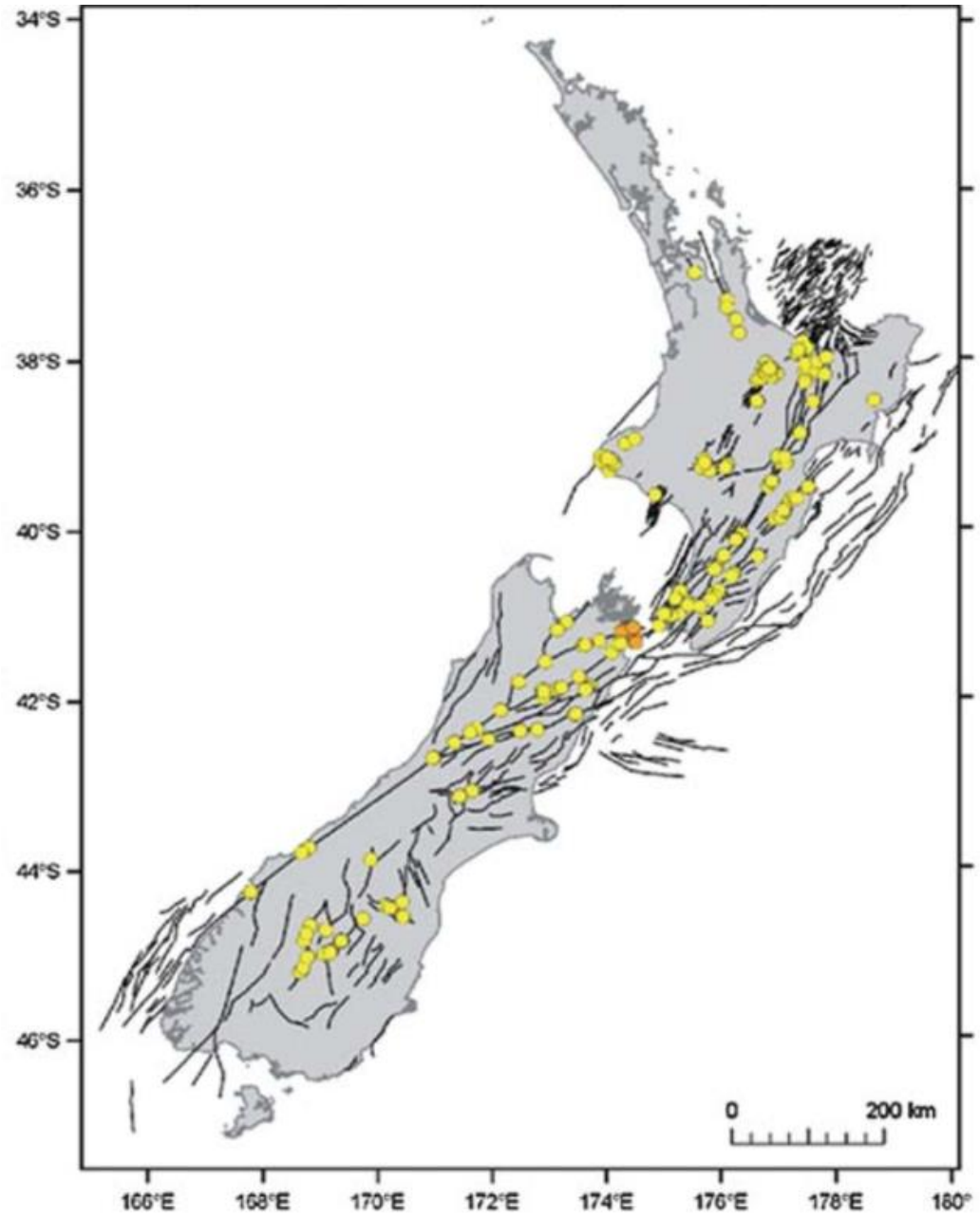

Figure 2.14 - Image of the Hamilton basin, illustrating where known studies have occurred in the Hamilton Basin. Image from Stirling *et al.* (2012).

Consequently, we recognize that a major knowledge gap regarding seismic hazard in the Hamilton Basin exists.

2.11 Summary

Literature regarding the Hamilton Basin is dated, and contains several major knowledge gaps, particularly regarding the presence of tectonic deformation within the Hamilton Basin. After reviewing literature, it is widely accepted that the Hamilton Basin has not itself been affected by tectonic deformation, only the surrounding region.

Recent discoveries however challenge these previously accepted hypothesis, and suggest that the Hamilton Basin is far more complicated than previously thought. Even in preliminary research phases, extensive evidence has been found that suggests faulting is present within the Hamilton Basin. Consequently, investigations conducted during this project, alongside studies completed by Kleyburg (2015), McKay (2017), Moon and de Lange (2017), Spinardi (2017) and Spindardi *et al.* (2017 (In Press)) aim to improve understanding of the Hamilton Basin, better identifying the extent of tectonic deformation, characterising movement that has occurred, alongside establishing the modern day risk.

Chapter 3

Methods

3.1 Introduction

The identification and characterisation of fault zones requires extensive field work. This chapter outlines research methods undertaken at both field sites involved in this investigation, alongside data processing methods. Geomorphic mapping, auger hole description and resistivity survey techniques are outlined for the Osborne Road field site, and facies description, structural data collection, mapping and modelling techniques used at the Kay Road field site are described.

3.2 Site selection

All field investigations took place within the Waikato Basin, New Zealand. The Kay Road field site was created when recent cuttings developed as part of the Hamilton Bypass portion of the Waikato Expressway were opened, exposing a complex fault zone through a hill. Located near the northern boundary of Hamilton City (37°42’40” S, 175°15’25” E (WGS84)), the site consisted of a deep cutting running approximately normal to the strike of the ridgeline, creating two exposures of the fault zone, one each side of the cutting. To the west of the ridgeline, an 85 m long by 35 m high embankment was exposed. Running parallel to the east, a 70 m long by 30 m high exposure was also uncovered. Two smaller faces to the south of the aforementioned faces were also exposed and studied at the Kay Road field site.

A second field site was identified for this investigation, and was located at Osborne Road (37°42'17.98"S, 175°14'10.74"E (WGS84)) near the northern boundary of Hamilton City (Figure 3.1). The site was first identified through study of LiDAR (light detection and ranging) data from the region. Study of LiDAR data illustrated a relationship between offset drainage patterns and ridgelines running through the Hamilton Basin, which coincide with a number of right angle bends in the Waikato River. A small offset can be traced across a number of paddocks at Osborne Road, exposing the inferred fault scarp. Consequently, Osborne Road was identified as a

particular zone of interest and a suitable field site. The locations of both the Kay Road and Osborne Road field sites in relation to northern Hamilton City are illustrated below in Figure 3.1.

Figure 3.1 - Satellite image illustrating the Kay Road and Osborne Road field sites. From Google Earth, 2017.

3.3 Methods

3.3.1 Site walkover

Field investigations at Kay Road began with a site walkover. During this walkover r, all exposed faces were observed alongside the general geomorphology of the field area. Exposed faces to be studied were then identified and named once a general feel for the site had been obtained. Exposed faces were named the North East (NE), North West (NW), South East (SE) & South West (SW) faces, relative to the approximate direction the expressway runs (Figure 3.2). Initial observations of the field site suggested that the Kay Road field site had experienced complex deformation. Therefore, understanding how the exposed faces relate to each other was essential during the site walkover. Photographs of the field area were then taken, and any deformation signatures were noted. An image showing the field site with pins depicting the four studied faces is shown below in Figure 3.2.

Figure 3.2 - A satellite image of the Kay Road field site. Detailed in the image are the four faces studied, along with directions of reference points. Image from Google Earth, 2017.

3.3.2 Field sketches

Field sketches of all faces were firstly drawn. This was done in an attempt to understand the overarching geology of the field site. Each face was then measured and scaled intervals were marked on the faces using spray paint. Depending on the accessibility and location of each of these faces, measurement markers ranged between 0–5 m interval marks across each face. These intervals were determined by the overall size of each face studied, and which scale was deemed most appropriate. Where suitable, horizontal level lines were constructed as reference points using nails and fluoro nylon builders line. Tape measures were then used to provide vertical and horizontal distance information about each of the faces. Graph paper was used to depict scaled down versions of the faces as accurately as possible. Noted in these sketches were changes in strata alongside structural observations and features. These sketches were drawn as close to scale as possible.

3.3.3 Unit descriptions and noting of anomalies

Geologic units and their boundaries were described. A Niwashi hand tool was used to clean representative areas and boundaries in the field. General unit descriptions were then undertaken using a template outlined by the New Zealand

Geotechnical Society (NZGS, 2017) whereby soil fraction, colour, structure, strength, moisture, bedding, plasticity and sensitivity were described. Each unit was then named, recorded and then labelled onto field sketches. Anomalies within the field area were then noted, including, but not limited to pinchouts of units, intrusion structures, tilting of beds and offset. Where it was clear that discernible offset had occurred, apparent offset was measured, recorded and transcribed onto corresponding field sketches.

3.3.4 Structural information

Dip and dip direction were recorded for bedding contacts, faults and anomalies at the Kay Road field site. Measurement of this structural information was recorded using GeoID, an IOS mobile application. Dip and dip direction were recorded in a style that best represented structural information of each feature, with each measurement recorded using a consecutive numbering system. These numbers were then added to field sketches so that each dip and dip direction could be recorded without field maps appearing too clustered. Field notes with the location of where structural information is attached as Appendices D (NW face) and Appendices J (NE face).

3.4 Kay Road processing methods

3.4.1 Digitising of maps

After field sketches were constructed in the field, they were converted into digital format, and field photographs were imported into Adobe Illustrator. Through the combination of photographs and field sketches, digital cross sections were created. These cross sections detailed faults, unit boundaries, and the dimensions of each face. These cross sections were drawn using the pen tool in Adobe Illustrator. Appropriate units were then added to the cross sections, alongside distance and location information, and legends defining annotations.

3.4.2 Geologic modelling

Geologic modelling of the Kay Road fault zone was undertaken using Leapfrog Geologic Modelling Software®. Firstly, digital cross sections constructed in Illustrator were imported into LeapFrog, and location parameters were entered. Conversion of GPS coordinates from WGS 1984 to NZTMP was required, and this

was carried out using the free LINZ converter website (http://apps.linz.govt.nz/coordinate-conversion/). Elevation data were then entered, and functional cross sections were generated. Once cross sections were to scale, a geologic modelling boundary was defined. Polylines were then drawn on each digital cross section to differentiate each lithology, and faults were then sketched as polylines. Fault polylines were categorized accordingly to differentiate them from polylines separating each lithology. Structural data points obtained in the field using GeoID were then added to respective locations on each cross section. Once structural data had been added, polylines and structural data were combined to generate meshes representing both the top and bottom contacts of each lithology.

A geologic model was then generated using fault planes and meshes. This produced an initial crude geologic model. Fault relationships, fault interaction and fault terminations with one another were then defined, generating a number of fault blocks within the model. Once these blocks had been defined, lithologies and structural relationships were entered for each block generated in the model. Topographic information was added, and preliminary models were constructed for both the NW and NE faces. Refining of models occurred continually until the Kay Road fault zone was modelled as accurately as possible.

3.5 Osborne Road Methods

3.5.1 Site walkover and geomorphic mapping

Research at Osborne Road also began with a site walkover. During this site walkover, the geomorphology of the field site, drainage networks and the inferred fault scarp were studied. An image illustrating the studied field area is shown below in Figure 3.3.

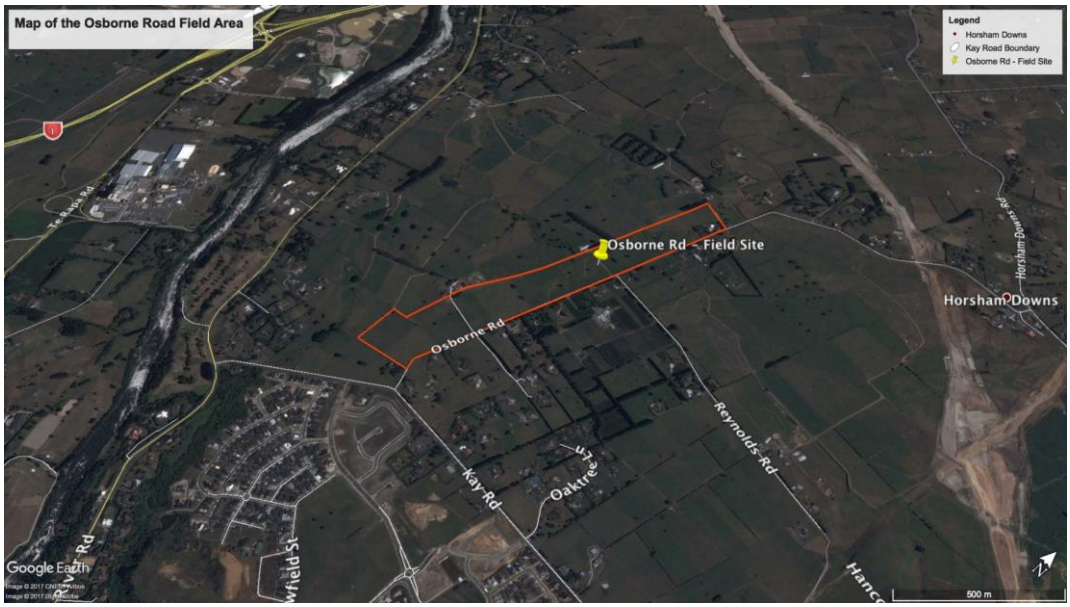

Figure 3.3 - Satellite image of the Osborne Road field site. The field site is contained within the red polygon. Image taken from Google Earth, 2017.

Once a site walkover had been undertaken, detailed geomorphic maps of the field site were created. LiDAR data and satellite images were prepared at a scale of 1:2500 in ArcMap, and were then printed. Using these base maps, a second site walkover was undertaken and surface geomorphology was recorded onto these base maps. Symbols used to describe the Geomorphology are provided below in Figure 3.4. Once field maps had been sketched, they were combined with LiDAR information, and satellite images of the Osborne Road field site were annotated. Using ArcMap, digital geomorphic maps were created.

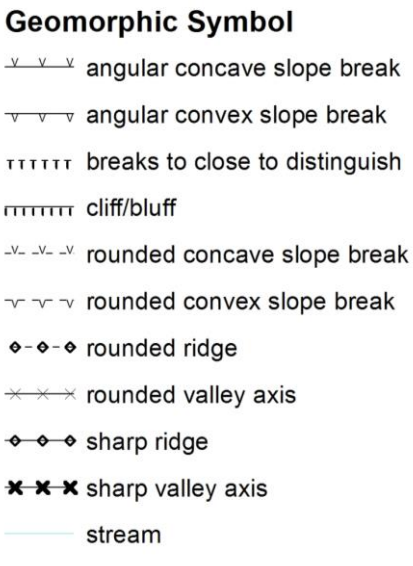

Figure 3.4 - Geomorphic symbols used for field mapping.

3.5.2 Soil Auger Sampling

Two soil auger transects were taken along the same line at the Osborne Road field site. The first was a 65 m transect extending east (E2707432, N6386163 (WGS 1984)) to west (E2707369, N6386177 WGS 1984)), with soil auger samples taken at 5 m intervals to a depth of 1.6 m. This was done using a Dutch auger with the same head as shown in Figure 3.5 (A), however this auger was slightly longer than that pictured (1.6 m). The head of the Dutch auger used was 50 mm by 185 mm. Each soil auger hole was described and photographed and descriptions were recorded onto field sheets. A second round of augering was then conducted using a telescopic 6 m long Dutch auger, with a head 50 mm by 185 mm Figure 3.5 (B). An image of the soil auger used is illustrated below in Figure 3.5 (C).

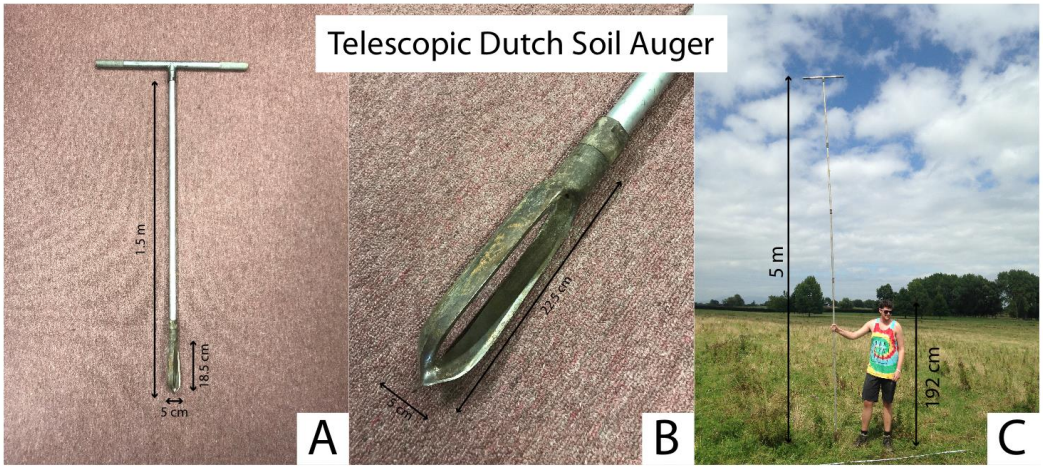

Figure 3.5 - Image of the telescopic Dutch soil auger used for soil sampling within the Osborne Road field site.

These auger holes were drilled at the 5 m, 30 m and 50 m marks of the previous profile line East (E2707432, N6386163) to west (E2707369, N6386177), however, due to inclement field conditions the sampled hole depth varied. As with the first round of augering, each soil auger hole was then logged, with photographs and descriptions of findings noted. The same soil description template outlined by NZGS (2017) was used to describe units at Osborne Road as was used at Kay Road. The line of the sampled soil auger transect with the location of deeper m auger sample holes marked is shown in Figure 3.6.

Figure 3.6 - Satellite image of the Osborne Road field site. Shown in the image is the transect of 5 m augers (yellow line), and the location of 3 deep auger holes. Image from Google Earth, 2017.

3.5.3 Soil resistivity surveys

Soil electrical resistivity surveys are a non-invasive method that can help improve understanding of spatial and temporal variability, alongside structure, water content and fluid composition of soils. Because the method is non-destructive, and very sensitive to changes within soils, it is an attractive tool that can help describe subsurface properties without digging (Samouëlian *et al.*, 2005). Electrical resistivity surveys determine the resistivity distribution of the surrounding soil volume. This involves generating artificial electric currents which are supplied to the soil. The resulting potential differences are measured, which in turn provide information on the form of subsurface heterogeneities and other electrical properties (Samouëlian *et al.*, 2005; Kearey *et al.*, 2013). Typically, soil electrical surveys can be performed in one, two or three dimensions, at centimetre scales to regional scales.

Soil resistivity measurements were conducted at Osborne Road using a SuperString R8 with a 28 electrode switch box made by Advanced Geosciences Inc. (AGI). Initial surveys were roll-along to 67 m, whereby multiple 15 m surveys were

taken with an electrode spacing of 1 meter used in a dipole-dipole array, and combined to generate a 67 m survey transect. Secondary surveys used an electrode spacing of 3 m, using a dipole-dipole with gradient array. All 28 electrodes were used to generate a quasi 3D survey, whereby multiple 2D surveys were taken parallel to each other, then combined into a 3D data set. Instrument settings were at factory defaults. An image showing the location of soil resistivity surveys is shown in Figure 3.7.

Figure 3.7 - Satellite image of the Osborne Road field site, illustrating the location of soil electrical resistivity surveys. An initial 2D Survey was conducted at the same location as soil augering, and a second round of electrical resistivity surveys to generate a 3D model was taken along pink lines (67 m). Image from Google Earth, 2017.

3.6 Osborne Road processing methods

3.6.1 Soil auger data processing

Data from Osborne Road were digitized for clarity. The first round of auger data was processed in Adobe Illustrator. Individual soil profiles were sketched from each auger hole, and then a working cross section of auger holes was generated to illustrate the change in soil type across the Osborne Road soil sample transect. To generate this fence diagram, a scaled elevation profile of the transect was created in ArcMap. This was then traced in Adobe Illustrator, and formed the basis

of the working profile. Soil logs sketched in Adobe Illustrator were then placed in their respective positions along the soil sampling transect. The second round of processing involved data obtained from 6 m auger samples, and was also completed in Adobe Illustrator. This involved digitizing soil logs and refining descriptions taken in the field to align with the NZGS template.

3.6.2 Resistivity data processing

Following resistivity surveys, data were processed using EarthImager 2D and EarthImager 3D software. JPEG images of surveys were then generated at various angles to best illustrate survey results. Data processing generated a number of 2D and 3D images that showed various perspectives.

Chapter 4

Results - Kay Road

4.1 Introduction

The Waikato Expressway is a key strategic transport corridor for the Waikato, connecting the region to both Auckland and the Bay of Plenty regions. Spanning approximately 102 km throughout the central North Island, the Waikato Expressway project has involved large scale earthworks throughout the greater North Island, offering a unique insight into the geology of the Waikato region through large scale earthworks. At the time of this investigation, a large cutting (Kay Road cutting) through a hillslope near the boundary of northern Hamilton was occurring. This hillslope aligned with a ridgeline running through the Hamilton Basin, thought to be an area of tectonic deformation.

Although the Kay Road field area was not initially the focus of this investigation, preliminary site investigations at the Kay Road cutting showed clear tectonic deformation of geological strata. Discussion between geologists working onsite for Coffey Geotechnics, the New Zealand Transport Authority (NZTA) and the University of Waikato then occurred, and permission to access and undertake a site investigation within the Kay Road portion of the Waikato Expressway project was granted.

The scale of earthworks involved in Waikato Expressway project is best shown by Figure 4.1 which shows a satellite image of the Kay Road field area prior to construction of the Waikato Expressway (2014), and Figure 4.2 which shows a more recent image of the Kay Road field area during construction of the Waikato Expressway. As shown in Figure 4.1, the Kay Road field area was once a region of hilly topography. Figure 4.2 illustrates the extent of earthworks that have taken place in the Kay Road portion of the Waikato Expressway, and illustrate the drastically different topography.

Figure 4.1 - Satellite image of the Kay Road field area in 2014, prior to excavation of a hill slope for construction of the Waikato Expressway.

Figure 4.2 - A more recent satellite image of the Kay Road field site during construction of the Waikato Expressway. Shown in the image are the significant earthworks that have taken place during the construction of the Waikato Expressway project. Image taken from Google Earth, 2017.

A map generated in ArcMap using LiDAR information is shown below in Figure 4.3. Figure 4.3 illustrates the location of the Kay Road field site in relation to one another, alongside the location of field site in relation to the Hamilton City boundary. A ridgeline that can be traced through both a 90° bend in the Waikato River and the Kay Road field site is also depicted.

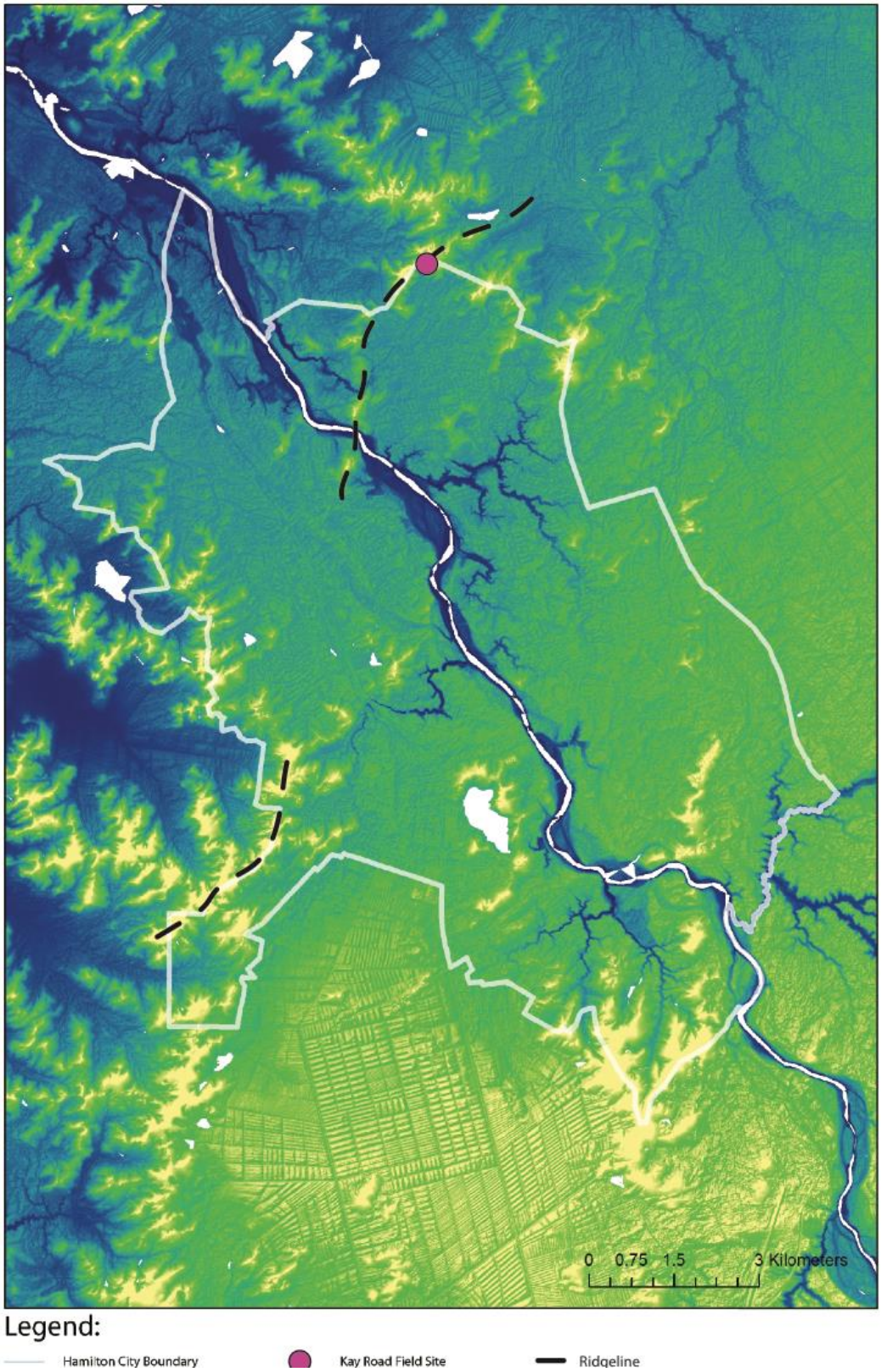

Figure 4.3 - LiDAR map illustrating the location of Kay field site. Shown in a faint white outline is the Hamilton City Boundary. Running through the centre of the image is the Waikato River, marked by a solid white channel.

This chapter details the observations of the Kay Road field area, alongside presenting results from this investigation.

4.2 Kay Road field site

The Kay Road field site runs approximately perpendicular to the strike of a ridgeline running through the Hamilton Basin (Figure 4.3). At the time of this project, construction of the Waikato Expressway had exposed significant deformation of units within a hill section. These units ranged from the most recent Hamilton Ash Series, with youngest members dated between c. 0.18 Ma and c. 0.08 Ma, to the much older Walton Sub-group (1.8 ma) (Lowe *et al.*, 2001; GNS, 2017d).

4.3 Face descriptions

Investigations commenced with general detailing of the four identified faces (NW, NE, SW, SE). This included recording location parameter, measuring the horizontal and vertical extent of each face, and measuring the angle at which each face was cut. Initial field sketches are presented in Appendices A – Q.

4.3.1 NW exposure

The NW field site was the largest exposure in the field area, at 80 m long by 30 m high. The face was cut at a 57° angle, and was located at 37°71'09" S, 175°25'68"E (WGS84). The exposure was diverse in geology, containing members from the Hamilton Ash Series, Puketoka Formation and the Karapiro Formation. Various weathered tephra units were also found within the NW face. A photograph of the NW face is shown below in Figure 4.4.

Figure 4.4 - Photograph of the NW face. Pictured to the far left (above digger) is the upper extent of the SW face.

4.3.2 NE exposure

The NE face was located at 37°42'36.2"S, 175°15'27.0"E (WGS84). At 30 m high by 70 m wide, the NE face was slightly smaller than the NW face. The NE face was the most recent cutting in the Kay Road field area, and was cut at a 42° angle. Similar

to the NW face, the NE face contained members of the Hamilton Ash series, Kauroa Ash Formation, Karapiro Formation and Walton Sub-group. A photograph of the NE face is depicted below in Figure 4.5.

Figure 4.5 - Photograph of the NE face. On the right of the image, the highest point of the lower lying SE face can be seen.

4.3.3 SW exposure

The SW face was 6 m high by 16 m wide. The exposure was located at the 37°42'39.2"S, 175°15'25.9"E (WGS84), and was cut at a 50° angle. The SW face contained many variations of the Walton Sub-group, with some topsoil observed in the upper extent of the profile. The SW face appeared to be continuous with the lower lying units of the NW face. An image of the SW face is shown below in Figure 4.6.

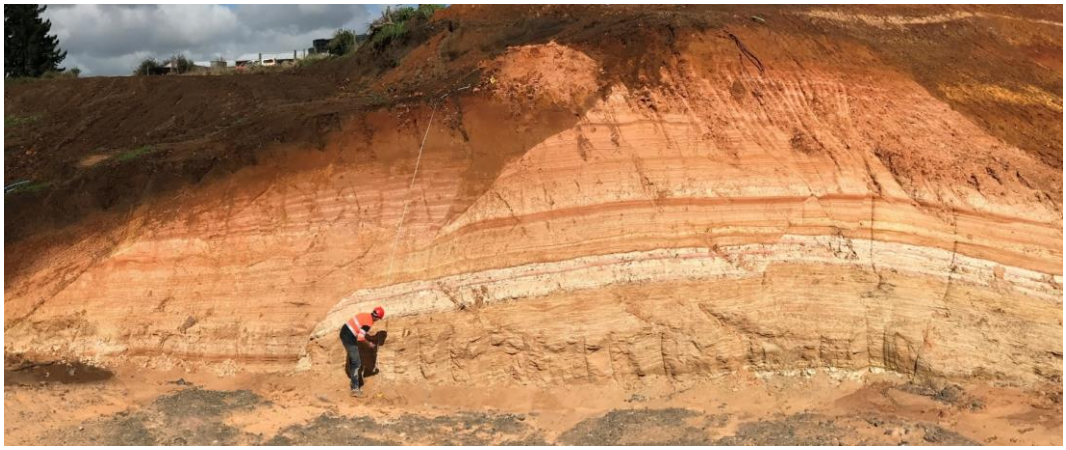

Figure 4.6 - Photograph of the SW face.

4.3.4 SE exposure

This SE face was located at the coordinates 37°42'39.6"S 175°15'28.8"E (WGS84) and was somewhat continuous with lower layers of the NE face. The exposure was

largely comprised of silts and clays, and showed evident offset within iron stained layers in the face (Walton Sub-group). The face exposure was 8 m high, by 26 m wide, and was cut at a 50° angle. Figure 4.7 depicts a photograph of the SE face.

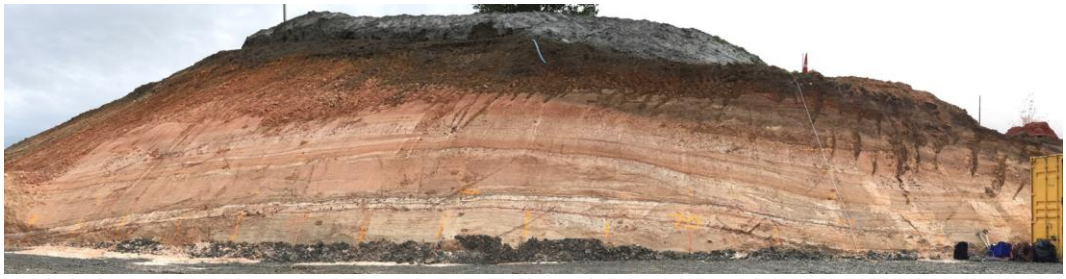

Figure 4.7 – Panoramic image of the SE face. In the top left of this image, the most southern extent of the NE face can be seen.

4.4 Unit descriptions

The field area was comprised of a variety of sands, silts and clays from both alluvial and volcanic origins. Units found within the field area were members of the Hamilton Ash Formation, Kauroa Ash Formation, Karapiro Formation, Puketoka Formation, alongside some slight variations of these formations. Both the Karapiro Formation and the Puketoka Formation form the Walton Sub-group, as per literature regarding the Hamilton Basin, however, the Karapiro Formation is presented as its own unit in this section. Descriptions of each of the units, and observed variations found within the field, are detailed below in Table 4.1. Unit descriptions of lithologies found within the NW of the field area, whereby informal unit identifiers specific to this study are described. These descriptions were taken using a general template outlined by the NZGS (2017).

Table 4.1- Unit descriptions of lithologies found within the field North West field area

Unit ID	Name	Description	Formation
T1	Topsoil 1	CLAY with minor silt. 10 YR 5/6 yellowish brown, slightly moist. Surficial organic soil layer that may contain living matter. Rootlets present in the top of the unit.	Topsoil

T2	Topsoil 2	CLAY with minor silt. 10 YR 5/8 yellowish brown. Slightly moist. Surficial organic soil layer that may contain living matter	Topsoil
R	Rangitawa Tephra	CLAY. 7.5 YR 7/1. Light brownish grey. Moist. Micaceous flakes present. Moderately plastic when wet. Weathered pumice present.	Hamilton Ash Series
WT1	Weathered tephra (Variation 1)	Clayey SILT. 7.5 YR 4/8 Brown. Unit grades down into lighter coloured 10 YR 6/4 dull yellow orange. Dry, stiff, moderately plasticity when wet.	Hamilton Ash Series
WT2	Weathered tephra (Variation 2)	SILT. 5YR 5/8 Bright reddish brown. Quartz and Manganese present. Weathered ignimbrite.	Hamilton Ash Series
K	Kauroa (Gold Paleosol)	Clayey SILT. 10 YR 8/6 Yellow Orange. Highly plastic. Moist. Weathered pumiceous nodules present.	Kauroa Ash Formation
K1	Karapiro (Variation 1)	Sandy CLAY. 5 YR 7/6 Orange. Slightly plastic. Manganese present alongside weathered pumice. Quartz, mica flakes, and heavy iron staining present.	Karapiro Formation
K2	Karapiro (Variation 2)	Sandy CLAY. 5 YR 6/8 Orange. Slightly plastic. Manganese present alongside weathered pumice. Quartz, mica flakes, strong iron staining.	Karapiro Formation
Intrusion Structure	Intrusion	Clayey SILT with sand minor. 10YR 7/8 Yellow orange. Lithics and crystals	Karapiro

		present within the unit. Very moist. Very sticky and somewhat plastic.	
W1	Walton (Variation 1)	Clayey SILT with trace sand. 7.5 YR 8/3 Pale yellow. Highly plastic. Wet. Heavy iron staining forming distinctive beds.	Walton Sub-group
W2	Walton (Variation 2)	Sandy CLAY. 2.5 Y 8/3 Pale yellow. Plastic. Muscovite and Quartz present. Pumiceous origins with some lithics.	Walton Sub-group
W3	Walton (Variation 3)	Silty CLAY. 2.5Y 8/2 Light Grey. High plasticity. Manganese staining, fine grained. Iron mottles and nodules present	Walton Sub-group
W4	Walton (Variation 4)	Clayey SILT. 2.5Y 8/6 Bright yellowish brown. Moist. Highly plastic. Muscovite and Manganese nodules present within the unit.	Walton Sub-group
W5	Walton (Variation 5)	Sandy CLAY. 7.5 YR 5/6 Bright brown. Highly plastic. Weathered pumice present in the unit.	Walton Sub-group
W6	Walton (Variation 6)	SILT with clay fraction. 7.5 Y 8/1 Light grey. Minor iron staining. Highly plastic. Pumiceous origins.	Walton Sub-group
Sp	Spoil	This unit was disturbed, and therefore could not be accurately described.	NA

4.5 Study area interpretations

The following section describes observations made within the Kay Road field site regarding each of the studied exposures. Each of the following sub-sections contains a digital cross section, illustrating the distribution of each of the relevant

units outlined Table 4.1. These are presented as Figure 4.8 to Figure 4.11, which illustrate the general distribution of units observed at each face. In these cross sections, fault planes are detailed with red lines.

4.5.1 NW face

The NW face contained the most diverse distribution of units within the Kay Road field area, and included formations ranging from the oldest Walton Sub-group to the most recent Hamilton Ashes. The south of the NW exposure was dominated by the Walton Sub-group, which is the oldest unit found within the field area. The Walton Sub-group exhibited obvious banding from iron staining; meaning offset within the unit was easily recognisable. Overlying the Walton Sub-group, various units were found irregularly distributed within the face. The lowest unit observed was weathered tephra 2 (WT2), which was distributed in 3 distinctive blocks. Within this unit, a number of intrusion-like structures were present, including a 100 mm wide sand channel running through the Karapiro Formation in the north of the NW face, alongside a small, liquefactions like intrusion structure Figure 4.25. The material found in this structure appeared to share characteristics with weathered tephra 1 (WT1). Younger units overlying the WT2 formation were the obviously deformed Kauroa beds. These beds exhibited significant deformation, appearing both tilted and rotated in an offset, repetitive pattern throughout the face. Blanketing these deformed units include a WT1 which does show offset, and the undisturbed Rangitawa tephra which was deposited 0.35 ma (Lowe *et al.*, 2001).

A number of blocks are found within the NW face; most of which exhibit some sort of deformation. The northern half of the NW face appears somewhat more complex than the southern half, with a definitive break in lithologies apparent. This is perhaps best indicated by the sharp boundary between WT1 and the Karapiro Formation.

Oldest units within the north of the NW face are the Karapiro Formation (K1), alongside more disrupted Kauroa Ash Formation. These are all offset however by two significant wedge structures, which appear to belong to be similar in characteristics to the Karapiro Formation, however these formations were notably

different in colour. These wedge structures are observed in Figure 4.22, and also shown by a large triangular polygon in the northern most point of the Figure 4.8, as anomaly *1 in the right of the image. Blanketing this northernmost point of the NW face were two units; one deemed ‘spoil’, as it had been disrupted through earth works and consequently could not be defined, alongside the Rangitawa tephra. Soil augering samples taken within the zone of spoil suggested that the Rangitawa Tephra was continuous throughout the NW face, as it was sampled across a transect within the spoil zone.

Deformation within the NW face was immediately apparent with offset found throughout the majority of units in the NW of the Kay Road field area. Normal faulting was the primary means of offset identified, however, overarching deformation of the face is chaotic. An image shown below in Figure 4.8 illustrates the complex distribution of units within the NW Kay Road exposure.

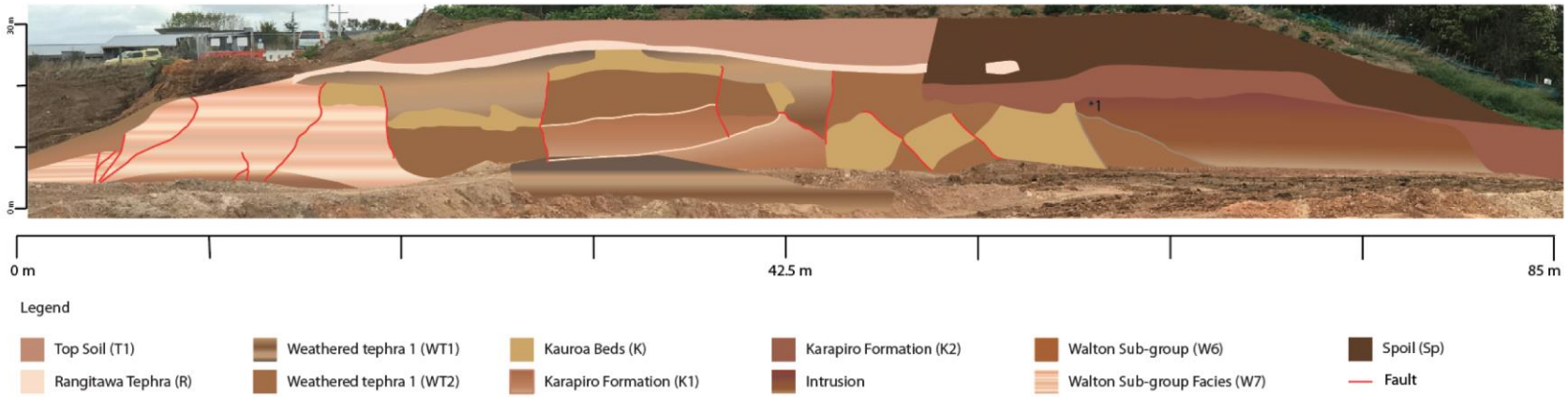

Figure 4.8 - Digital cross section of the NW face at the Kay Road field site. This cross section was generated in Adobe Illustrator, and combines digitally drawn polygons with a photo to best illustrate structural features and unit boundaries. Pictured in red are inferred fault lines.

4.5.2 NE face

The NE face had similar geology to the NW face, however the exposure was somewhat smaller, and appeared somewhat more simple. The oldest unit in the field was the Walton Sub-group. Banding was present in the unit making deformation obvious by means of steeply dipping normal faults, and associated offset bedding. These faults appeared steep in nature in lower units of the NE face, before shallowing out in younger sediments. This is thought to be attributable to soft sediment characteristics of the younger, overlying units (Karapiro Formation and younger variations of the Walton Sub-group).

Influenced by faulting were the multiple variations of the Walton Sub-group observed in the field area, alongside units derived from the Karapiro Formation (K1 and K2), the Kauroa beds and those members forming the Hamilton Ash Series. Units within the NE face appear to show signs of soft sediment deformation, including ragged boundaries and abnormal distribution patterns as shown in anomaly two (*2) in Figure 4.9. The Rangitawa Tephra was found undisturbed in the field area, blanketing deformation within younger, lower-lying units. An image illustrating observations of the NE face is shown below in Figure 4.9.

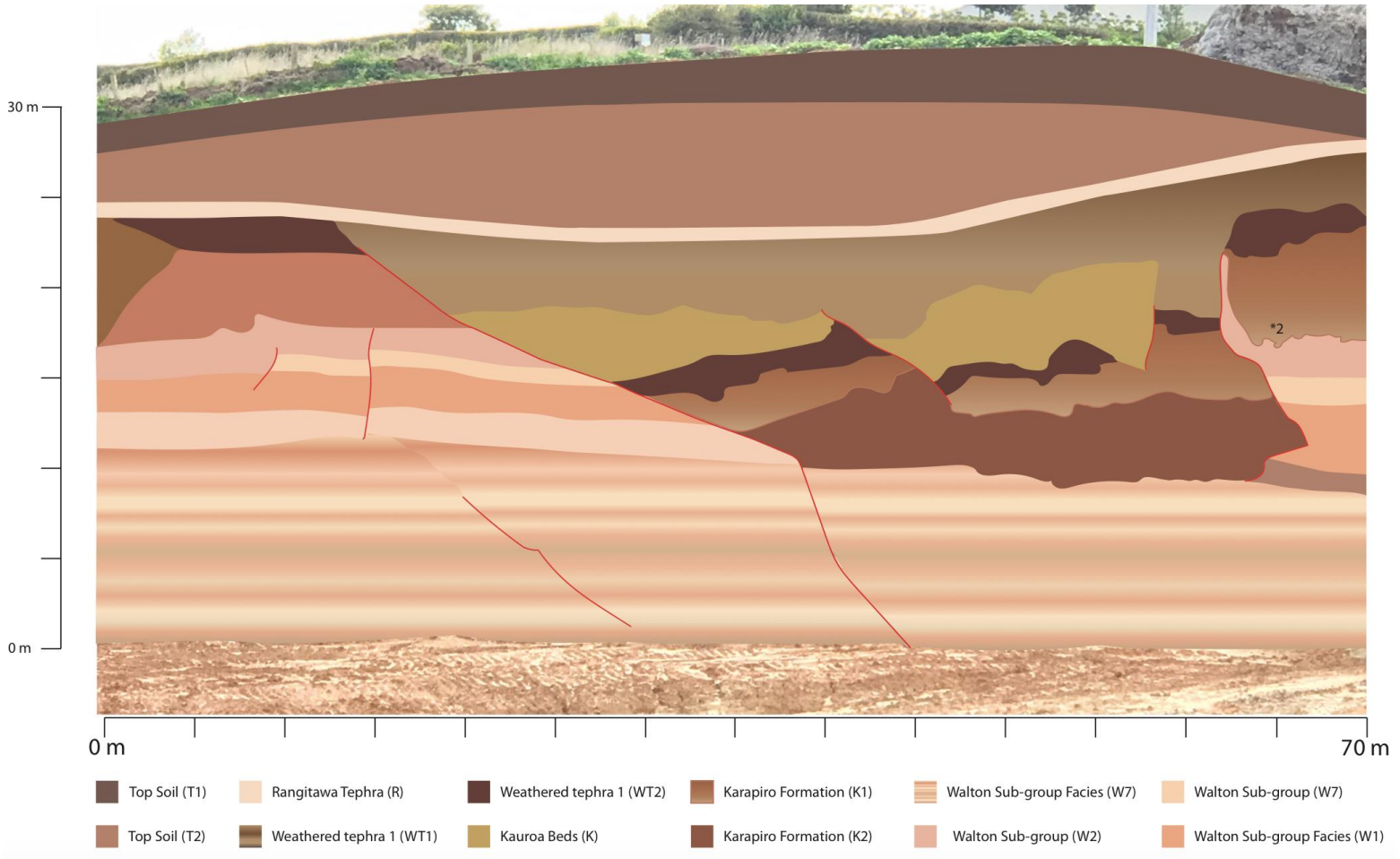

Figure 4.9 - Schematic illustrating structural features and unit distributions observed on the NE face

4.5.3 SW face

The SW face was dominated by variations of the Walton Sub-group. The northernmost part of the SW face was continuous with the NW face; however, unlike the NW face the SW face had relatively simple geology. Within the face, W1, W2, W3, W4, W5, W6 and W7 were recognised, alongside a generic top soil blanketing younger members of the Walton Sub-group at the top of the exposure.

Faulting was found within all of the aforementioned units, excluding the topsoil. These faults appeared normal in nature, resulting in overall down-throw of the southern block of the face. An image detailing units and their distribution within the SW face is shown below in Figure 4.10.

Similar to the NW and NE faces, the Walton Sub-group exhibited distinctive bedding.

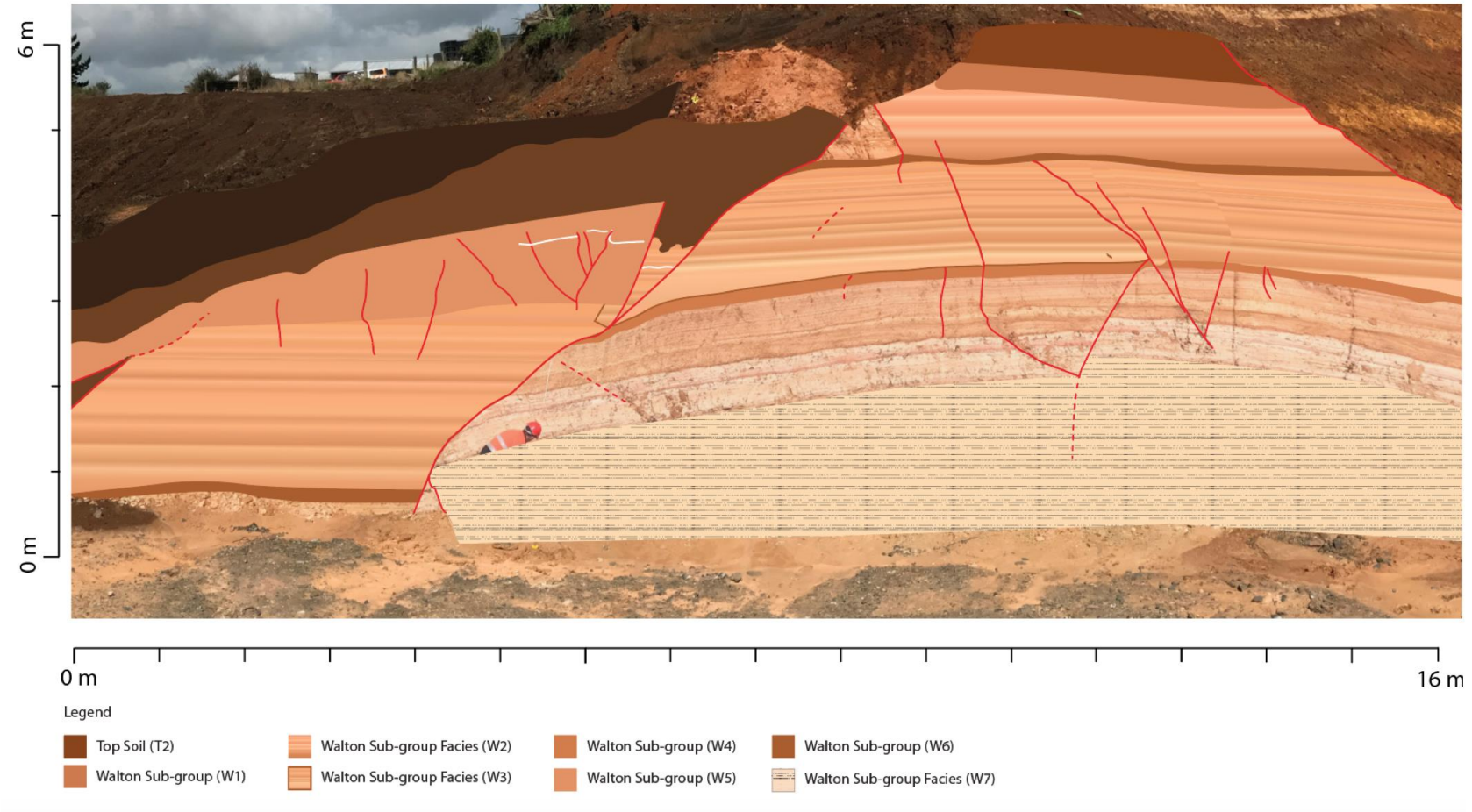

Figure 4.10 - A digital cross section of the SW face. This cross section was generated in Adobe Illustrator, and combines digitally drawn polygons with a photo to best illustrate structural features and unit boundaries. Pictured in red are inferred fault lines.

4.5.4 SE face

Similar to the SW Face, the SE face contained a number of variations of the Walton Sub-group. These included variations of the Walton group W1, W2, W3, W4, W5, W6 and W7, as described in Table 4.1.

Distribution of units within the SE face was uniform throughout the SE exposure, aside from where deformation was observed. Deformation was, like the other faces, made easier to recognize through banding within the Walton Sub-group units. Faulting was evident in the south of the SE face, with faults appearing normal in nature. These faults were steeply dipping, and appeared throughout the face. A cluster of normal faults was observed in the southernmost extent of the SE face.

Overall, the SE face had similar geology to that observed in the SW exposure at the Kay Road field site. An image of the SE face is shown below in Figure 4.11.

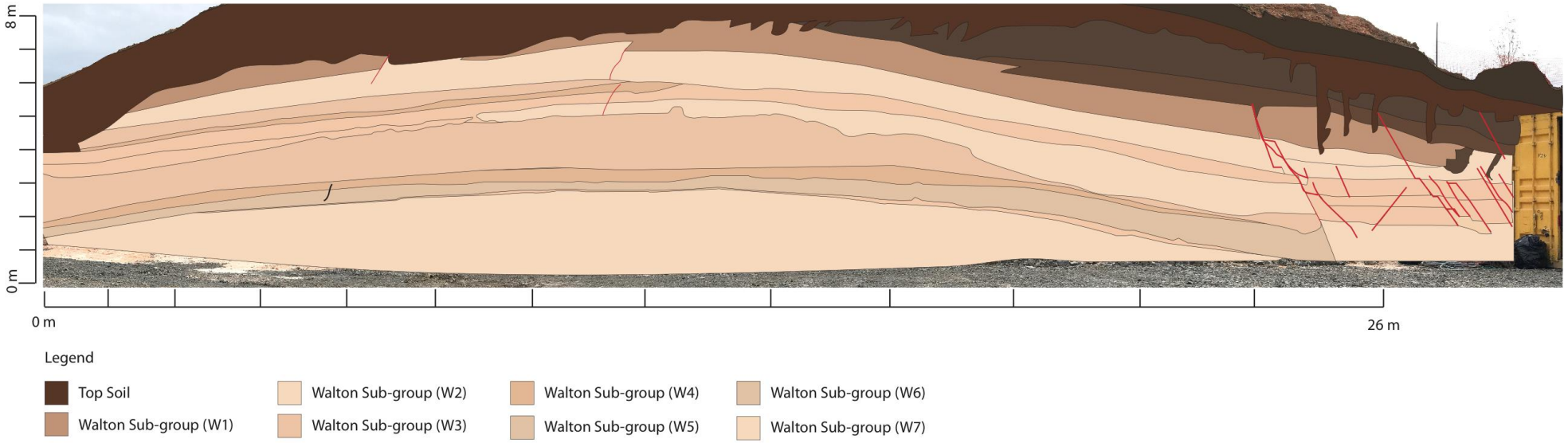

Figure 4.11 – Cross section of the SE face. This cross section was generated in Adobe Illustrator, and combines digitally drawn polygons with a photo to best illustrate structural features and unit boundaries. Pictured in red are inferred fault lines.

4.6 Structural information

Dip and dip direction of unit boundaries, and structural features were recorded in the field using GeoID. These measurements were then translated into a field note book alongside sketches to show the location of where structural information was obtained.

Structural information recorded on the NW face is outlined below in Table 4.2. The measurement number column relates to the numbers shown in Appendices D. The location column details the nature of the contact along which each dip/dip direction measurement was recorded, with direction and dip columns representing structural measurements.

Table 4.2 – Dip and dip direction measurements obtained from the NW face.

Measurement Number	Direction	Dip	Location
1	14	11	Base of Rangitawa
2	103	11	Weathered tephra under Rangitawa
3	117	7	Weathered tephra under Rangitawa
4	199	7	Weathered tephra
5	117	53	Weathered tephra
6	154	39	Karapiro Formation
7	163	38	Base of Kauroa
8	282	66	Fault plane
9	109	86	Fault plane
10	152	12	Karapiro
11	163	52	Base of Rangitawa
12	63	7	Weathered tephra
13	184	71	Weathered tephra/Kauroa
14	135	21	Kauroa/Walton Sub-group
15	140	42	Kauroa/weathered tephra
16	53	5	Karapiro

17	345	8	Fault plane
18	120	60	Fault plane
19	103	51	Fault plane
20	176	22	Weathered tephra/Kauroa Contact
21	175	29	Karapiro/weathered tephra Bed
22	169	37	Base of Rangitawa
23	177	57	Weathered tephra under Rangitawa
24	99	17	Weathered tephra/Rangitawa
25	108	9	Intrusion structure
26	135	8	Karapiro/Intrusion
27	93	8	Karapiro
28	53	10	Karapiro
29	163	13	Intrusion Within Karapiro
30	147	20	Intrusion Within Karapiro
31	12	23	Karapiro/Walton
32	22	35	Karapiro/Walton
33	207	43	Walton
34	188	16	Intrusion structure
35	248	79	Kauroa/Walton Sub-group
36	154	10	Top of Rangitawa
37	148	5	Rangitawa/Weathered tephra
38	186	6	Weathered tephra
39	254	20	Weathered tephra/Kauroa
40	279	60	Fault plane
41	275	45	Fault (Kauroa)
42	74	24	Fault (Kauroa)
43	100	6	Rangitawa Tephra
44	173	18	Weathered tephra

45	275	45	Weathered tephra/Kauroa
46	74	25	Karapiro formation
47	256	6	Intrusion Structure
48	335	2	Base of Rangitawa
49	222	25	Weathered tephra/Karapiro
50	71	31	Karapiro
51	74	32	Karapiro formation/Intrusion structure
52	260	26	Displaced block

A stereonet presenting structural data obtained in the NW face is shown in Figure 4.12. Important to note however is variation that was observed in measurements, as plotted by clusters in Figure 4.12, but all reflect an approximately N/S strike. The dip and dip direction of faulting in the NW face was 63°/280°, giving a strike of 010° which aligns with an inferred fault line offsetting the Waikato River. The fault angle measurements taken also align with observations made by Skempton (1966), who suggests that under near-perfect faulting conditions that failure angles (dip) typically range around ~60°.

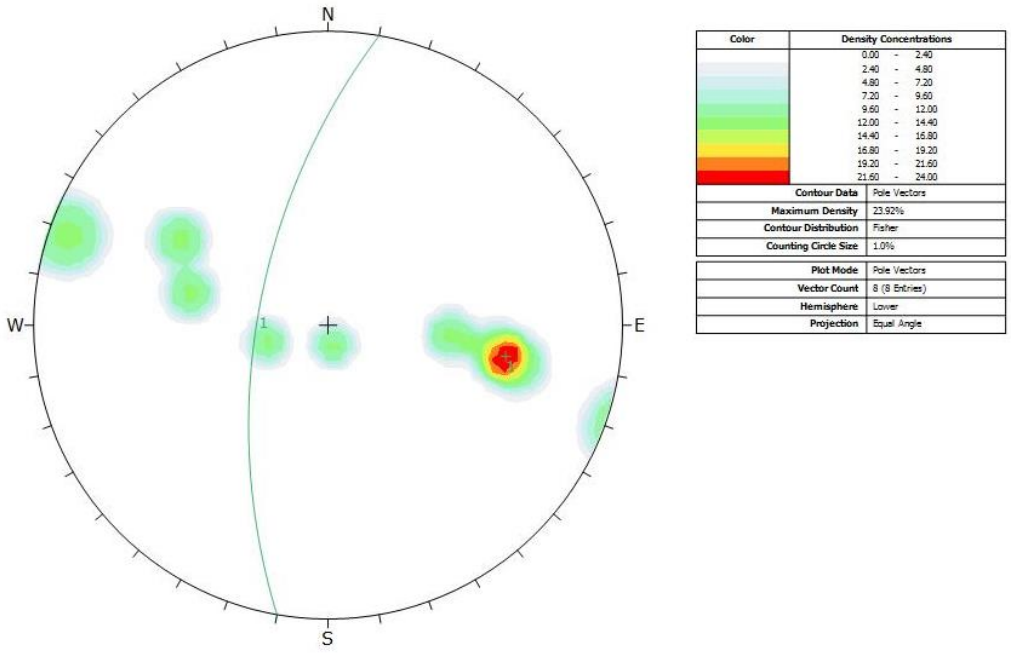

Figure 4.12 – Stereonet illustrating structural information of faults obtained in the NW field area.

A stereonet illustrating structural information of beds found in the NW of the field area is shown in Figure 4.13. As shown in this image, beds were generally dipping at shallow angles. The dip/dip direction for the central cluster of geologic beds observed in the NW face was 05°/130°.

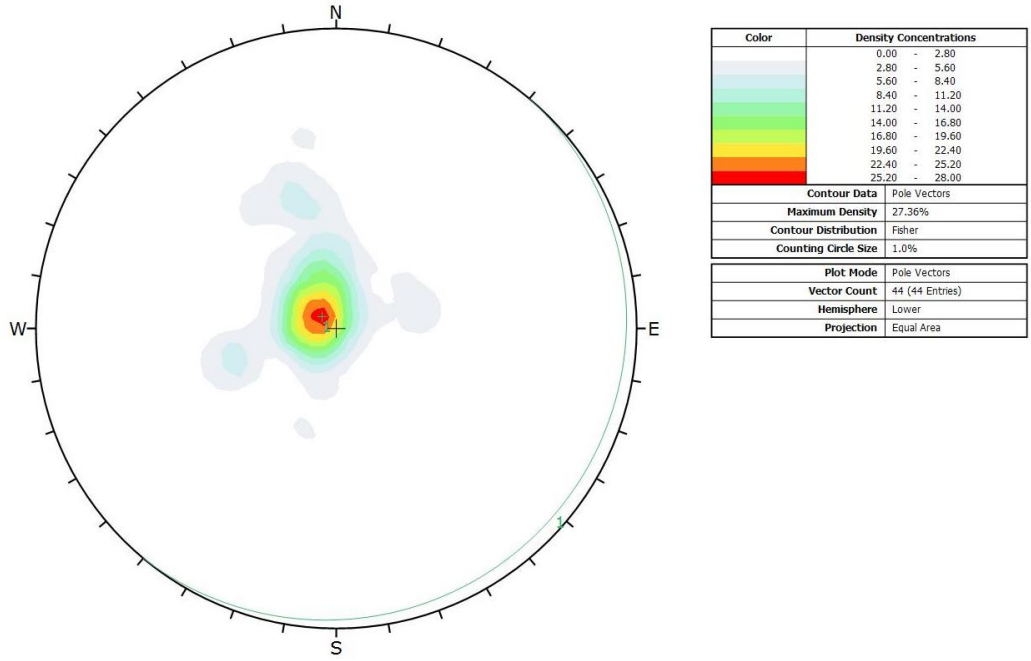

Figure 4.13 - Stereonet illustrating structural information of beds obtained in the NW field area.

Similar methods were used to record structural information on the NE face. A similar Table to Table 4.2 is detailed below. Table 4.3 shows measurement dip and dip direction measurements, alongside an approximate location on the face, plus a measurement number which shows the location of the measurement on field sketches. These locations are detailed in a field sketch of the NE face (Appendices J).

Table 4.3 – Recorded dip and dip direction measurements taken on the NE Face, and corresponding locations.

Measurement Number	Direction	Dip	Location
1	346	9	Top of Rangitawa
2	349	17	Bottom of Rangitawa
3	249	29	Rangitawa/weathered tephra

4	212	73	Weathered tephra
5	126	78	Fault
6	247	28	Karapiro/Weathered tephra
7	135	76	Karapiro
8	216	44	Karapiro
9	104	14	Fault (Offset Karapiro)
10	280	71	Fault
11	226	11	Rangitawa
12	289	17	Weathered tephra
13	279	6	Weathered tephra
14	279	42	Weathered tephra/Kauroa
15	211	75	Kauroa
16	136	3	Karapiro
17	91	45	Karapiro/Walton Sub-Group
18	51	59	Fault
19	59	13	Walton Sub-group
20	120	7	Fault
21	245	14	Bottom of Rangitawa
22	233	10	Weathered tephra
23	40	24	Weathered tephra/Kauroa
24	NA	NA	NA
25	74	68	Fault
26	28	5	Karapiro
27	315	14	Bottom of Rangitawa
28	261	1	Weathered tephra
29	187	34	Weathered tephra/Karapiro
30	171	9	Karapiro
31	21	2	Karapiro
32	72	57	Fault

A stereonet illustrating structural data of faults obtained in the NE face is shown in Figure 4.14. As shown in this image, two fault sets are identified. The first set had an average dip/dip direction measurement of 10°/111°, with the second averaging and 62°/073°. The subsequent strike of these two sets of faults are 021° (NNE) and 343° (NNW), as presented in Figure 4.14.

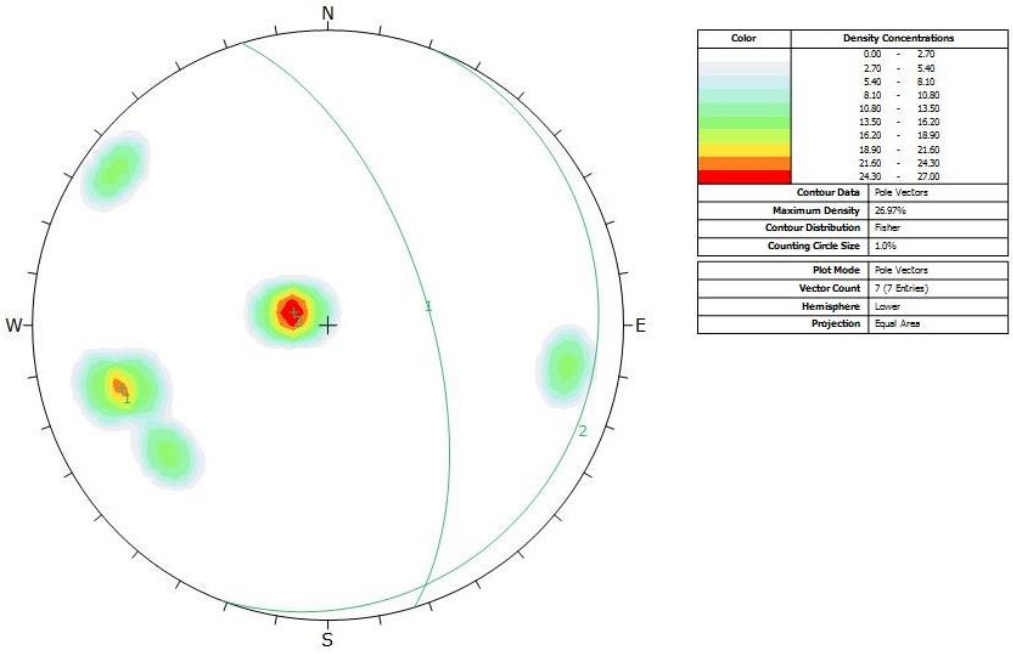

Figure 4.14 - Stereonet illustrating structural information of faults obtained in the NE field area.

A stereonet illustrating structural information of geologic beds is shown in Figure 4.15. These geologic beds dip at a shallow angle compared to structural features observed within the NE face. A general dip and dip direction measurement of 04°/238° was observed for structural beds. This differs somewhat to that observed in the NW of the field area, however this is expected due to the displacement observed.

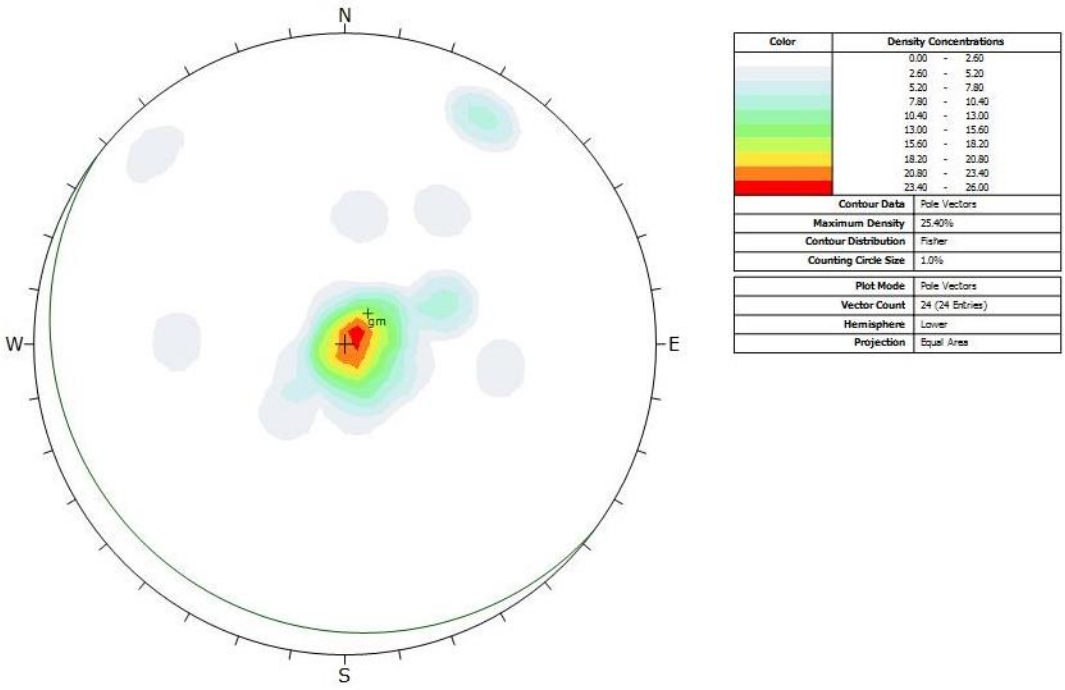

Figure 4.15 – Stereonet illustrating structural information of geologic bedding obtained in the NE field area.

Structural information obtained in the field was then used to generate geologic models of the NW and NE faces. This was done so using Leapfrog® geologic modelling software, and is discussed in Section 4.8.

4.7 Deformation structures

Tectonic deformation of strata is commonly associated with distinctive geologic and geomorphic signatures. Throughout the Kay Road fault zone, a plethora of these structures were observed, suggesting that tectonic deformation has severely impacted the field area. This section illustrates evidence of the type of deformation structures found within the field area.

4.7.1 Offset bedding

Offset bedding of strata is often a clear indicator that tectonic deformation has occurred by means of faulting. Within the Kay Road field area, extensive offset of beds within the Walton Sub-group was recognised. This offset ranged significantly within the field area from 40 mm on the SE face, to 3.6 m in the SW face. Figure 4.16 shows offset of beds as a result of normal faulting within the SE face. Iron staining within the beds makes identification of offset easier.

Figure 4.16 - Image showing offset within the Walton Sub-group in the SE of the Kay Road field area. As shown in the image, the block to the right (southern block) appears to be down-thrown, a result of normal faulting within the Walton Sub-group. Also shown in Figure 4.16 is clear banding, a phenomenon observed throughout the Walton Sub-group in the field area.

More offset bedding is shown in Figure 4.17 and Figure 4.18 which depict further offset within the Walton Sub-group. Figure 4.17 shows vertical displacement of approximately 320 mm, observed in the SE face.

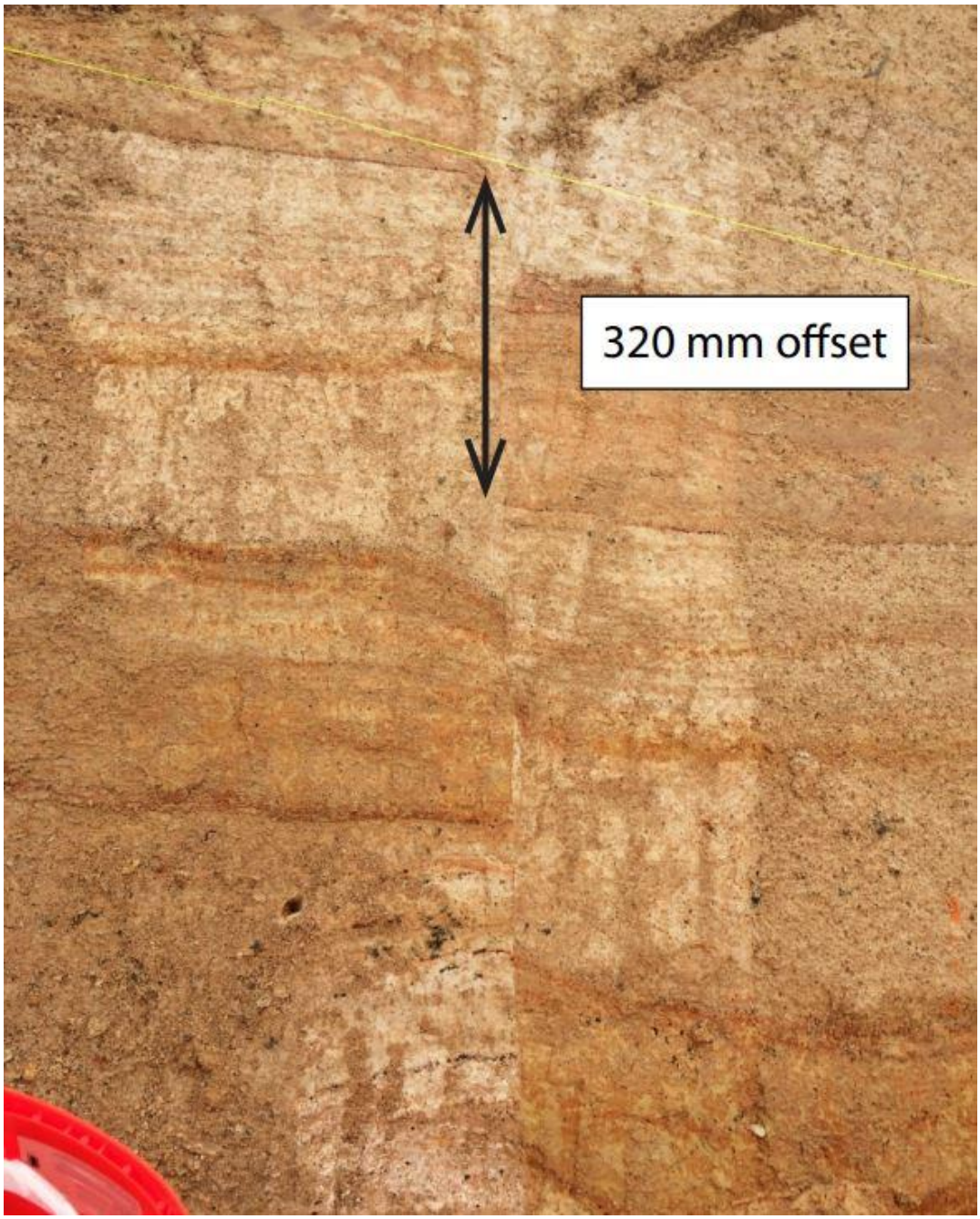

Figure 4.17 – Offset beds within the Walton Sub-group in the SE face, a consequence of normal faulting.

Shown in the left of Figure 4.18 is down-thrown, whereby the hanging wall is the southernmost wall. Down-throw of the southernmost block was a common trend observed within the Kay Road field area.

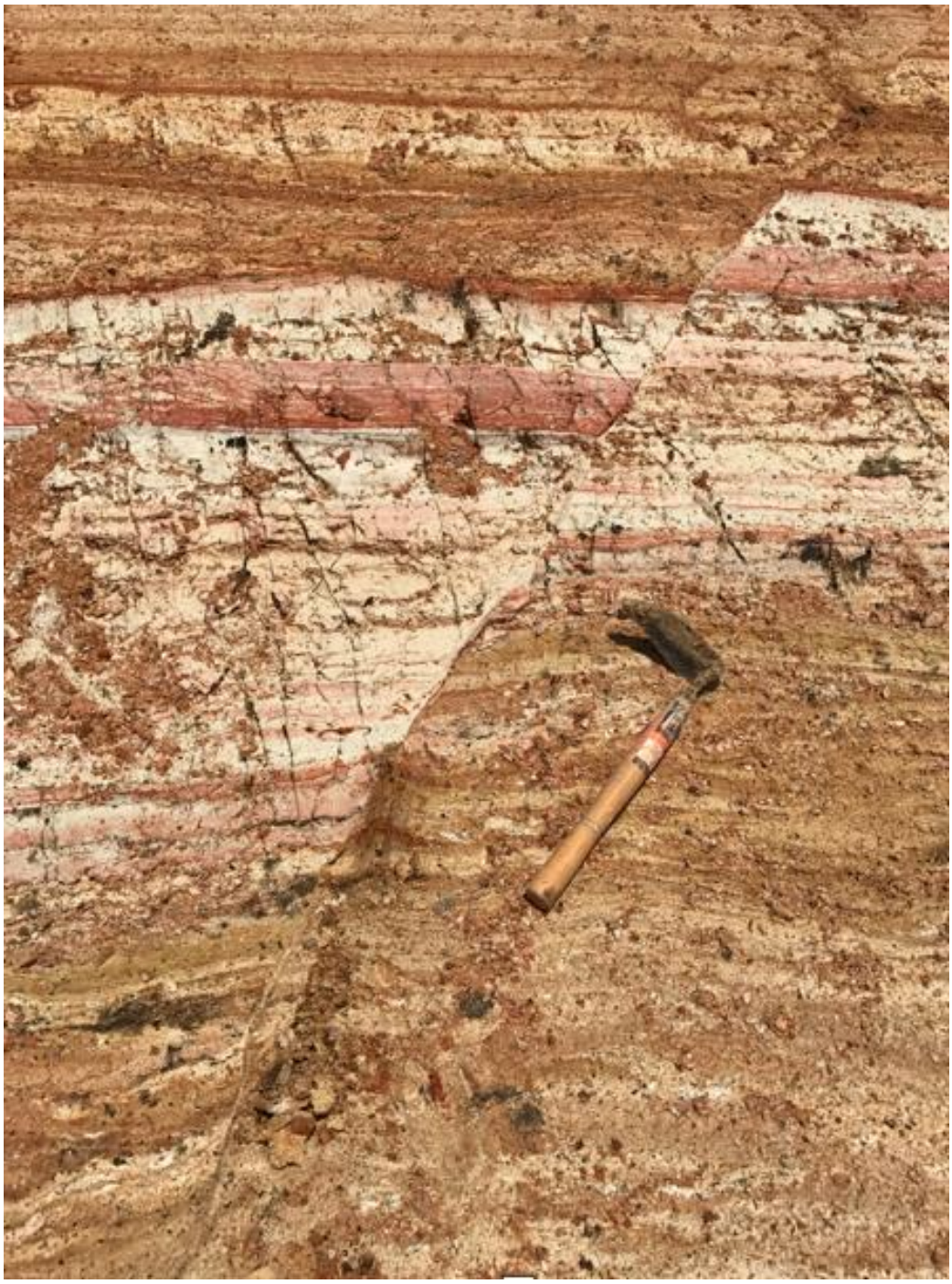

Figure 4.18 - Normal faulting within the Walton Sub-group, resulting in the Southern block (left of image) being down-thrown in the SW face of the Kay Road field area.

Figure 4.19 below illustrates the same normal faulting within the Walton Sub-group. This image is taken from a wider perspective however, and illustrates the scale of faulting observed within the SE face. Similar to Figure 4.18, the

southernmost block of the face is the down-thrown block (right of image in Figure 4.19).

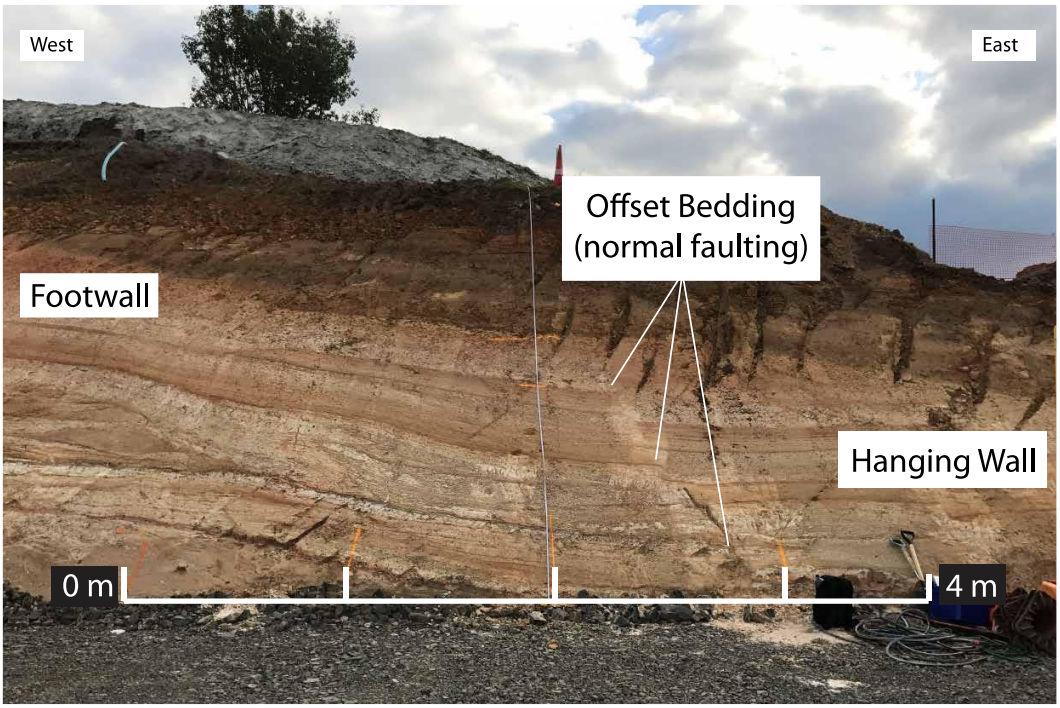

Figure 4.19 - Image showing deformation of the Walton Sub-Group within the South Eastern face. Pictured to the right is a spade for reference. The total height of the face was 8 m high.

4.7.2 Intrusion structures

Deformation of strata within the Kay Road fault zone also included the presence of intrusion structures. Within the field area multiple intrusion structures were observed in both the east and west of the field area. Clear boundaries between the inferred intrusions and surrounding structures were able to be drawn.

A number of intrusion-like structures with significantly different characteristics are presented below from Figure 4.20 to Figure 4.28. Figure 4.20 shows an intrusion-like structure found within the lower lying units of the NW face. This intrusion structure was thought to be a variation of the Karapiro Formation (K2), as the unit was sandy clay with 5 YR 6/8 orange colouring. As shown in this image, clear boundaries are observed within the formation, with thin white accumulations being found on the top of the intrusion unit. This banding of white material is also shown in Figure 4.21, and noted in field sketches (Appendices C and D). Although this material could not be identified; it was deduced that the material was not

calcareous. Overlying this intrusion structure is a distinctive boundary between the Karapiro Formation and the tilted Kauroa beds.

Figure 4.20 - Clear boundaries with white cementations found around the boundary of this structure.

An alternate perspective of the intrusion like structure found within the Karapiro Formation, next to the Kauroa Ash Formation is shown in Figure 4.21. Shown in this image is the pinch out of an orangey brown sandy clay (unit K2).

Figure 4.21 – An Intrusion structure observed on the NW face. As shown in the image, clear boundaries between the intrusion structure, overlying Kauroa bed to the right and overlying Karapiro formation to the left exist.

A much larger intrusion structure was found in the north of the NW face. This structure was wedge shaped, and had distinctive boundaries between the overlying weathered tephra units and adjacent Karapiro Formation. This structure is detailed in Figure 4.22, and explicitly noted in Appendices E. Also shown in Figure 4.22 is a number of identified units, and relative. The easternmost portion of the block was deemed a variation on the Karapiro Formation, which overlies an apparent intrusion structure. To the left of this is obviously tilted and rotated Kauroa Ash Formation, overlain by WT2. Figure 4.22 shows the significant portion of spoil, which was created during construction of the Waikato Expressway. Obvious displacement is apparent within the Figure, however this deformation is confined to units older than the Rangitawa Tephra.

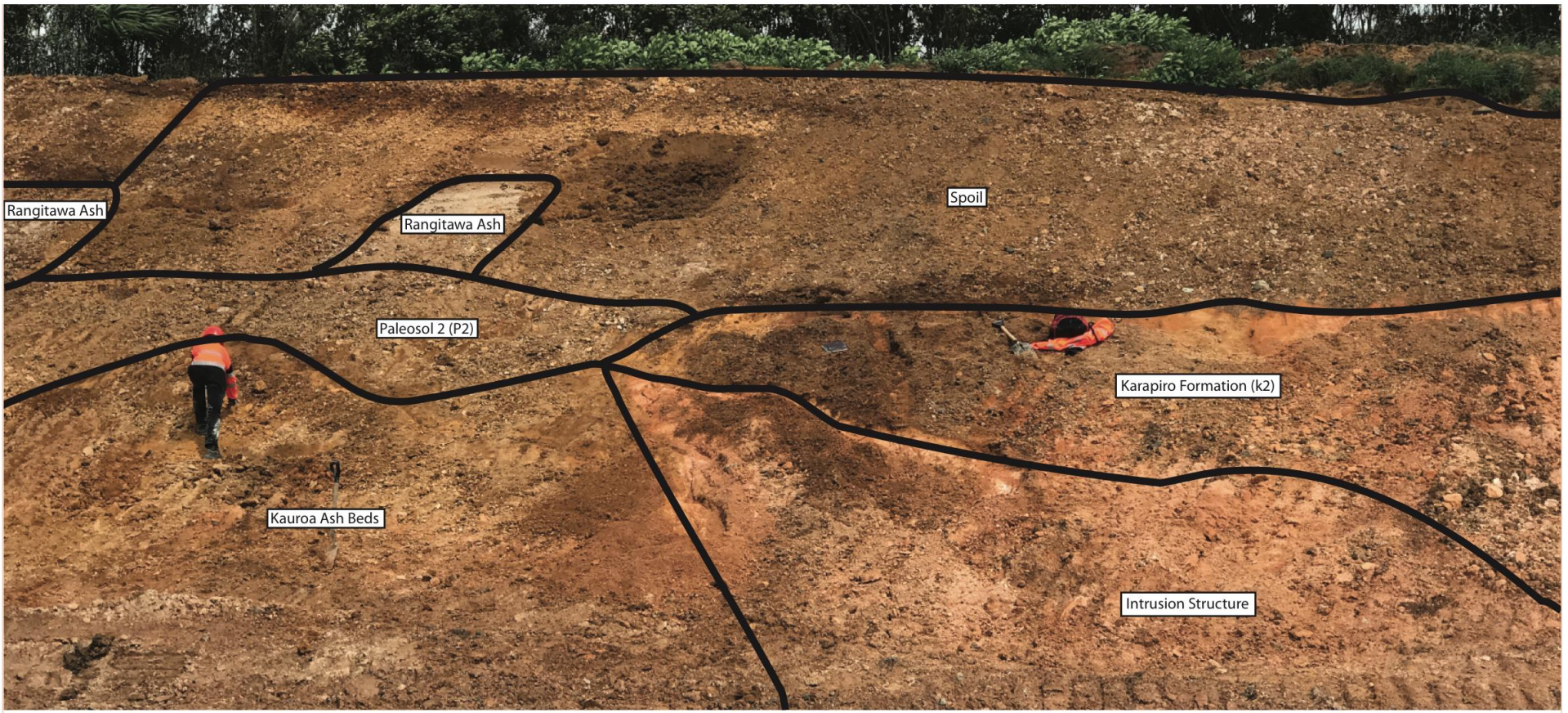

Figure 4.22 - Intrusion of a large sandy unit, wedging into the North Western face. Clear deformation of units is observed in this Figure.

All intrusion structures were found below units older than the Karapiro Formation, suggesting that deformation has not occurred within the previous 0.35 ma.

A much smaller intrusion structure, similar to a sand blow was found in close proximity to this intrusion structure.

4.7.3 Intrusion structures

An intrusion structure was found a few metres to the left of the aforementioned wedge intrusion in the NW face (Figure 4.22). This structure was approximately 100 mm wide throughout the intrusion channel. This structure spanned from apparent ground level at the Kay Road field site, through some 14 vertical metres of the NW face. At the base of the structure, a lateral channel approximately 2.2 metres long was found. Images of this structure are detailed below in Figure 4.23 and Figure 4.24.

Figure 4.23 - What appears to be a clay intrusion structure within the Walton Sub-group unit.

An alternative image of the intrusion structure is shown below in Figure 4.24. Shown in Figure 4.24 is a lateral channel, branching off this structure. Primarily, this intrusion structure was fine-grained, brown clay unit. This structure dissipated before penetrating the Rangitawa Tephra.

Figure 4.24 – The base of an observed intrusion structure in the NW face of the Kay Road field area. A lateral channel is shown at the base of this structure, branching toward the right of the image.

A much smaller intrusion like structure was found within younger units of the NW face, towards the southernmost portion of the NW face. Spanning to just below the Rangitawa Tephra, the second intrusion structure was approximately 40 cm long. This structure is shown below in Figure 4.25, with an accompanying field sketch shown in Appendices F. The lithology of the structure appeared to have similar characteristics to the underlying weathered tephra unit (WT1).

Figure 4.25 – An intrusion like structure found proximal to weathered tephra units in the field. As shown, this intrusion structure is significantly smaller than that pictured in Figures 4.20 to 4.24.

Following preliminary field investigations and detailing of the NE, NW, SE and SW faces, further excavation occurred at the Kay Road field site resulting in a deeper cutting into the lower units of the Walton Sub-group. Within the lower units, further studies occurred, whereby a larger intrusion structure was discovered. Running through the Walton Sub-group, the intrusion structure appeared to be continuous throughout both the Western and Eastern faces of the lower cutting.

This however this is speculation, as the structure could not physically be traced due to gravel that had been placed to form the base of the Waikato Expressway. Images of this intrusion structure which aligned on the west and east of the field area are shown below in Figure 4.26 through Figure 4.28. Important to note is investigation of lower Walton Sub-group strata was conducted following fresh hydro-seeding. As such, a grey matrix covers most of the Walton Sub-group, which may alter the appearance of the unit in the following pictures.

Shown in Figure 4.26, the intrusion structure can be seen running through the Walton Sub-group unit. Close up images of the intrusion structure show distinct boundaries between the outermost whitish-grey silt boundary within the Walton Sub-group, alongside the innermost boundary between sand and clay within the structure. The sand channel was a coarse grained, greenish brown unit, dominated by quartz; and appeared heavily weathered. The formation appeared well sorted.

Conversely, the silt channel was very fine grained, white, non-plastic silt. This outermost unit within the structure varied in thickness within the structure, fluctuating between ~10 mm wide to ~80 mm at its thickest point.

Figure 4.26 – An intrusion structure cutting through the massive Walton Sub-group. As shown in this image, the intrusion structure is > 6 m long. Also shown in the image is clear boundaries within the intrusion structure, with an inner sand channel being surrounded by a clay matrix. Due to logistics of the field site, the total height of the structure could not be measured, as the slope face was too steep to scale.

A close up image of the Intrusion structure is shown below in Figure 4.27. This image is taken on the east of the field site, converse to Figure 4.26 which was taken in the west of the field area. As shown in Figure 4.26 and Figure 4.27, the characteristics both structures share suggest that they are continuous.

Figure 4.27 - An intrusion structure found on the western face of lower units within the Walton Sub-group. Shown in the image are clear boundaries between the brownish-green sand and white silt channels within the structure.

A zoomed out image shows the same feature pictured in Figure 4.28. As shown at the top of this image, the structure appears to splinter into smaller features in the uppermost regions of the lower Walton Sub-group.

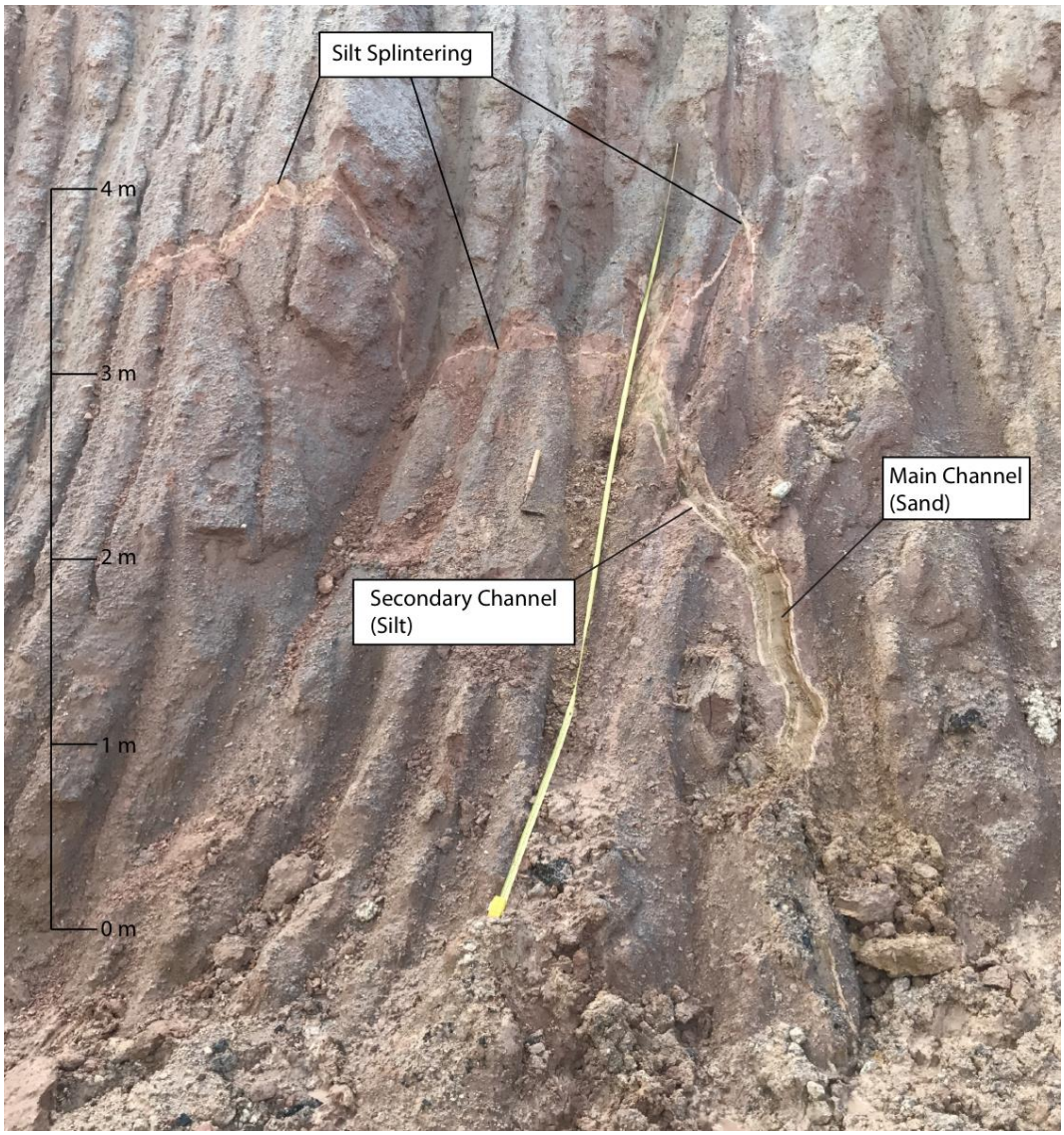

Figure 4.28 – An image of an intrusion structure observed in the east of the field area. As shown in this image, the intrusion structure appears to splinter of into a number of distinct channels. Pictured in Figure 4.28 is a 4 m tape measure for scale.

The feature shown in Figure 4.26 to Figure 4.28 showed distinct boundaries within its internal structure. This suggests that the structure may have been subject to deformation multiple times, whereby the first intrusion channel was an injection of silt, followed by a second deformation process involving the injection of sand. It appeared that this unit continued into the upper reaches of the Walton Sub-group, however due to the nature of the face the formation was unable to be traced due to safety concerns.

4.8 Geologic modelling

4.8.1 Geologic modelling of the NW face

Geologic models of the Kay Road fault zone were produced to help illustrate the extent of deformation within the field area. Primarily, models show extensive deformation throughout the Puketoka Formation and the Karapiro Formation (Walton Sub-group), alongside the uppermost units of the Kauroa Ash Formation. No deformation was modelled within the Rangitawa Tephra, so subsequent younger units. An assortment of models of the NW face are shown below in Figure 4.30 through to Figure 4.34, and models of the NE face are shown through Figure 4.35 though to Figure 4.42. Figure 4.29 below illustrates units used in the NW model.

Figure 4.29 - Legend of units within the NW model.

Figure 4.30 illustrates the NW geologic model as a whole. In this image, the model is unsliced. Shown in this image is a blocky, repetitive pattern observed in the Kauroa Ash Formation, alongside the Karapiro Formation. Important to note in the eastern portion of Figure 4.30 is a large portion of spoil which dominates the model. Structural information regarding this spoil unit was unable to be obtained, and thus the unit is presented as a solid block.

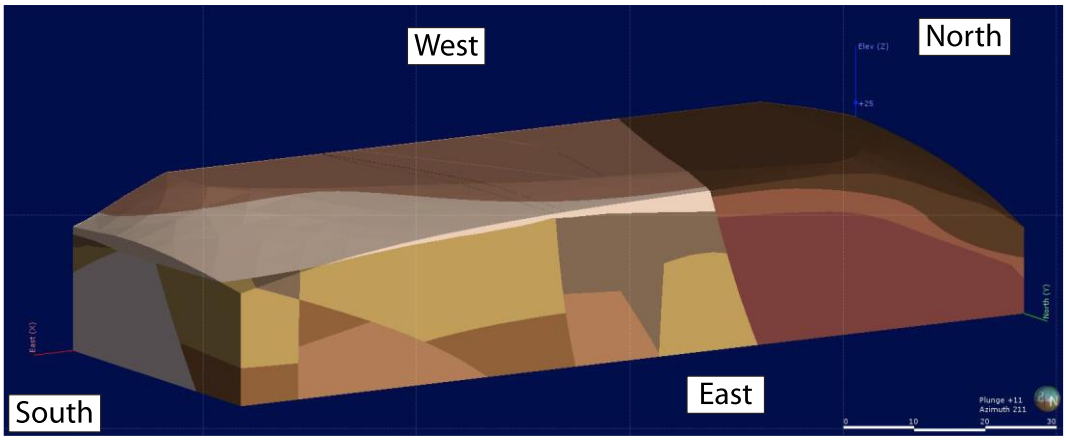

Figure 4.30 - Image of the NW geologic model. In this image the perspective is viewing the NW model from a SE location. As shown in the model, extensive deformation is present within the Kauroa Ash Formation (gold), which exhibit significant displacement.

Anomaly *A marked in Figure 4.8 shows a clear boundary between an intrusion structure and the rest of the geology in the NW face. Above this intrusion, contacts are modelled artificially, as this unit was spoil it had no structural information so was modelled as a definitive block. It is known however that the Rangitawa tephra continues throughout the NW face, as evidenced by soil auger sampling.

Figure 4.31 below shows a similar perspective of the NW model, however the image is from a higher view angle looking down, and the model is sliced to show the inner geology of the model. Shown in Figure 4.31 with red lines are fault planes, with a dashed blue line representing an artificial boundary between modelled geology and the spoil unit.

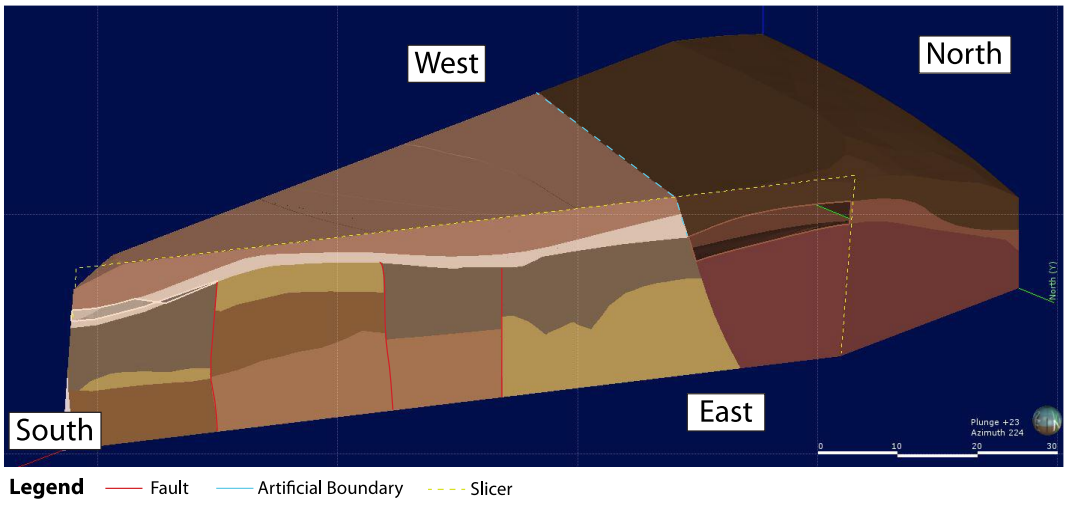

Figure 4.31 - Geologic model illustrating offset within the Kauroa Ash Formation. This model is a similar perspective to Figure 4.30, however the image is sliced to show deformation within the Kauroa beds. 8 m of offset is present in the southernmost part of the model. Also shown in this image is that deformation is confined to a time period prior to deposition of the Rangitawa Tephra. The right hand side of the model illustrates where excavation of the NW face occurred. Due to the significant disturbance that occurred in the area, geology could not be accurately depicted. Consequently, the right hand of the model is modelled as a simple block shape labelled spoil.

Figure 4.32 below looks at the NW model from the south, looking north; perpendicular to the perspective of the cross section. As shown in this image, displacement is present in the Kauroa Beds. No offset is visible within the Rangitawa Tephra unit.

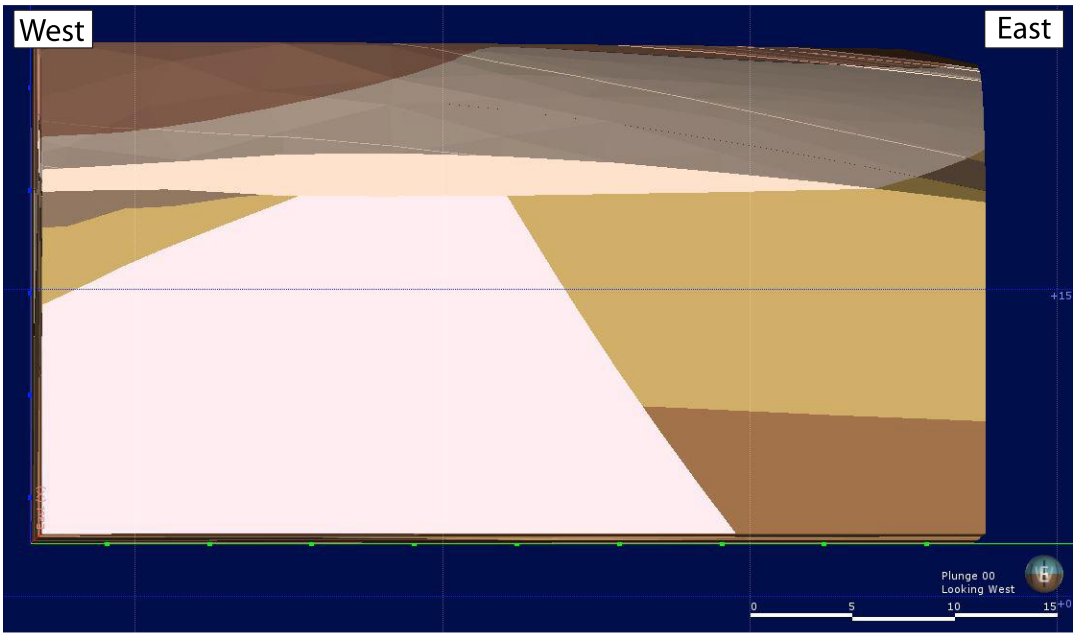

Figure 4.32 – An image of the NW geologic model from a northward facing perspective. Shown in this image is significant displacement of the Kauroa (gold) beds, and also a wedge of the Walton Sub-group which is steeply dipping.

A sliced image of the NW model is shown in Figure 4.33. Clear uplift and deformation of the Kauroa Ash Formation is shown by the blocky, tilted repetitive nature of the gold wedge shown at the bottom of this image.

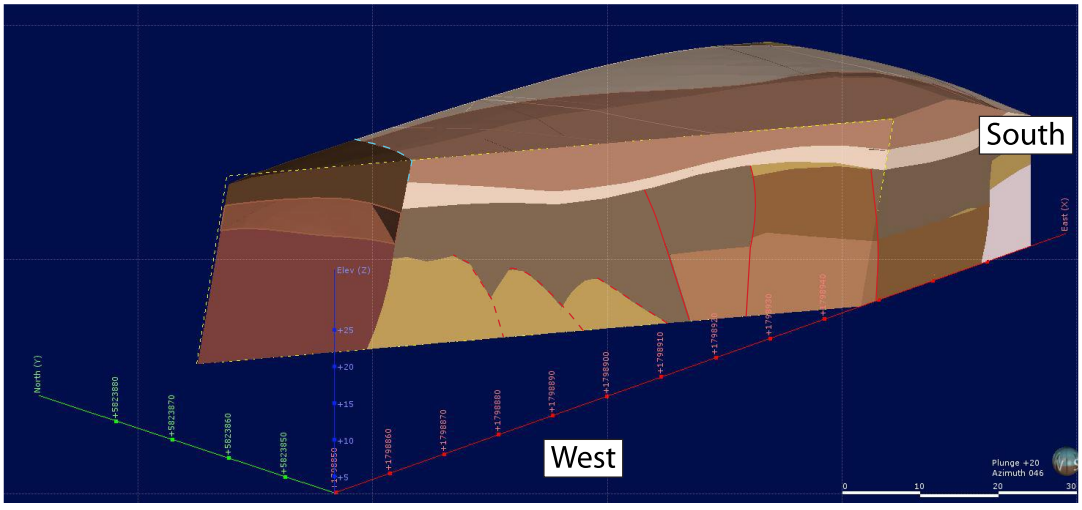

Figure 4.33 - The NW model showing repetitive displacement of the Kauroa Ash Formation. The perspective of this model is taken from the west, looking east; a perspective not possible without geologic modelling of this section of the Kay Road fault area. Important to note in Figure 4.33 is the dashed yellow boundary around the cut face of the model. When studied, a clear distinction between the 2D perspective that has been sliced (that we look at head on), compared to the original 3D perspective of the model on the right hand side of the image.

Figure 4.34 below shows the NW model from the perspective that the cross section was sketched.

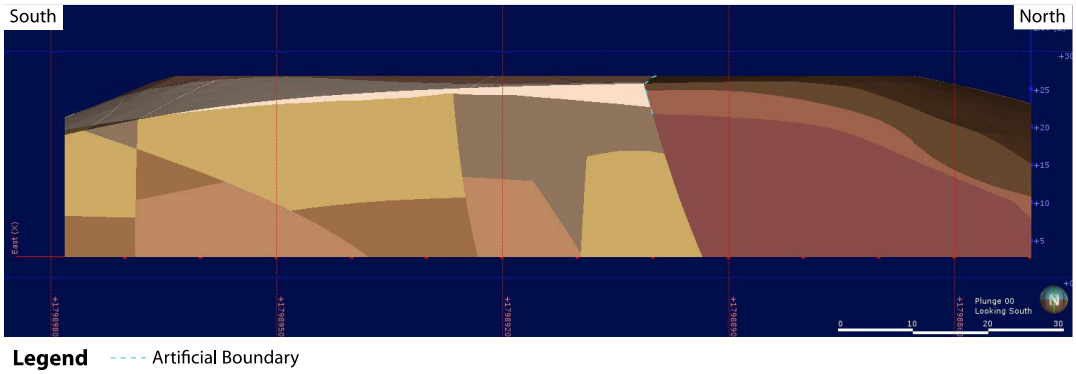

Figure 4.34 – A capture of the model taken looking directly at North Western geologic model as one would in the field. As shown in Figure 4.31, the model is unsliced. Shown to the right is the apparent intrusion structure (pink). Not shown in the right hand side of the model is the Rangitawa Tephra, as structural information on the Rangitawa Tephra could not be extracted from the spoil. Consequently, the model only shows where the Rangitawa unit was found within the field, undisturbed. Soil augering in the field did show, however that the Rangitawa Tephra is continuous throughout the entirety of the NW face (not shown in model).

What we recognise from observations of geologic modelling is that the NW face exhibits complex deformation of multiple units. Involving pinchouts of units, intrusion structures, significant displacement and multiple discontinuities, deformation within the NW model is extensive. Hence, deducing the exact means of deformation is difficult. What we can recognise however is that the Rangitawa Tephra unit (lowest unit of the Hamilton Ash Series) remains intact throughout the entirety of the Kay Road field area. Consequently, we know that deformation is confined to a time period older than the deposition of the Rangitawa Tephra (0.35 Ka)(Lowe *et al.*, 2001). We also recognise that the Kay Road field site is a fault zone, as opposed to a single fault plane. This is shown by the presence of multiple faults, and the chaotic deformation observed in field sketches, descriptions and geologic modelling of the NW face. Generally, these faults were steeply dipping normal faults.

Also shown in the NW is significant offset of a number of older units. Offset is presented in various ways, however most noticeable within the figures is the uplift, rotation and offset of the gold Kauroa beds. Deformation is clear within this unit, and is shown particularly well in Figure 4.33. Similarly, offset is observed

easily in the Karapiro Formation, which shows clear deformation by means of intrusion structures and displacement of units. These intrusion structures are best shown by Images in Figure 4.20 through Figure 4.28.

Geologic modelling of the NW face recognised three major faults, alongside three inferred faults. The three recognised faults were steeply dipping at approximately ~66°, and appeared to be normal faults. Inferred faulting within the NW field area was somewhat shallower, with an average dip of 35° recorded.

Geologic modelling of the NW face shows that deformation is clearly significant, with extensive displacement observed throughout the Walton Sub-group, alongside the Kauroa Ash Formation. Offset from these faults ranged in size, with largest offset measured at 8.5 m. This is thought to have been caused by reverse faulting, and associated crustal compression. Many smaller faults were also found offsetting the Kauroa Ash Formation, ranging upward from ~3 m. This movement is thought to have been induced by normal faulting. Further analysis of deformation within the NW field site is continued in Chapter 6.

4.8.2 Geologic modelling of the NE Face

Geologic modelling of the NE face was completed using the same methodology as the NW face. The nature of deformation within the face did however prove more challenging during modelling. A legend of units used in the NE model is shown below in Figure 4.35.

Figure 4.35 - Units used in the geologic modelling of the NE face.

Various perspectives of the NE model are shown below in Figure 4.36 -4.42. Figure 4.36 shows an image of the unsliced NE model. The perspective of the image is looking perpendicular to the angle at which the NE cross section was drawn.

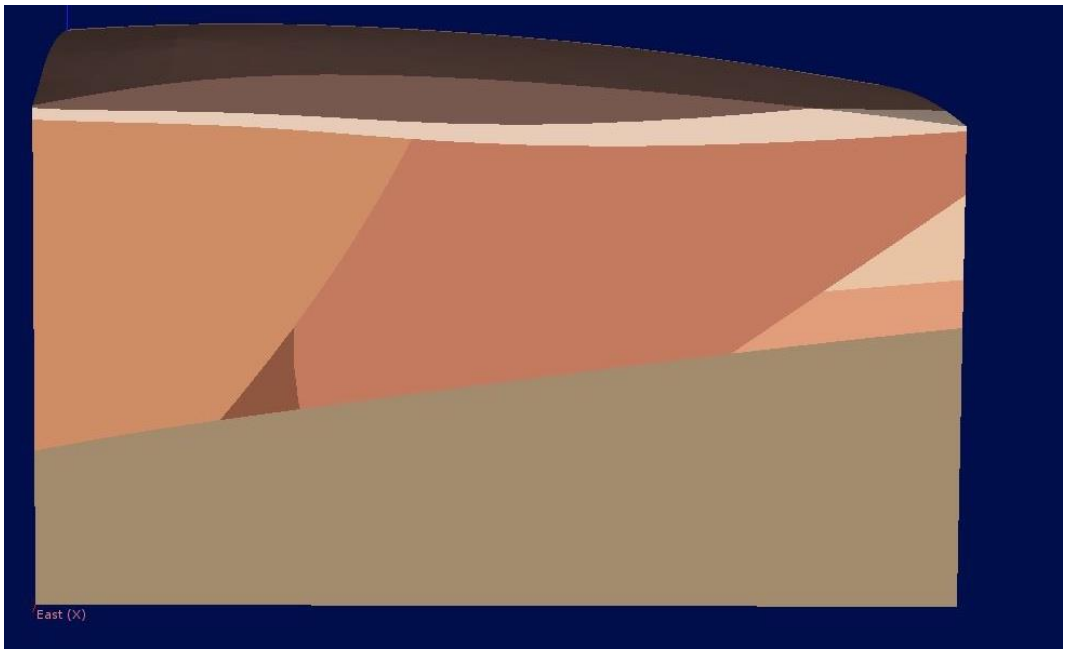

Figure 4.36 - Image of the NE model south to north. Shown in this image is the Walton Sub-group, which was gently dipping within the field area

An alternate perspective of the unsliced NE model is shown below in Figure 4.37. Shown in this model is an apparently chaotic, blocky deformation of the NE face, alongside multiple fault planes as illustrated by distinct, irregular unit boundaries.

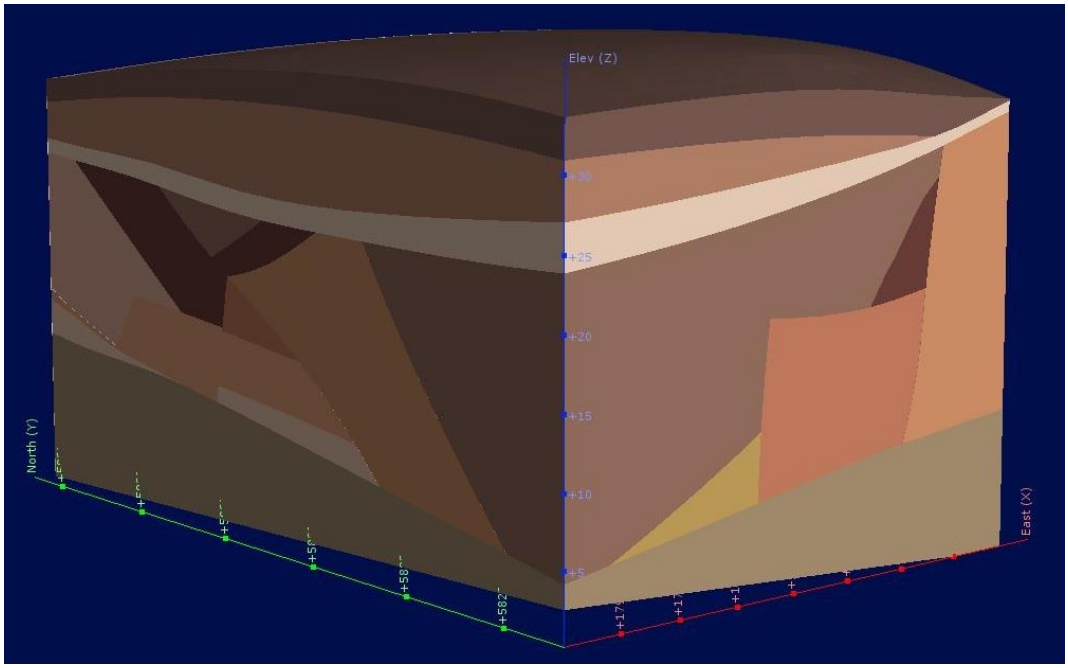

Figure 4.37 - An image from the SSE looking NNE of the NE geologic model. The image is unsliced, and no deformation is observed within the overlying Rangitawa Tephra unit at the top of the model (greyish-white unit).

Figure 4.38 below shows a sliced image of the NE model, which exhibits complex deformation within geologic units. Undisturbed in the model however is the Rangitawa Tephra. This model is taken looking from an opposite perspective to that from which the field sketch was taken (looking at the NE face from behind).

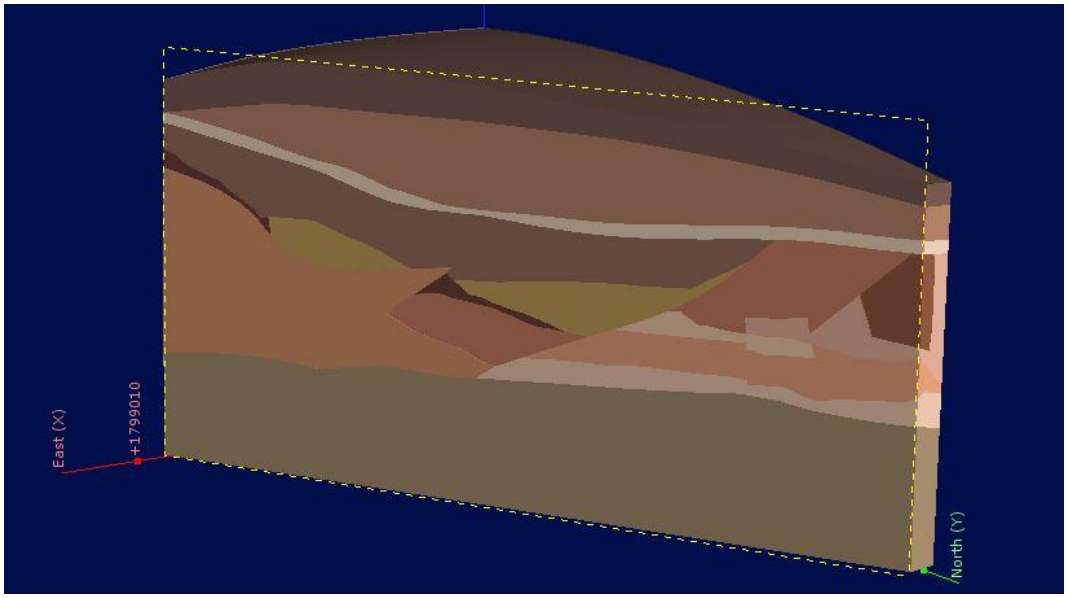

Figure 4.38 - Looking South East from the North East of the NE model. As shown in this image, no deformation has occurred within the Rangitawa Tephra unit, however significant deformation of the Karapiro Formation, Kauroa Ash Formation and Walton Sub-group is observed.

Another sliced version of the model is shown below in Figure 4.39.

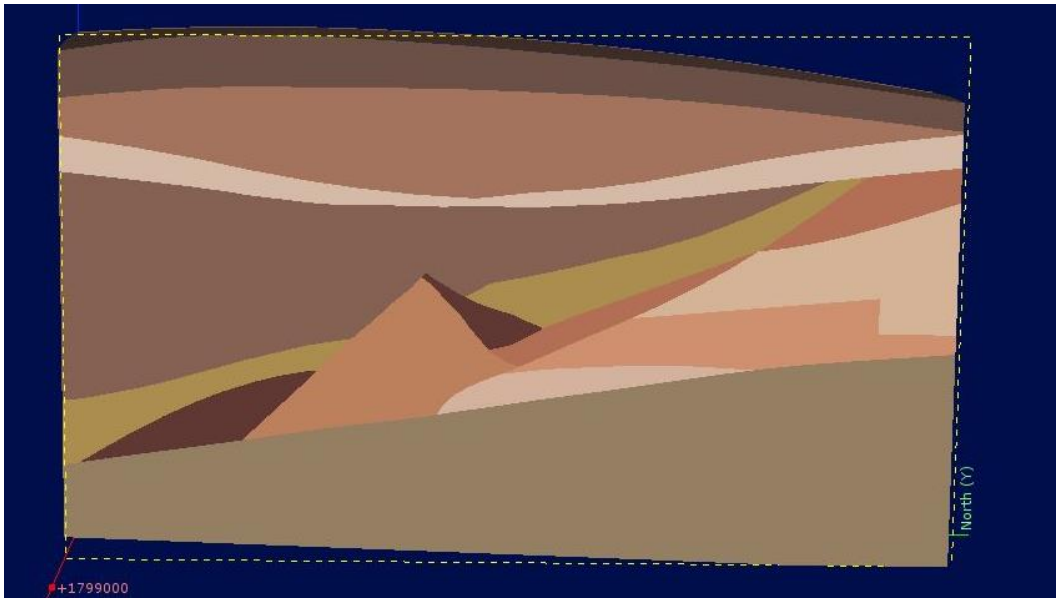

Figure 4.39 - Model of the NE face that has been sliced East/West through the middle of the model. Shown in this image is deformation of the Kauroa Ash Formation, by means of an apparent intrusion of the older Karapiro unit. The Kauroa Ash Formation, and Walton

Sub-group also show extensive deformation, associated with down-throw of units from normal faulting.

An alternate perspective of the sliced model is shown below in Figure 4.40 that has been sliced perpendicular to the cross section. This is running through approximately they middle of the NE model.

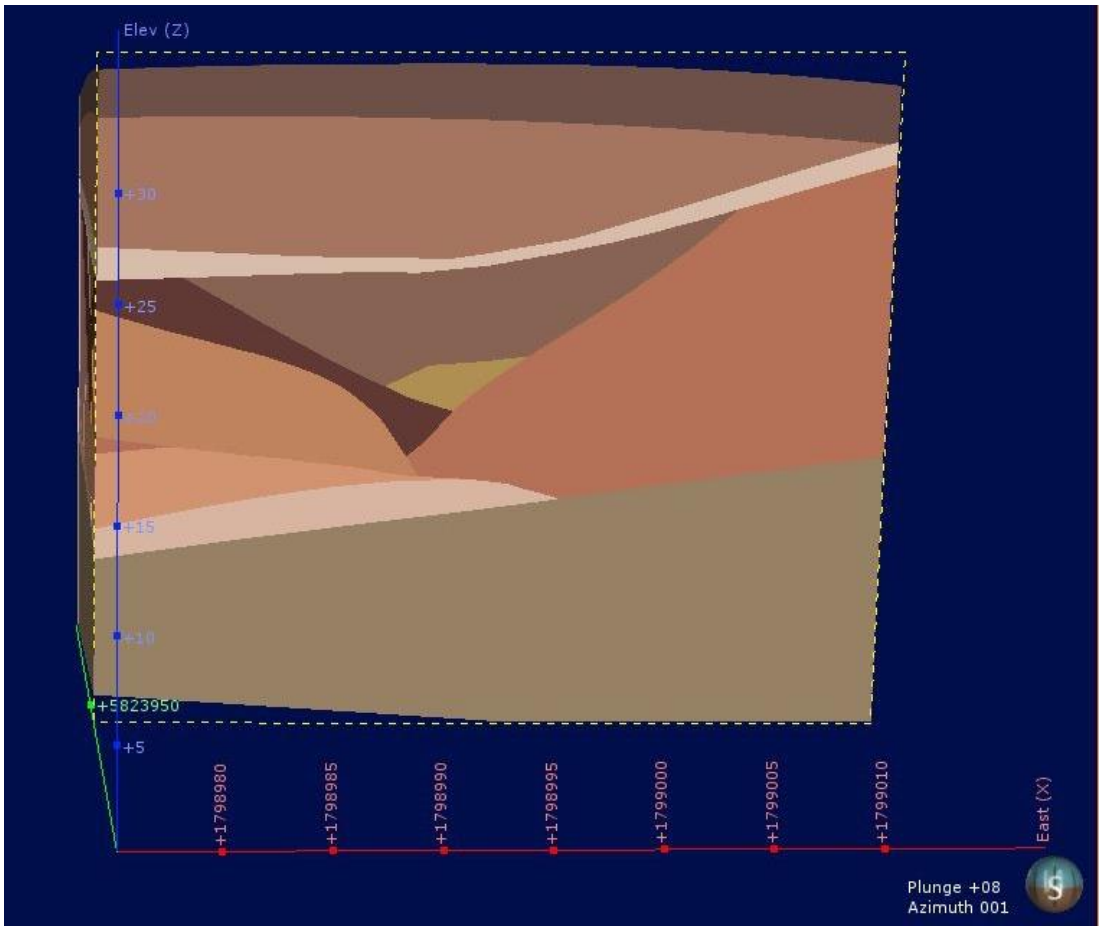

Figure 4.40 - An image of the NE geologic model that has been sliced east to west, looking at the face from the south. The Rangitawa Tephra is shown near the top of the model, undisturbed.

Shown below in Figure 4.41 is a sliced version of the NE model from a SE perspective. Shown in this Figure is complex deformation.

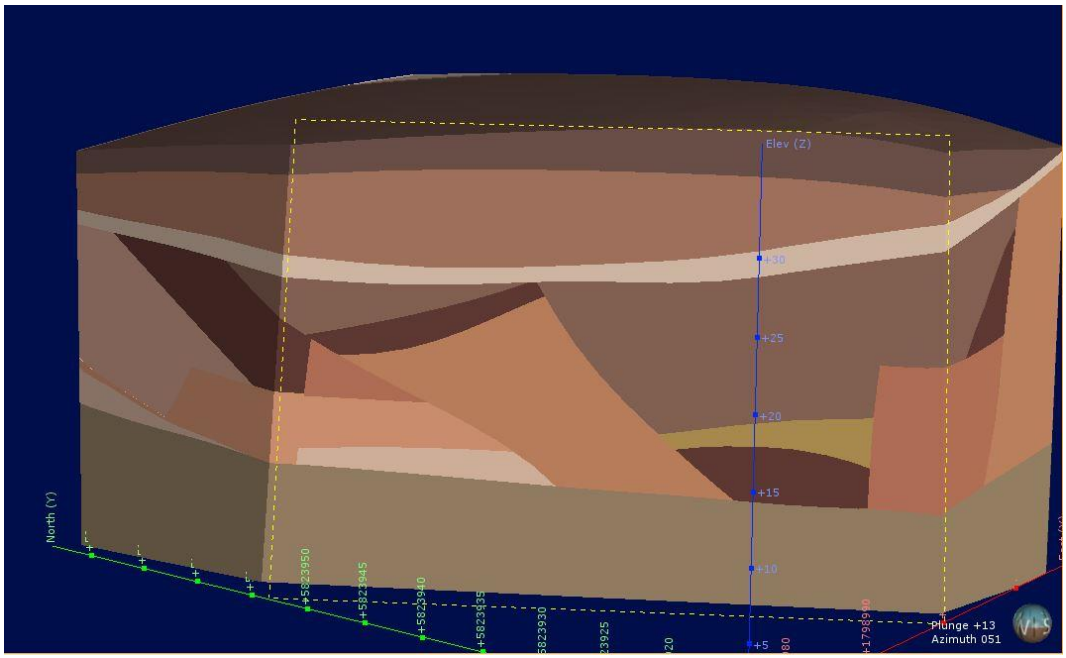

Figure 4.41 - An image of the NE face, viewing from west. The image is sliced to show an alternate perspective of the model. As shown in the model, chaotic, blocky deformation of the NE field site is present..

A sliced view of the NE model from a bird's eye perspective is shown below in Figure 4.42. This slicer was approximately 5 m from the top of the model.

Figure 4.42 - A Birdseye view of the NE geologic model. Shown in this model is the undisturbed Rangitawa unit, with topsoil layered above it. Shown in the model is blocky deformation of the NE face.

Geological modelling of the NE face indicates chaotic deformation. Similar to the NW model, I note that deformation is contained to units older than the Rangitawa Tephra.

Although geologic modelling of the NE face was completed, it is thought that logistically, development of the NE model was somewhat unsuccessful compared to the NW face. Primarily, this is due to some uncertainty of the geologic phenomenon modelled, and that these phenomena may not be geologically possible. Although structural geology of the NW model is credible when modelled directly from the cross section, when this information is extrapolated out credibility of findings does appear to decrease. This may be associated with the significant presence of diverse faulting within the field.

Geologic modelling of the Kay Road field site did produce sensible results that, for the most part corroborated findings from the field. Key findings from geologic modelling is that deformation within the field area is confined to a specific time period older than the Rangitawa Tephra, and significant offset is present within the field area. Most influenced by deformation was the Kauroa Ash Formation, alongside the Karapiro Formation and older members of the Walton Sub-group.

Within the NE model, seven major fault planes have been modelled. Consequently, geologic modelling of the NE face shows complex, multiple slips that have occurred along fault planes. Fault planes within the NE face varied in characteristics, with faults tending to shallow out as they penetrated younger units. Within the NE face, faults trended along an average plane of 080° (N/S), with an average dip of ~51°, somewhat shallower than those modelled in the NW face. Chaotic geology of the NE face shares some characteristics with wider hypothesis that listric faulting is present within the basin. This is evidenced best by Figure 4.41, which illustrates a smaller scale, listric like model of deformation within the model. Further analysis of deformation within the NE field site is continued in Chapter 6.

4.9 Displacement in Kay Road field area

Displacement observed in each of the faces is detailed below in Figure 4.43, Figure 4.44, 4.45 and 4.46. Figure 4.43 and Figure 4.44 illustrate annotated cross sections of the faces (NE and NW), whereby Figure 4.46 and Figure 4.43 illustrate offset annotated onto photographs of the SE and SW faces.

This section presents various offsets determined through measurement of relative up-throw and down-throw of units within the field area. These total offset images were generated using field measurements, the ruler tool in Leapfrog® Geological Modelling Software, and Adobe Illustrator. Shown in the figures are fault planes, depicted by red lines, and blue lines which illustrate the location of measured offset along fault planes in each face. Arrows depicting up-throw and down-throw, alongside displacement measurements are also depicted on the relative figures.

4.9.1 Offset within the NE face

An image showing total offset found within the NE face is shown below in Figure 4.43. The NE face was dominated by normal faulting, with significant offset observed. Largest offset found in the NE face was 15.3 m of offset observed within the Kauroa Ash Formation, in the centre of the face along a steep-angle fault trace. Offset was also observed extensively throughout the Walton Subgroup, albeit smaller.

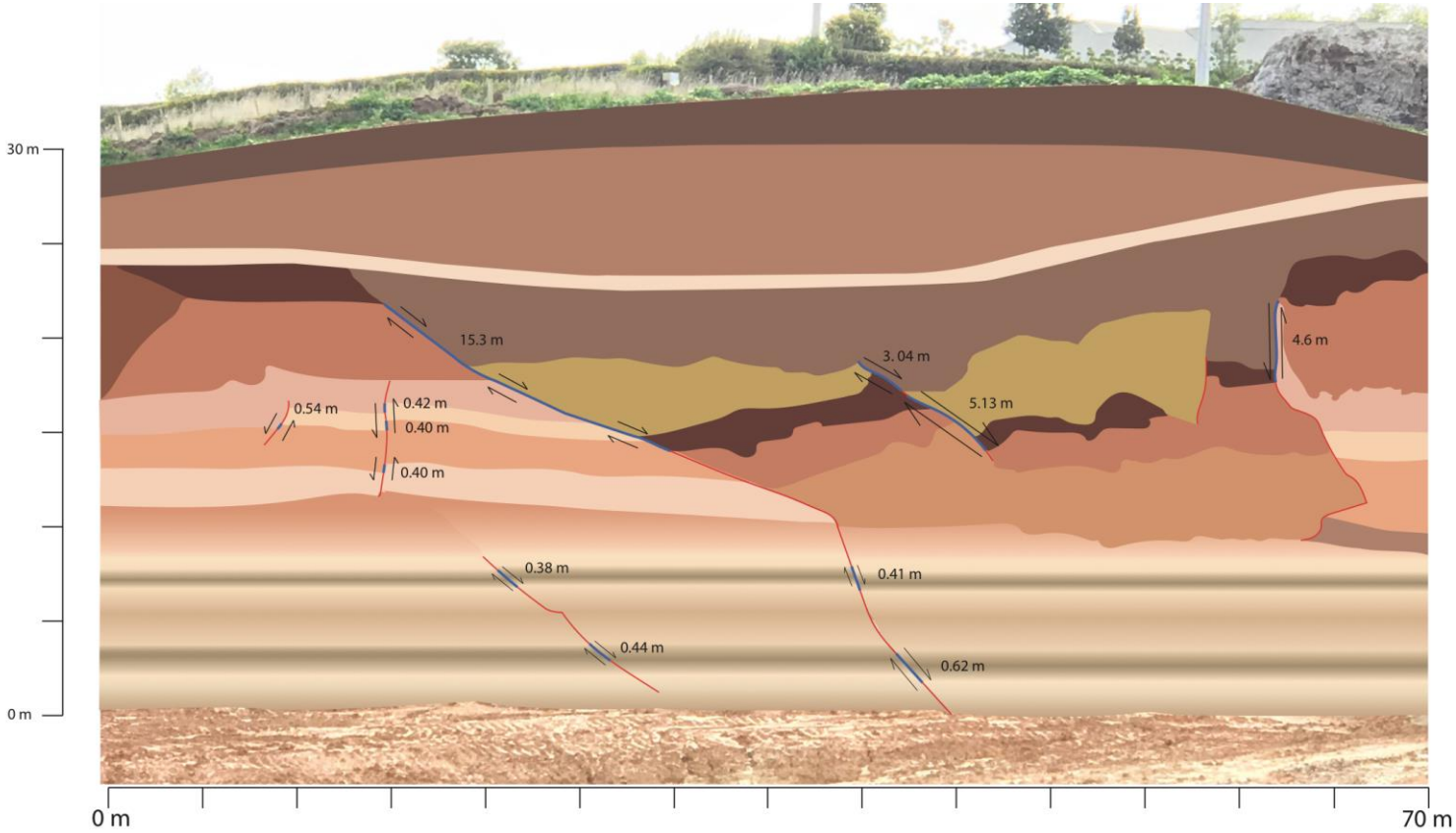

Figure 4.43 - Image showing displacement within the NW face. Measurement of offset is noted on the face next to the location of offset, alongside up-throw and down-throw of units.

4.9.2 Offset within the NW face

An image showing total offset found within the NW face is shown below in Figure 4.44. Offset within the NW face varied significantly, ranging between 3 m in the Kauroa Ash Formation to 15.3 m within the WT1 unit. A blocky, repetitive pattern of deformation was observed within the middle of the Kauroa Ash Formation, alongside significant displacement of the unit within the southernmost portion of the NW face.

Measurement of offset within the NW face is shown in Figure 4.44. A large portion of the south of the NW face does not have offset described, as this is better detailed in Figure 4.45 which was continuous with the NW face.

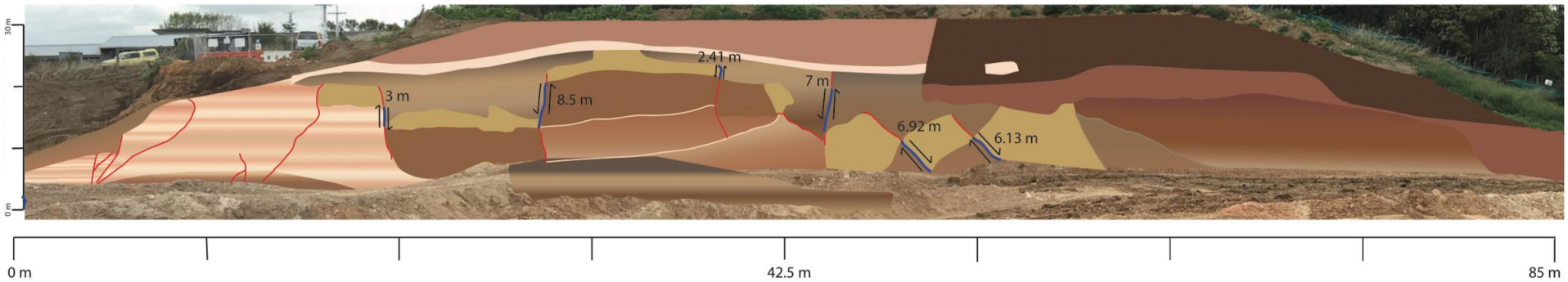

Figure 4.44 - Figure showing displacement within the NW face. Measurement of offset is noted on the offset location, alongside up-throw and down-throw of units depicted by arrows. As shown in this image, the Kauroa Ash Formation exhibits the most extensive deformation in the NW face.

4.9.3 Offset within the SW face

An image showing total offset found within the SW face is shown below in Figure 4.45. The SW face was continuous with the NW face, however the SW exposure showed the lower lying Walton Sub-group unit. Largest offset within this face was 3.6 m, and smallest offset within the face was approximately 0.04 m. Due to the logistics of the SW exposure, access to the top of the face could not be obtained, and some offset as unable to measured. Offset that was measured, however, was easily recognisable in the SW face due to iron staining and bedding within the Walton Sub-group.

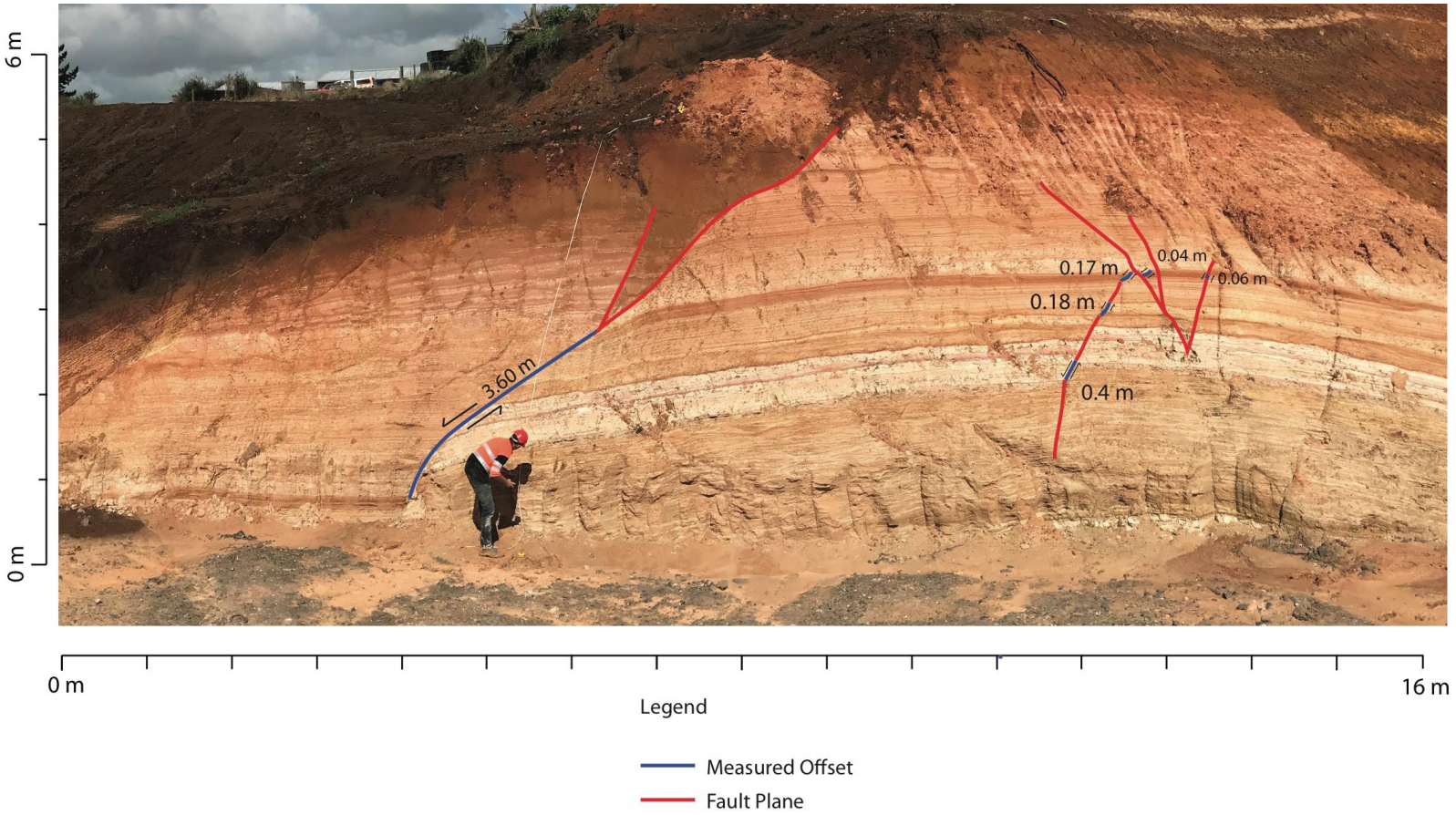

Figure 4.45 - Figure showing displacement within the SW face. Noted on the face are offset measurements, alongside up-throw and down-throw of units. Major displacement of the Walton Sub-group is shown around the 4 m mark. Between this major displacement and measured displacement in the east of the image, some smaller offset was observed, but not measured.

4.9.4 Offset within the SE face

An image showing total offset found within the SE face is shown below in Figure 4.46. Offset within the SE face was similar to the SW face, and was dominated by normal faults. The SE face clearly exposed the Walton Sub-group, with the southern portion of the SE face containing the majority of deformation. Offset within the SE face was most noticeable due to iron-stained beds within the face. Offset within the SE face ranged from 0.07 m to 0.063 m. Similar to the SW face, the south block of the SE face appeared down-thrown.

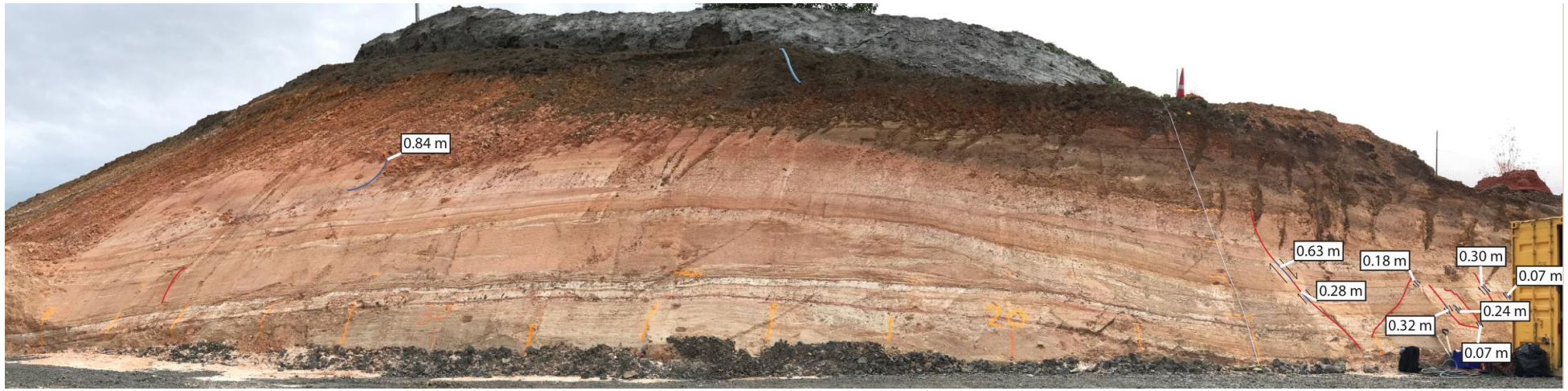

Figure 4.46 - Figure showing displacement within the SE face. As shown in this image, displacement was concentrated in the southernmost (right of image) portion of the SE face.

4.10 Total throw of the Kay Road field area

Total throw of the Kay Road field site has been difficult to calculate, due to the chaotic nature of deformation found at Kay Road. Consequently, producing a single number to best represent deformation in the field area is difficult. Table 4.4 to Table 4.7 below illustrate location and size of offset, alongside the relative movement type and whether offset of units appears to have been up-thrown or down-thrown, relative to proximal offset geology. Table 4.8 then summarises the Kay Road field site in general, establishing the total throw of the Kay Road field area.

Table 4.4 – Apparent vertical offset within the NE face.

Measured offset	**Location**	**Movement Type**	**Relative Throw**
15.3 m	Weathered tephra 1	Normal Faulting	Down
0.54 m	Walton Sub-group	Reverse faulting	Up
0.42 m	Walton Sub-group	Normal faulting	Down
0.4 m	Walton Sub-group	Normal faulting	Down
0.4 m	Walton Sub-group	Normal faulting	Down
0.38 m	Walton Sub-group	Normal faulting	Down
0.44 m	Walton Sub-group	Normal faulting	Down
0.41 m	Walton Sub-group	Normal faulting	Down
0.62 m	Walton Sub-group	Normal faulting	Down
3.04 m	Kauroa Ash Formation	Normal faulting	Down
5.13 m	Weathered tephra 2	Normal faulting	Down
4.60 m	Weathered tephra 2	Normal faulting	Down

The total movement observed within the NE face was 27.9 m of relative down-throw towards the south.

A summary Table of offset measurements obtained in the NW of the Kay Road field area is shown below in Table 4.5.

Table 4.5 - Summary of offset measurements observed in the NW face.

Measured offset	**Location**	**Movement Type**	**Throw**
3m	Kauroa Ash Formation	Normal fault	Down
8.5 m	Kauroa Ash Formation	Reverse fault	Up
2.41 m	Kauroa Ash Formation	Normal Fault	Down
7 m	Weathered tephra 2	Reverse Fault	Up
6.92 m	Kauroa Ash Formation	Normal Fault	Down
6.13 m	Kauroa Ash Formation	Normal Fault	Down

Total throw within the NW of the Kay Road field area was 2.96 m of relative down-throw towards the south.

A summary Table of movement within the SW face is shown below in Table 4.6

Table 4.6 - A summary table of measured offset within the SW face.

Measured offset	**Location**	**Movement Type**	**Throw**
3.6 m	Walton Sub-group	Normal	Down
0.4	Walton Sub-group	Normal	Down
0.18	Walton Sub-group	Normal	Down
0.17	Walton Sub-group	Normal	Down
0.04	Walton Sub-group	Normal	Down

0.06	Walton Sub-group	Normal	Down

The total throw observed in the SW face is 4.45 m of relative down-throw towards the south.

A summary table of movement within the SE face is shown below in Table 4.7.

Table 4.7 - A summary of measured offset within the SE face.

Measured offset	**Location**	**Movement Type**	**Throw**
0.84 m	Walton Sub-group	Normal	Down
0.63 m	Walton Sub-group	Normal	Down
0.28 m	Walton Sub-group	Normal	Down
0.18 m	Walton Sub-group	Normal	Down
0.32 m	Walton Sub-group	Normal	Down
0.24 m	Walton Sub-group	Normal	Down
0.07 m	Walton Sub-group	Normal	Down
0.30 m	Walton Sub-group	Normal	Down
0.07 m	Walton Sub-group	Normal	Down

Total throw within the SE of the Kay Road field area was 2.93 m of relative down-throw towards the south.

A summary Table comparing all movement within the Kay Road field area is shown below in Table 4.8.

Table 4.8 - Summary of all measured movement within the Kay Road field area.

Face	**Dominated by**	**Total Throw**
NW	Normal Faulting	-2.96 m

NE	Normal Faulting	-27.9 m
SW	Normal Faulting	-4.45 m
SE	Normal Faulting	-2.93 m

The total throw observed in the Kay Road field area was 7.41 m of relative down-throw toward the south, measured in the west of the field area. This was calculated by measurement of offset within the western margin of the Kay Road field area, as the western portion of the field showed clearer, more extensive faulting. As faults in the west and east were not recognised as the same faults, only the total throw of the west is presented, to ensure the most accurate total throw measurement. Some uplift of units within the Kay Road field area was recognised, however this was negligible in comparison to down-thrown units.

4.11 Summary

The Kay Road field site is comprised of an extensive hill cutting near the northern boundary of Hamilton City. Created during construction of the Waikato Expressway, the Kay Road field site offers a unique perspective into the deformation of hillslope units within the Hamilton Basin. Running through an inferred fault zone, the Kay Road field area exposed a number of geologic units, including weathered tephra units, sands, silts and clay; later identified as the Hamilton Ash series, Kauroa Ash Formation, Karapiro Formation and Puketoka Formation.

Through geologic detailing, sketching and measuring of the Kay Road field site, evidence of deformation was found within the Walton Sub-group (Karapiro Formation and the Puketoka Formation) and more recent Kauroa Ash Formation. Deformation signatures identified within the field area included, but were not limited to, offset beds, displaced units and the presence of intrusion structures. Consequently, these features were recorded and detailed, and geological models of the fault zone were constructed to best characterise the region. The construction of models allowed for an improved understanding of each of the exposed faces, and helped illustrate field observations in a tangible way.

Geological modelling of the region also provided alternate perspectives of the fault zones which would not have otherwise been recognised.

Immediately apparent from the construction of Leapfrog models was that the field area was dominated by steeply dipping normal faults; however, some more recent shallow faults were also identified within the field area. Collectively, 7.41 m of down-throw was observed in the west of the Kay Road field area and some 30.83 m observed in the east. As models generated for the west of the field area appeared more successful, the total throw within the Kay Road field area was generated by adding the total throw of the NW and SW faces. This 7.41 m of relative down-throw toward the south supports the idea that the Kay Road field area has been subject to normal faulting.

Within the field area, the deformation of units was immediately apparent, especially in lower beds of the Kay Road field area. Clear offset within the oldest Walton Sub-group units was made obvious through offset iron staining within the field. Offset within the Walton subgroup varied significantly, with few mm to up to 15.3 m of offset observed within the field area.

Units overlying recognised offset also exhibited deformation. This was shown through stark contrasts between unit boundaries, including the Kauroa Ash Formation, the Karapiro Formation, and various tephra units found within the field. The chaotic distribution of these units, alongside the presence of both intrusion and intrusion structures is irrefutable evidence that the region has been deformed tectonically.

As the structural distribution of these units was so varied, it was measured and recorded in this investigation. Primarily, faults within the field region were thought to be trending along a N/S plane when averaged. This aligns with ridgelines identified in LiDAR maps of the Hamilton Basin, and corroborates the idea that the Hamilton Basin has been subject to tectonic deformation. Important to note however is that no recent deformation has occurred within this field site as all deformation identified at Kay Road has been confined to a time period older than 0.35 Ma, which was when the undisturbed Rangitawa Tephra unit was deposited.

Chapter 5

Results – Osborne Road

5.1 Introduction

The Osborne Road field site is located at 37°42'19.53"S, 175°14'12.11"E (WGS84) near Horsham Downs in northern Hamilton. Owned by Andrew Kimpton, access to several paddocks running parallel to Osborne Road was kindly granted to allow investigation of an inferred fault zone. A satellite image depicting the location of the Osborne Road field site, alongside northern Hamilton City is shown below in Figure 5.1.

Figure 5.1 - Satellite image of Hamilton City, with the Osborne Road field site marked. Image taken from Google Earth, 2017.

A closer perspective of the Osborne Road field site is depicted below in Figure 5.2. This image depicts the location of Osborne Road alongside the Kay Road field site. Shown in orange is the boundary of the Osborne Road field site, which is approximately 1.4 km by 0.17 km.

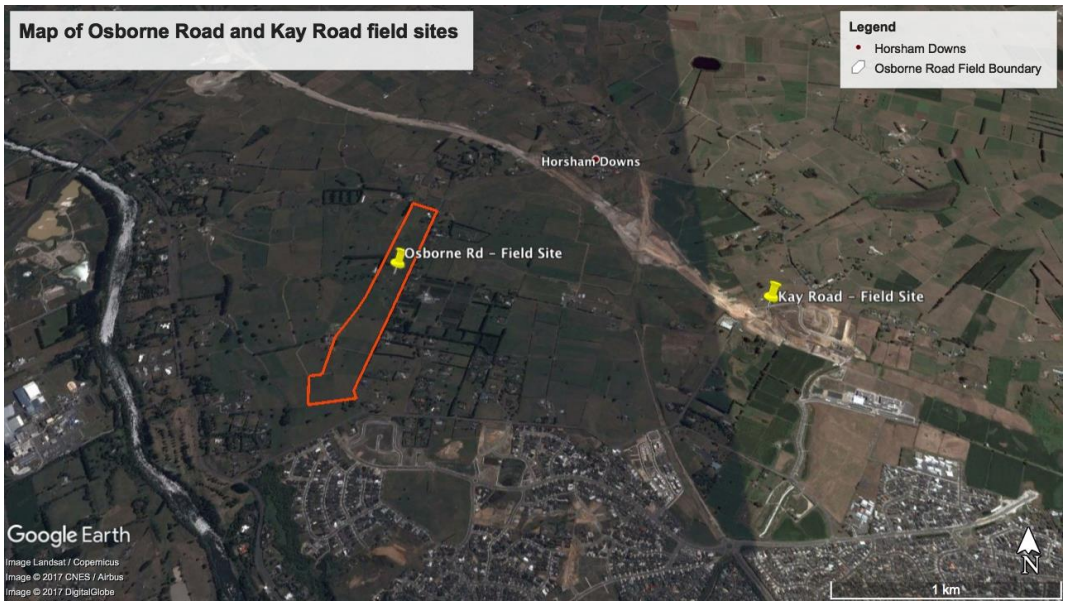

Figure 5.2 - A satellite image detailing the Osborne Road field site, alongside the Kay Road field site. The Osborne Road field site is depicted by an orange polygon.

The Osborne Road field site was first identified as a potential field site due to unique geomorphic signatures within the landscape. A distinctive, continuous break in slope is found running through the east of the field site, creating an escarpment approximately 2 m high. Initial investigation of this escarpment and the surrounding landscape unearthed a number of features indicative of tectonic deformation on. This evidence of deformation includes, but is not limited to, offset within the Waikato River channel, abnormal parallel drainage patterns around the Osborne Road field area, and the obvious physical displacement within the Osborne Road field site. This chapter details results of preliminary investigation of the Osborne Road field site, alongside evidence indicative of tectonic deformation.

5.2 Site walkover and geomorphic mapping

Field investigations at Osborne Road began with a thorough site walkover. Completed to help attain a general feeling for the field site, the site walkover included observation of geomorphic features, together with the noting of drainage patterns and soil exposure within the Osborne Road field site. Where soils were exposed, brief descriptions and photographs were taken.

Following an initial site walkover, geomorphic mapping of the field area was undertaken. This was completed using standard geomorphic mapping symbols. Using these symbols, multiple site walkovers were undertaken and geomorphic

symbols representing different landscape features were sketched onto both topographic and LiDAR maps generated in ArcMap. These maps were continually refined as understanding of the field area improved, and other phenomena within the field area such as drainage patterns were noted. Field sketches were then studied and refined in a laboratory environment. Multiple geomorphic maps of the Osborne Road field area were produced, illustrating geomorphology overlain on satellite and LiDAR images. These figures are shown in Figure 5.3 – Figure 5.5 below.

Figure 5.3 shows a satellite image of the Osborne Road field area that has been annotated with geomorphic mapping symbols. The same geomorphic map is shown in Figure 5.4. However, the background here is an image generated from LiDAR information. Similarly, Figure 5.5 illustrates the same mapped geomorphology of the Osborne Road field site, but there is no image background image making the geomorphic symbols more legible.

Figure 5.3 - Satellite image of the Osborne Road field area with geomorphic mapping symbols.

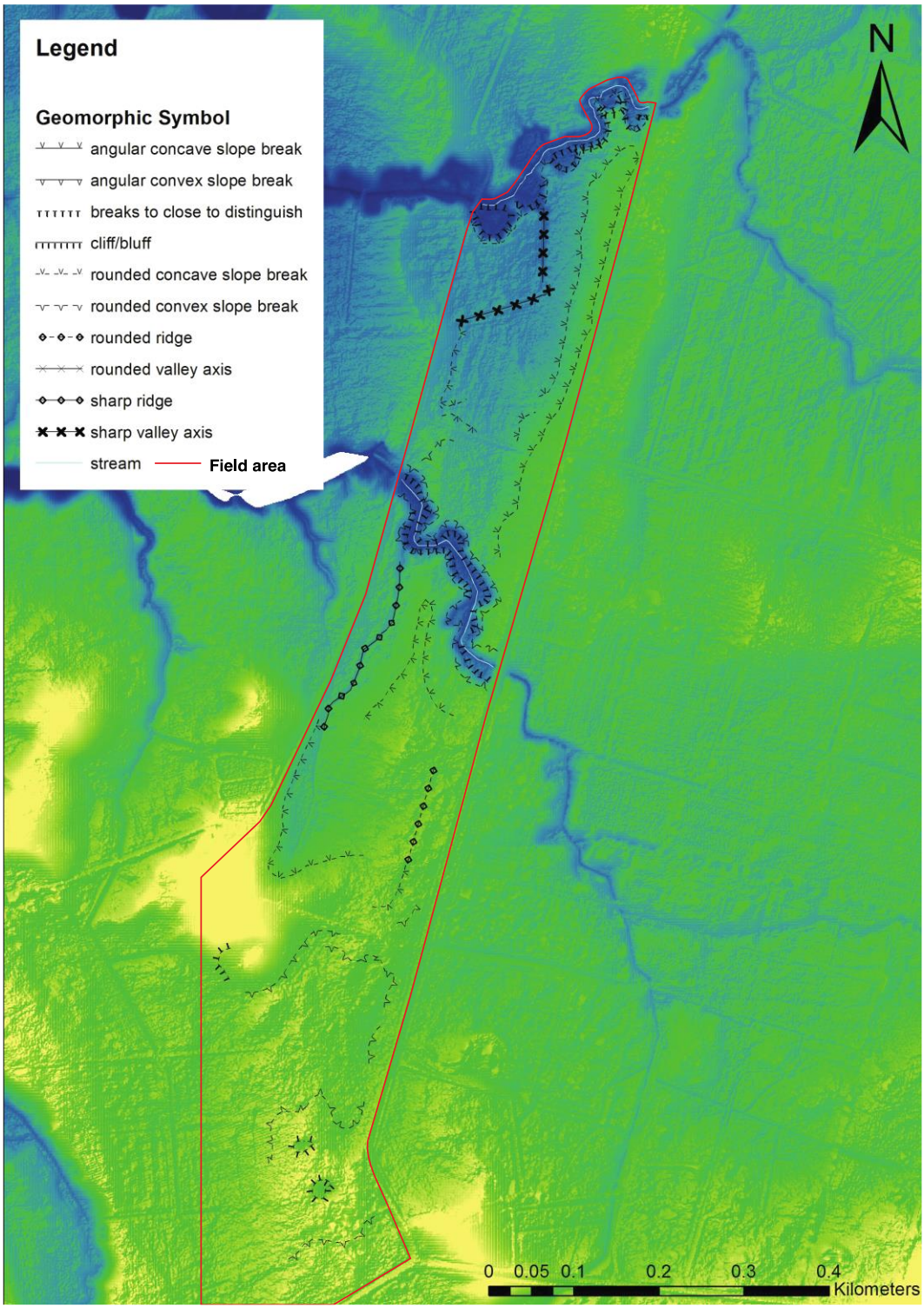

Figure 5.4 - Geomorphic map of the Osborne Road field area with LiDAR information also shown.

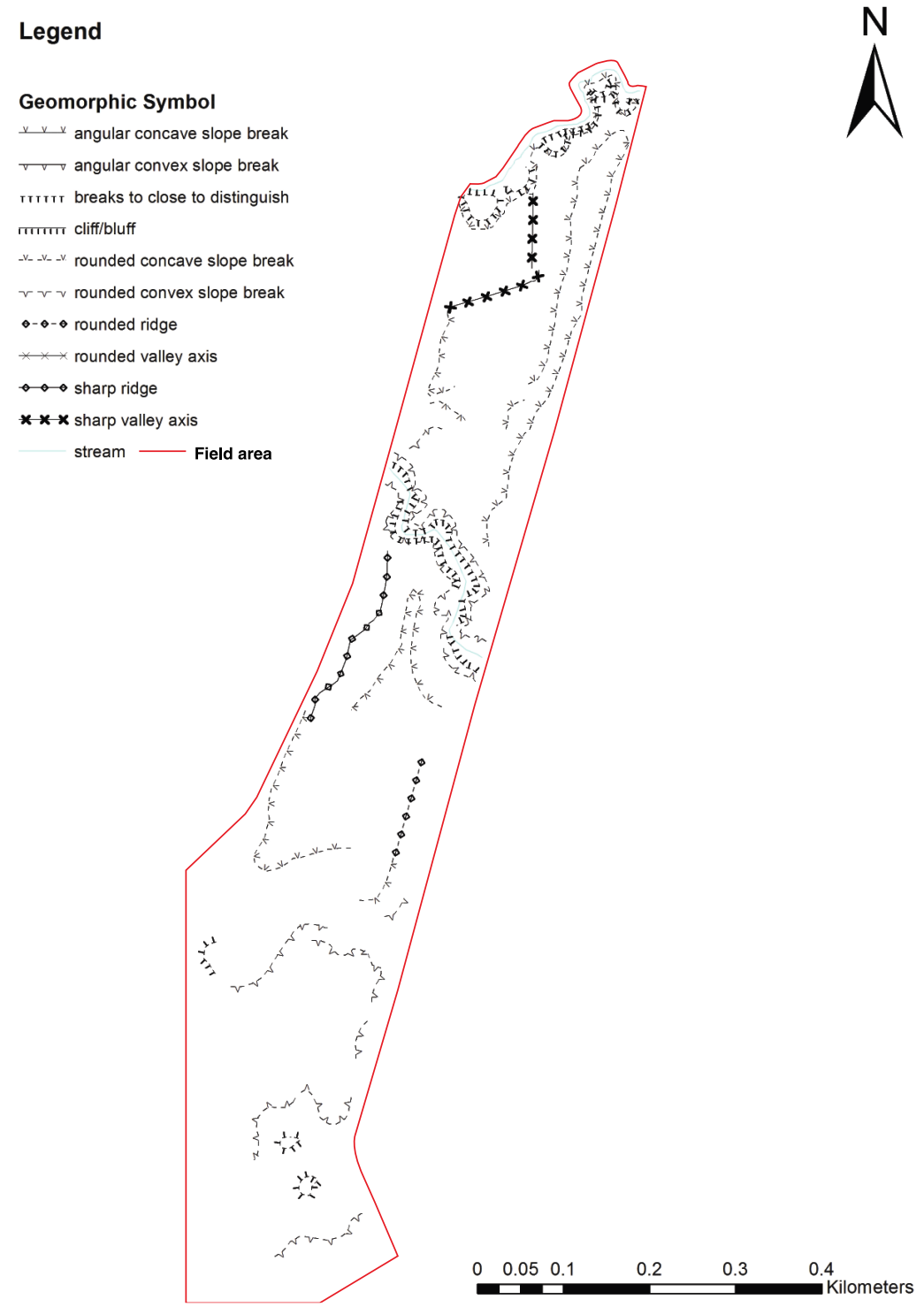

Figure 5.5 - A simple map depicting the geomorphology of the Osborne Road field site with no image behind geomorphic symbols. Map was prepared using ArcMap.

As shown in Figure 5.3 – Figure 5.5, the geomorphology of the Osborne Road field site is dominated by a slope break running through the easternmost portion of the field area, approximately parallel to Osborne Road. To the east of this ridgeline, land elevation is approximately 39 m above sea-level (ASL). To the west of this

break, a decrease in elevation is observed, with the average land elevation being 37 m ASL.

The Osborne Road field site is primarily used as a grazing paddock for a dairy farm. Further research into the field area suggests that some modification of the landscape may have occurred, as shown by Figure 5.6, which illustrates an old farm track that runs through the field area. This farm track ran through the northern half of the Osborne Road field area during 2002 – 2004. However, by 2008 it looked as though the farm track had been abandoned and that the landscape had begun to recover.

Figure 5.6 - Image showing the Osborne Road field site in 2002 and 2008. Shown in this image is the recovery of an abandoned farm track running through the northern portion of the field area. This track did have a minor influence on modern day geomorphology.

Notable geomorphic features within the field area include a distinctive drainage network in the north of the field area and a few valleys and ridgelines scattered throughout the field area. Albeit minor, and somewhat masked by the current land use, a number of changes in geomorphology are observed throughout the field area. The ridgeline found in the east of the field area can be traced throughout the majority of the field area, although it does appear to splinter off into smaller ridges in the south of the field area (Figure 5.4).

A region of more complex geomorphology is observed within the middle of the field area, characterised by a number of terrace-like features surrounding a stream/drainage unit. This feature appeared continuous through paddocks to the west and east of the studied field area, and is marked by minor bluffs (< ~1 m) and step-down terraces in regions adjacent to a river running across the Osborne Road field area.

Not shown in Figure 5.3 – Figure 5.5 above are the flat zones of the Osborne Road field area. This is best illustrated by a concentration of blue in the LiDAR image shown in Figure 5.4 between the ridgeline in the east of the field and drainage gulley to the west.

5.3 Soil auger transects

Soil auger transects were deemed necessary to aid in establishing whether or not the escarpment running through the east of the field area is a consequence of tectonic deformation, or whether it is some other geomorphic feature, or formed by human activities. Consequently, soil auger holes were taken as an initial approach to better understand the distribution of soil units and the characteristics of soils found within the Osborne Road field area.

5.3.1 Initial transect

Preliminary soil auger descriptions began with a 65 m transect running east to west across the north of the Osborne Road field site. Initially, soils were sampled and described at 1 m intervals, however due to time constrains the interval was subsequently changed to 5 m. In total, four soil auger samples were taken at 1 m intervals, and 11 soil auger holes were taken at 5 m intervals. Descriptions of these auger holes were recorded onto field sheets, before being digitized and presented

as a fence diagram. This fence diagram (Figure 5.7) shows the relief of the Osborne Road field site, together with the distribution of identified units.

Soil sampling indicated that silts tend to dominate the Osborne Road field area. Although multiple units were identified within the Osborne Road field area and presented below, it was quickly established that many shared similar characteristics. This was particularly true with silts found in the field area, which were only differentiated due to minor differences in grain size or slight colour differences.

Noted during the sampling of soils within the Osborne Road field area was the discernible difference in the characteristics of soils found on either side of the ridgeline. To the east of the major ridgeline running north-south, material sampled was generally coarser grained (silty sands). To the west of the ridgeline, materials were dominated by finer-grained material, primarily sandy silts and clays. This break in soil characteristics is illustrated in Figure 5.7, 5.9, 5.10 and 5.11.

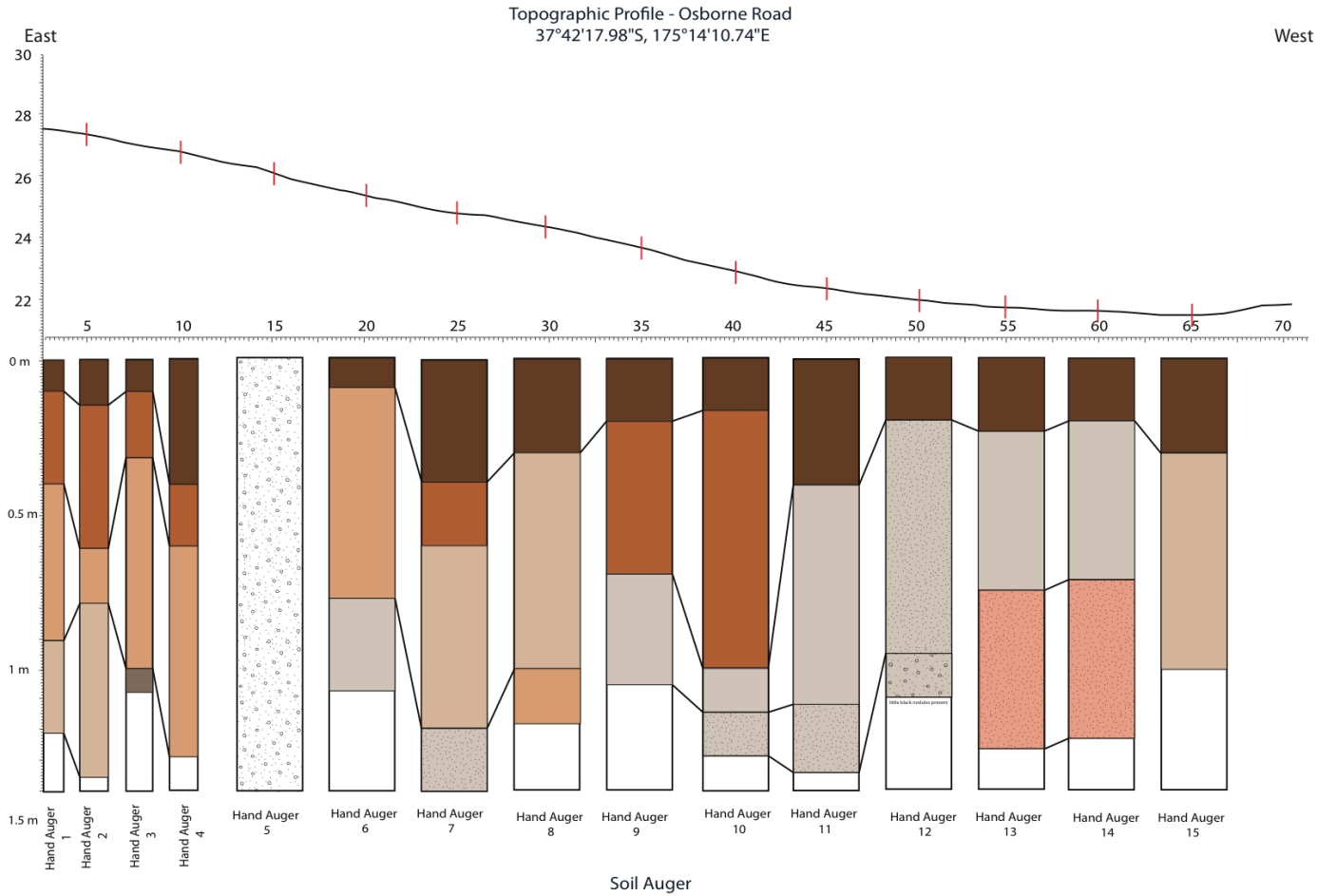

Figure 5.7 - Fence section of soil auger descriptions taken from the initial Osborne Road soil auger sampling transect. Shown in the top of this figure is the topographic relief of the Osborne Road field site (east to west). The middle of the transect illustrates horizontal distance across the profile, whilst the Y axis shows elevation on the top half, and soil auger sampling depth on the lower half. A description of the units shown in Figure 5.7 is depicted below in Figure 5.8.

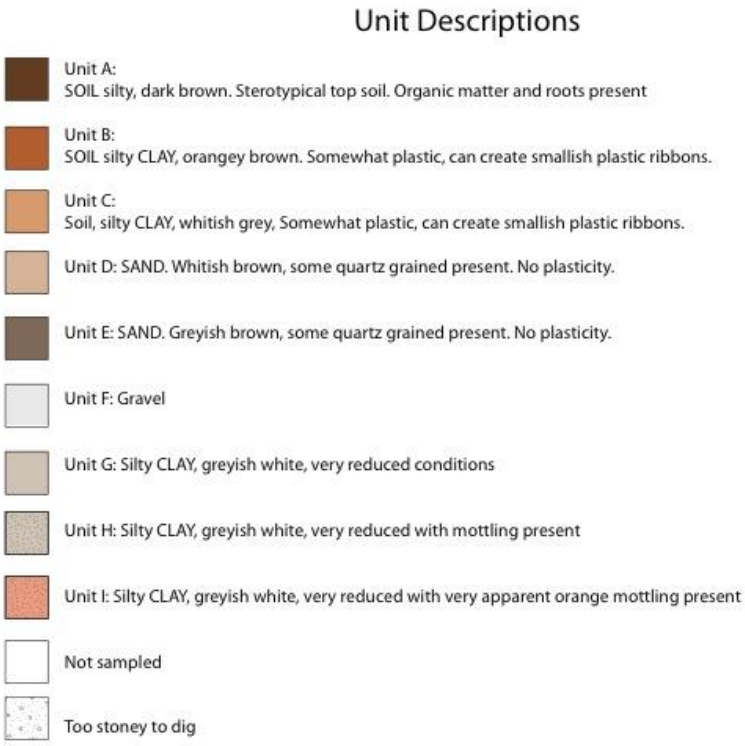

Figure 5.8 - A legend to accompany units illustrated in Figure 5.7. Units described in this legend all appear to be derivatives of the Hinuera Formation.

The soil description logs taken during soil auger sampling used to compile this fence section are attached as field notes (Appendices Q1 – Q15).

5.3.2 Secondary transect

Preliminary soil augering rounds showed a distinct break in soil units at the Osborne Road field site. Consequently, a second round of deeper soil auger holes using a 6 m Dutch auger was undertaken. Due to adverse climatic conditions and the saturation of lithologies of the units being surveyed, however, the depth of these soil auger holes varied significantly. Logs describing the units found in the secondary round of soil auger sampling are illustrated below in Figure 5.9 to Figure 5.11.

Three soil auger holes were taken along a single transect; these are labelled auger holes A, B and C. Transect sample A is shown below in Figure 5.9. As shown in this Figure, the profile was firstly dominated by silts, with a sharp transition into coarser sandy materials from the 1.5 m mark. This auger hole was taken 13 m west of the Osborne Road eastern fence line.

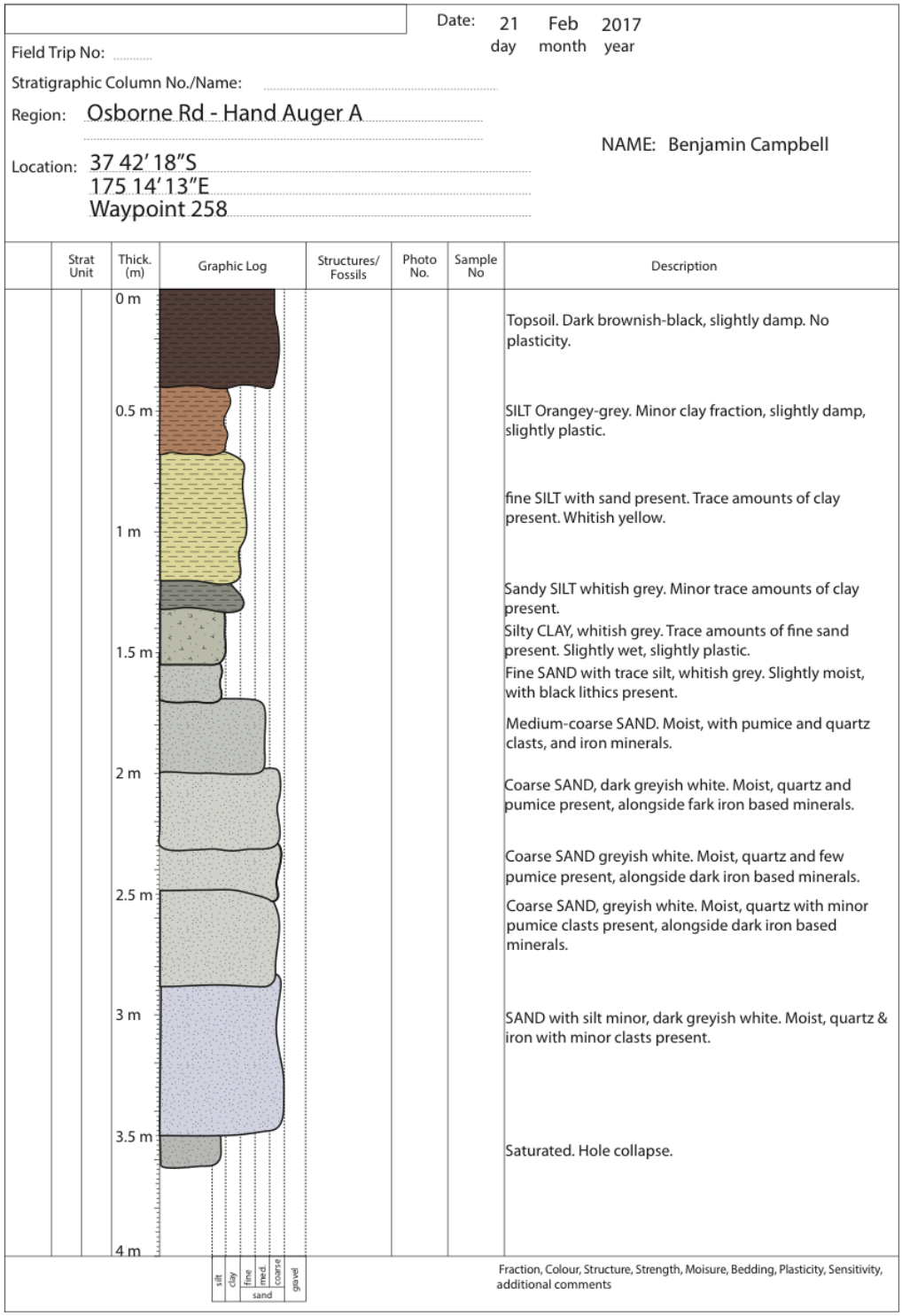

Figure 5.9 - The eastern-most transect taken at the Osborne Road field area.

Figure 5.10 details auger hole B findings which was taken in the middle of the field site, approximately 45 m west from the eastern fence line. As shown in Figure 5.10, the soil profile taken at hole B differs significantly from that of hole A (Figure 5.9). Found without the profile in Figure 5.10 is finer-grained clays and silts. Sandy

layers are present around the 2 m and 3 m mark in this profile. Generally speaking the profile was much finer grained than hole A (Figure 5.9).

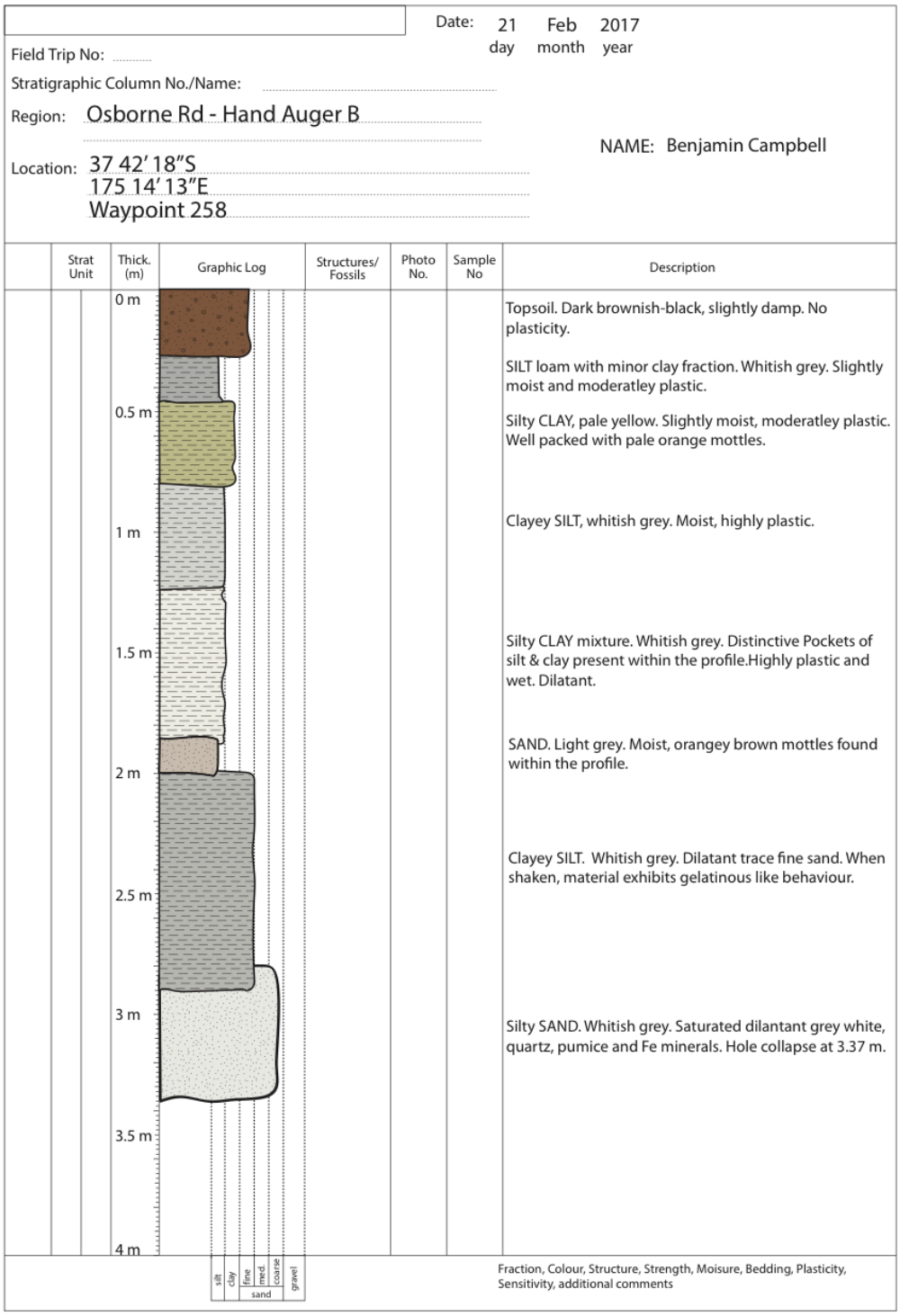

Figure 5.10 - Hand auger description log B. Taken in the approximate middle of the Osborne Road soil sampling transect.

Figure 5.11 shows the soil profile sampled at hole C; approximately 85 m west of the eastern fence line of the Osborne Road field site. As shown in this log, soil at location C was predominately silt. Due to saturation of the field area, the profile

could only be sampled to a shallow depth. A transition into sandy material was observed around the 1 m mark.

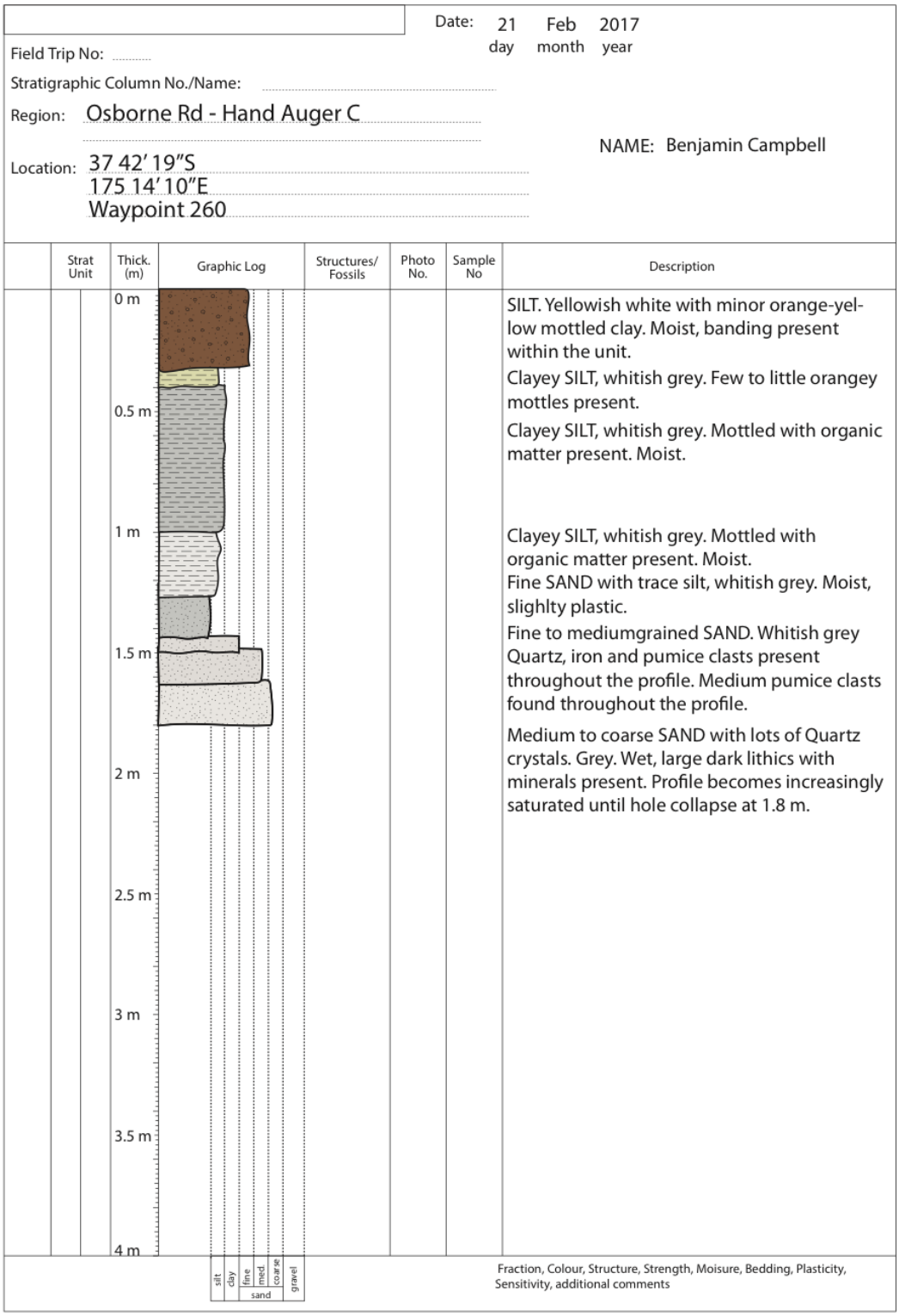

Figure 5.11 - Hand auger description log C. Taken approximately 85 m west of the eastern fence line at the Osborne Road field site.

As shown in the three soil auger description logs, clear differences in lithologies is apparent throughout the transect in the Osborne Road field area. To better understand the varied distribution of units within Osborne Road, soil resistivity surveys were conducted.

5.4 Soil electrical resistivity surveys

Soil electrical resistivity surveys were taken at Osborne Road to best establish characteristics of units within the field area. Processed results of soil surveys are shown below in Figure 5.12 - Figure 5.19.

Figure 5.12 shows a simple inverted resistivity transect of the Osborne Road field area. This resistivity survey was conducted across the same transect as initial soil auger samples (37°42'17.98"S, 175°14'10.74"E WGS84). As shown in Figure 5.12, areas shaded in cooler colours (blues) are areas of low electrical resistivity like silts and clays.

Hazreek *et al.* (2015) found that gravelly sands often have a higher approximate soil electrical resistivity values between 278 Ωm & 285 Ωm, compared to finer grained materials such as silty sands that had an approximate electrical resistivity between 223 Ωm & 199 Ωm. On the basis of this, we interpret that areas of blue in Figure 5.12 as reflecting silty material, with warmer areas (red – yellow) reflecting coarser sandy material.

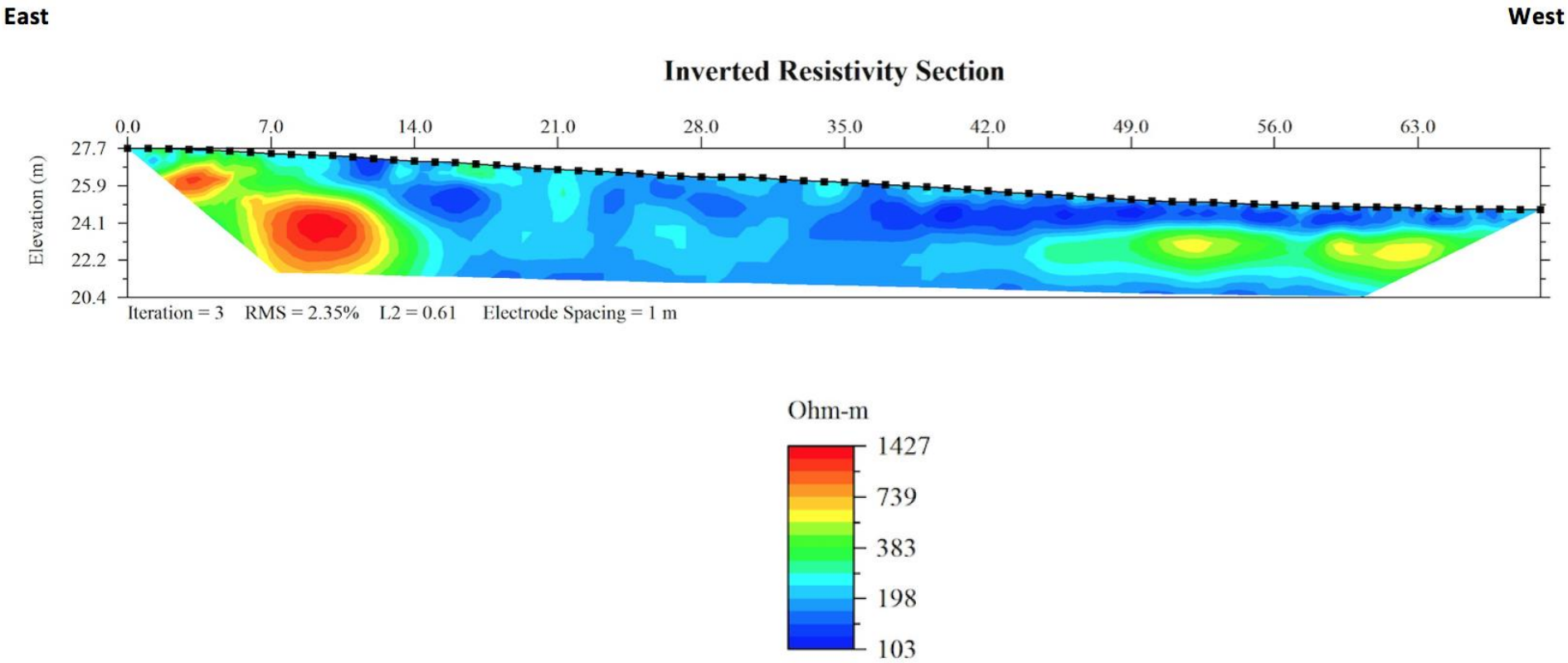

Figure 5.12 - A 2D inverted resistivity survey completed at Osborne Rd. Higher electrical resistivity occurs in the east of the field area, with an increase in resistivity also observed in the western-most region of the Osborne Road field site. Shown in the middle of this image is a concentration of lower soil electrical resisitivity, believed to be an area of finer grained materials.

An accompanying apparent resistivity crossplot is shown below in Figure 5.13. Figure 5.13 compares electrical resistivity measured in the field on the X axis, with simulated results generated by software shown on the Y axis. The integrity of data is improved the closer to 1:1 results are plotted. As shown in this image, an obvious relationship appears between measured vs. calculated values, suggesting that the data measured in this survey is credible.

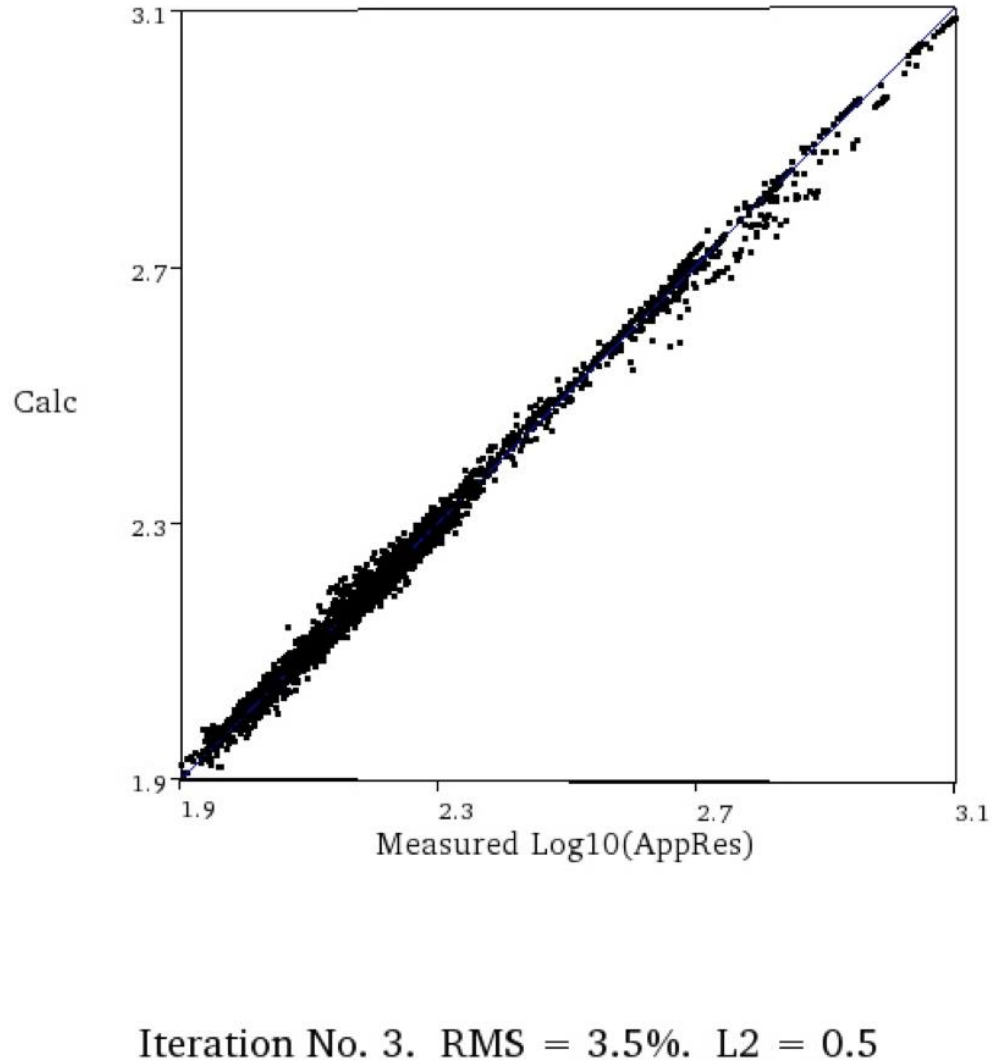

Figure 5.13 – A graph showing an apparent resistivity crossplot. Shown in this image, few outliers are plotted, and the relationship between measured and calculated data resembles 1:1. This supports the robustness of resistivity surveys undertaken within the Osborne Road field area.

Figure 5.14 shows clear variation in the electrical resistivity of material surveyed. This implies variability in the materials themselves. Also observed is a concentration of high resistivity volumes in the east of the field area – with such distinctive boundaries, and such different characteristics (both electrical resistivity

and grain size sampled during soil auger sampling), we infer that faulting has occurred due to the clear offset and differentiation of units.

With initial survey results corroborating the idea that tectonic deformation has occurred in the Osborne Road field area, alternate surveys were taken to improve the understanding of this deformation. A 3D resistivity survey was carried out, with Figure 5.14 - Figure 5.17 illustrating the results of this 3D survey.

Figure 5.14 below shows results of a 3D inverted resistivity survey. This was generated using methods outlined in Chapter 3. Similar to Figure 5.12, higher electrical resistivity is occurs to the east of the ridgeline running through the field area. Inverted resistivity image modelled from 3D survey is shown below.

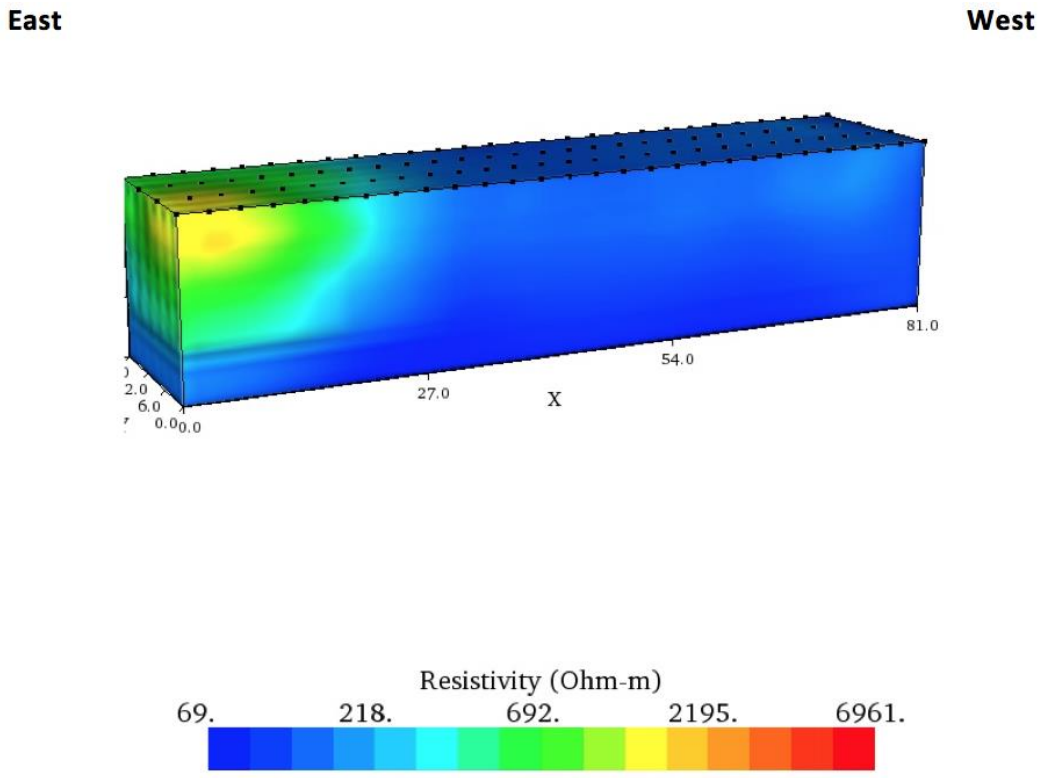

Figure 5.14 – A simple block model showing a 3D perspective of the surveyed area. Black dots shown on top of the resistivity image represent each sample electrode, and the lines joining these dots illustrate the surveyed transects.

A sliced version of the survey from an alternate perspective is shown below in Figure 5.15. Observed in this image is a concentration of materials with high electrical resistivity in the 2nd transect.

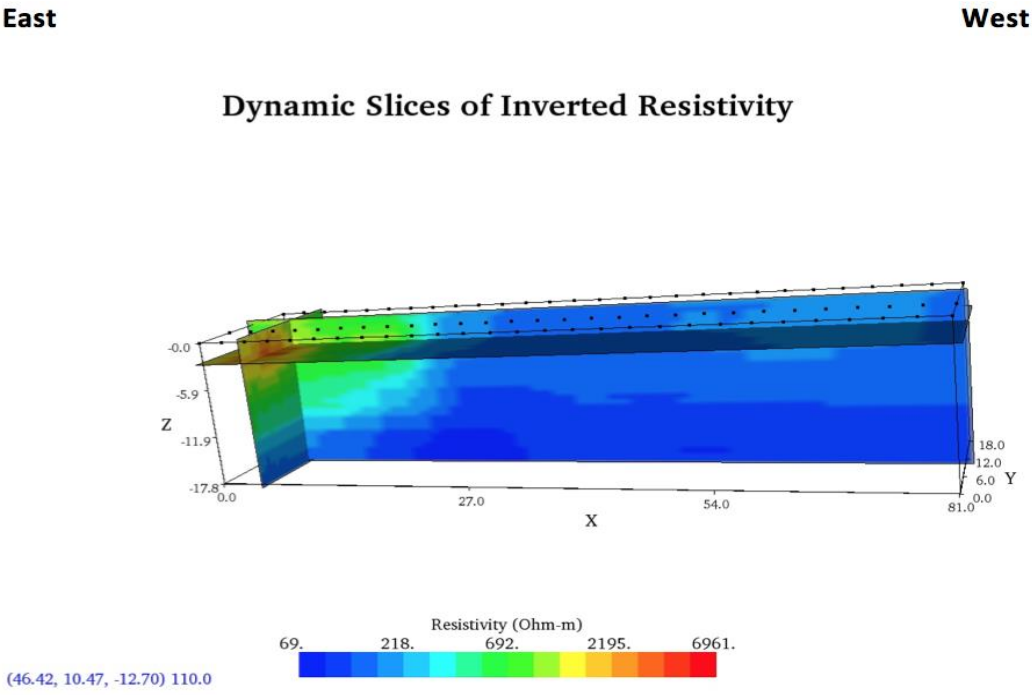

Figure 5.15 – A sliced perspective of the 3D resistivity survey conducted at the Osborne Road field site.

Figure 5.16 below illustrates bands of common resistivity observed within the profile. As shown in this image, a clear distinction between the concentrations of material with higher soil electrical resistivity in the east of the profile can be made, compared to areas of lower soil electrical resistivity to the west.

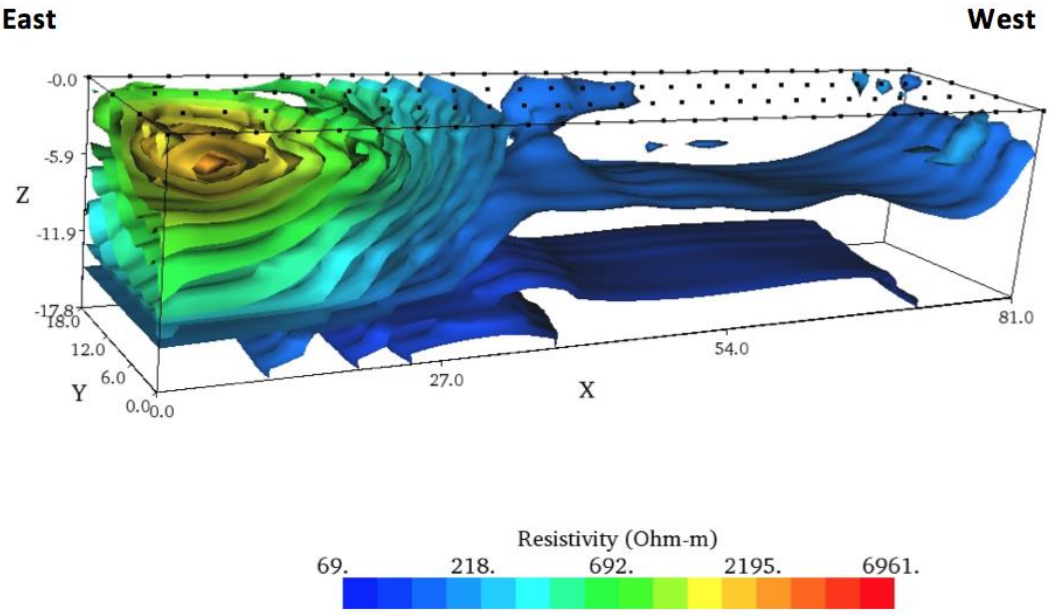

Figure 5.16 - A contour plot illustrating soil electrical resistivity taken across transects in the Osborne Road field area. Shown in this image are black dots at the top of the image to illustrate where electrodes were placed for this survey.

An alternative perspective of the same survey is depicted below in Figure 5.17. Shown clearly in Figure 5.17 is a concentration of material with higher electrical resistivity in the east of the field area, alongside the inferred break in soil characteristics.

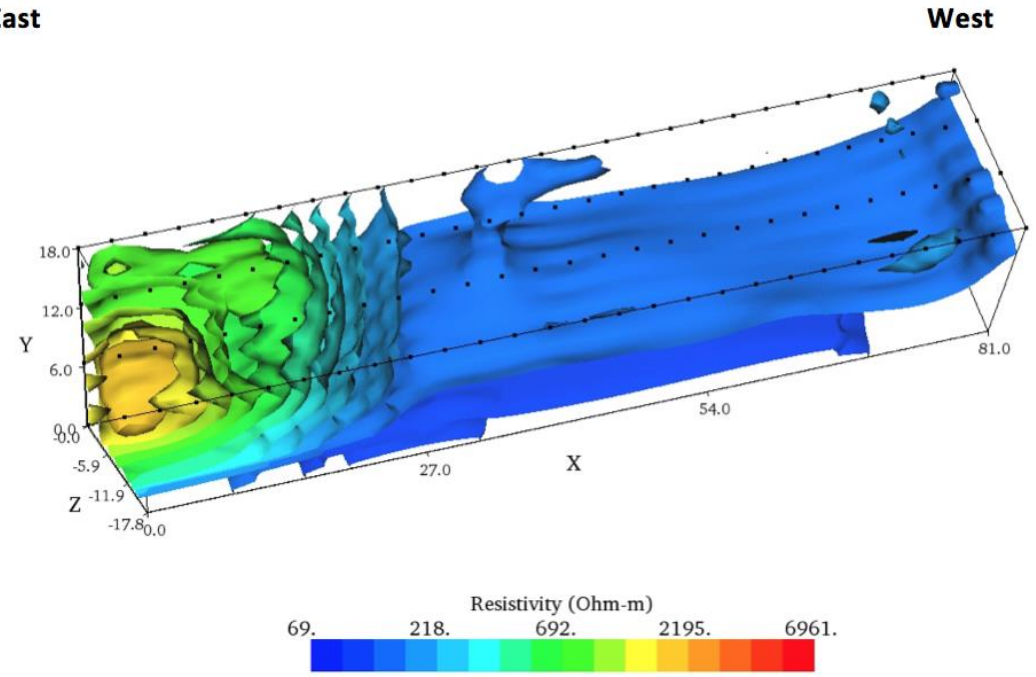

Figure 5.17 – A birds-eye view perspective of the 3D survey conducted within the Osborne Road field area.

As shown in the soil resistivity surveys, a clear concentration of material with higher electrical resistivity is observed in the north east of the field area, with resistivity peaking at approximately 2200 Ohm-m. Conversely, material of significantly lower resistivity (~69 Ohm-m) is found widely distributed throughout the western portion of the field area. This change in resistivity aligns with the mapped break in slope shown by geomorphic mapping of the field areas.

This clear change in electrical resistivity is a trend that is easily observed in Figure 5.14 - Figure 5.17. Such a sharp change in resistivity is somewhat uncharacteristic, and consequently I infer some sort of deformation to have taken place in order for present day units distributed in their current form at Osborne Road. Figure 5.16 and Figure 5.17 support the idea that deformation has occurred at Osborne Road by the pattern of resistivity that is shown, and the inferred break in material observed.

5.5 Hybrid models

When electrical resistivity surveys are compared to soil auger transects, clear similarities between the material found in soil auger sample holes and the level of electrical resistivity appear. A legend of the units found within the field area and included in Figure 5.19 is shown in Figure 5.18. An overlay comparing electrical resistivity observed in the Osborne Road field site, with soil auger logs is shown in Figure 5.19.

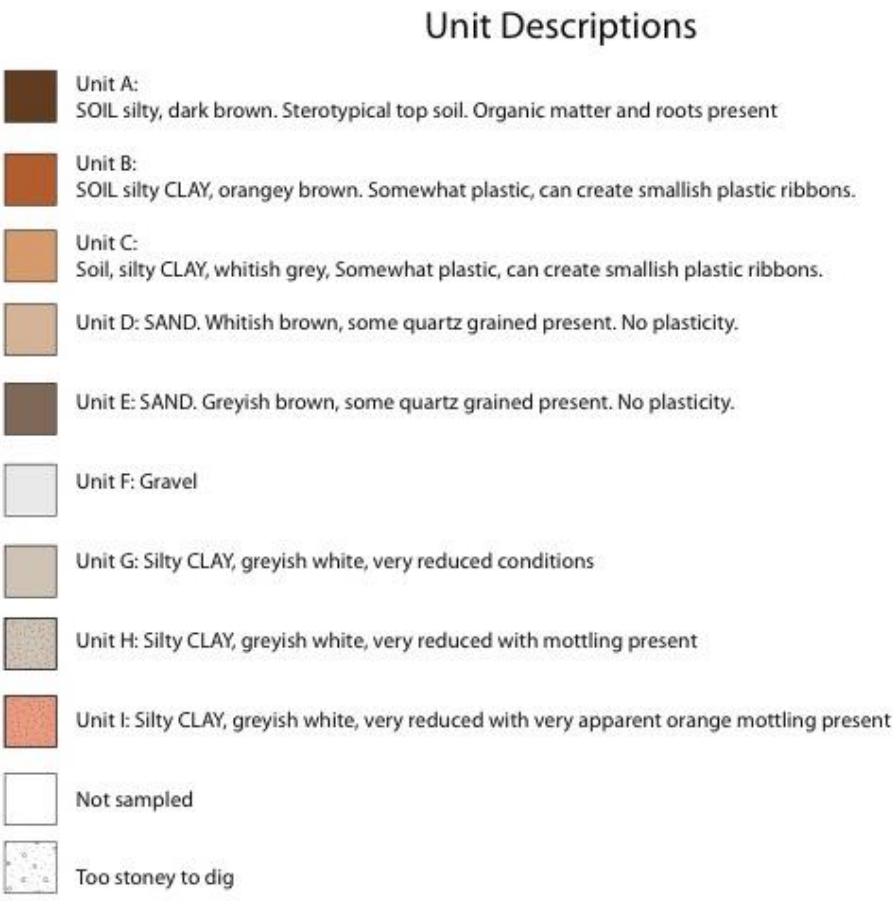

Figure 5.18 - Legend of units found within the Osborne Road field area that have been used in Figure 5.19.

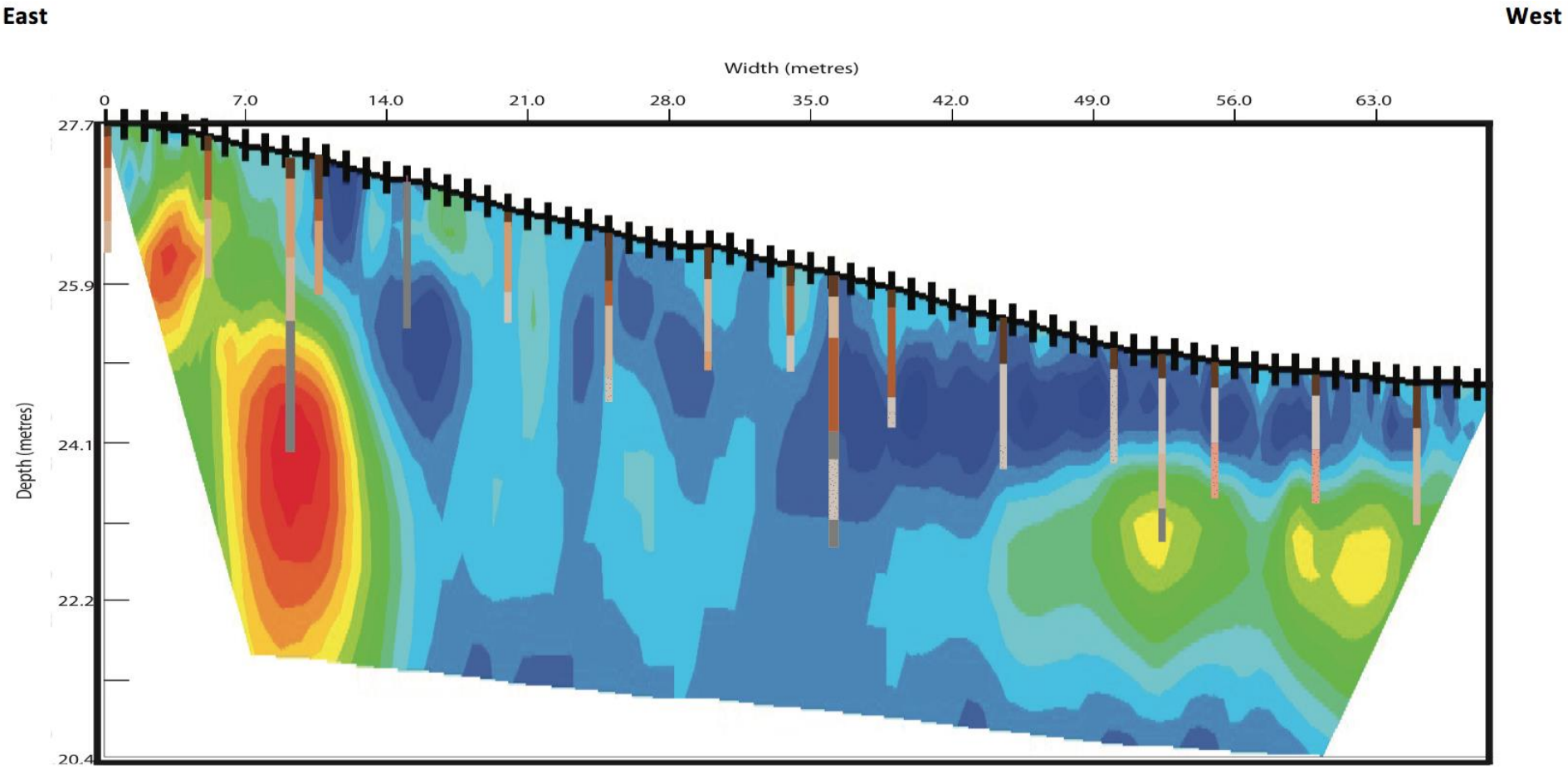

Figure 5.19 - Hybrid model combining soil electrical resistivity information with sampled soil auger logs. A legend describing soil units used within this model is shown in Figure 5.18.

Figure 5.19 illustrates the distribution of units within the Osborne Road field area, as well as offering insight into potential deformation within the field area.

Immediately apparent is the correlation between electrical resistivity and various units found within the field area. Clearly shown in Figure 5.19 is a link between higher levels of electrical resistivity and the coarseness of material. As shown in the east and west of the field area, increased electrical resistivity is found in regions with warmer colours. Incidentally this is where the coarsest materials observed in the field area were located. Areas of lower resistivity (cooler colours) were found where finer grained units, including silts and clays were predominantly found. To the east of the inferred fault, we observe coarser grained sands, typical of the Hinuera Formation. Conversely, the west of the fault exhibits silts and clays typical; also units typical of the Hinuera Formation.

The matching of soil units and the link to electrical resistivity is a consistent trend that is observed throughout the profile. Also observed throughout the profile is a distinctive boundary between soil units. This is documented by both soil auger samples and electrical resistivity surveys, which show a clear break in what should be a continuous soil unit. This change in soil properties is marked by a concave slope break located between 37°42'15.56"S, 175°14'12.51"E (WGS84), and 37°42'31.53"S, 175°14'6.75"E (WGS84). To the west of this slope break (inferred fault), silts and clays were discovered. For present lithology observed in the east of the field area, it is suggested that the Osborne Road field area has been subject to reverse faulting, whereby the eastern block has been occurred. Further discussion of this inferred faulting is presented in Chapter 6.10.

5.6 Summary

The Osborne Road field site was first identified through observation of geomorphic signatures within the landscape. Tied to a ridgeline that offsets the Waikato River, the Osborne Road field site contained a number of geomorphic features, indicative of tectonic deformation.

Consequently, site investigation at the Osborne Road field site was undertaken. Investigation began with geomorphic mapping of the Osborne Road. Geomorphic mapping showed a clear break in slope running through the eastern portion of the

Osborne Road field area, believed to be a fault scarp. Whilst other geomorphic features noted supported the idea that the field area was deformed, it became increasingly apparent that the inferred faulting was contained to the east of the field site, due to a lack of features observed in the west of the field area.

Soil augers were then undertaken across this inferred fault zone. Results indicated that the east of the inferred fault was primarily derived of younger sands with some silts of the Hinuera. As soil augering is somewhat limited, soil electrical resistivity surveys were conducted, to characterise the presence of units within the field area. These surveys corroborate hypothesis that the east of the field area was dominated by coarser material, compared to finer grained material observed in the west of the field area.

Evidence suggesting tectonic deformation has occurred within the Osborne Road field area is substantial. Discussion of this evidence, and subsequent analysis of the Osborne Road field area are presented in Chapter 6.10.

Chapter 6

Discussion

6.1 Introduction

Literature regarding the Hamilton Basin is confined to a few authors across a relatively small time period. Consequently, significant knowledge gaps exist, particularly in regards to structural features and deformation within the Hamilton Basin. Studies regarding the extent of tectonism have been limited, suggesting that only the outer extent of the Hamilton Basin has been subject to tectonic deformation. Recent investigations by McKay (2017), Moon and de Lange (2017), Spinardi (2017), Spinardi *et al.* (2017 (In Press)) and Kleyburg (2015) suggest otherwise however, proposing that the Hamilton Basement is more complex than previously thought.

The identification of multiple deformation features within the Basin has led to funding from the EQC and the Waikato Regional Council, encouraging further investigation within the Hamilton Basin. Through study of sidescan and multibeam data within the Waikato River, and LiDAR information of the Hamilton Basin, more evidence was found further supporting hypotheses that faulting is present within the Hamilton Basin. As a consequence of this increased interest, discussion regarding deformation within the geological communities has occurred, with many members of the geotechnical community noting evidence of deformation within the Hamilton Basin. Ultimately, the identification of offset within the Kay Road field site through workers involved with construction of the Waikato Expressway is how one of the cornerstones of this investigation (Kay Road field site) was discovered.

This chapter expands on research undertaken in this investigation, and involves discussion of deformation within the Hamilton Basin through a focus on the Kay Road and Osborne Road field sites. Firstly, units found within the Kay Road field area are outlined, with any irregular features found in these units presented. The whole Kay Road field area is then assessed, with sections addressing fault orientation, structural features recognised, deformation signatures discussed with

deformation then assessed, followed by comparison with literature. The chapter then discusses results of investigation at the Osborne Road field site, touching on evidence of faulting within the field area, irregular soil distribution, evidence of reverse faulting, and an assessment of the overall field area. Implications of evidence of deformation found at both the Osborne and Kay Road field sites are then discussed, alongside the implication this has for the Hamilton Basin.

6.2 Kay Road

A significant ridgeline thought to be a fault scarp (Figure 4.3) was first noted through observation of LiDAR data of the Hamilton Basin. Initial ideas that this ridgeline may be associated with tectonic faulting were confirmed during construction of the Waikato Expressway, and the resulting investigation described in this study was undertaken.

Study of the Kay Road field area showed that geologic units are typical of those found throughout the Hamilton Basin, with the Hamilton Ash Beds including the Rangitawa Tephra, Kauroa Beds, Karapiro Formation and Puketoka Formation found within the Kay Road field area. Arranged chronologically from youngest to oldest, Figure 6.1 below shows the expected distribution of these units, as reported by Lowe *et al.* (2001).

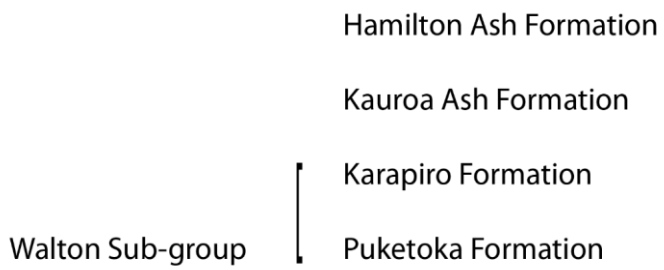

Figure 6.1 - A simplified stratigraphic interpretation of hills throughout the Waikato Region, interpreted by Kamp & Lowe (1981).

The oldest unit in the field, the Walton Sub-group incorporates the Karapiro and Puketoka Formations. With oldest members dated 3.0 Ma (Kear, 1961) and youngest members dated between 2.58 - 1.26 Ma (Nelson *et al.*, 1988; GNS, 2017c), the Walton Sub-group is diverse in both characteristics and distribution. Overlying these units is the Kauroa Ash Formation, dated at c. 2.25 Ma (Lowe *et al.*, 2001), which encompasses the gold coloured Kauroa beds found extensively

throughout the Kay Road field site. Younger still, is the Hamilton Ash series, which is comprised of paleosols and multiple weathered tephra units, and can be found blanketing the older Kauroa Ash Formation and Karapiro Formation. Included in the Hamilton Ash Formation is the Rangitawa Tephra, at the base age of 0.35 Ma (Lowe *et al.*, 2001).

It is expected that these units would be found distributed within the landscape similar to that presented in Figure 6.1, however this was not the case at the Kay Road field site. As shown by Figure 4.8 and Figure 4.9 which illustrate the distribution of units within the Kay Road field area, extensive deformation is present, with irregular distribution of the Walton Sub-group, Kauroa Ash Formation and the Karapiro Formation found scattered throughout the exposed profiles (NE, NW, SE and SW).

6.2.1 Walton Sub-group

The Walton Sub-group was the oldest and lowest lying unit found in the Kay Road field area, and exhibited many characteristics synonymous with tectonic deformation. Observed in all studied faces (NE, NW, SE and SW), the Walton Sub-group incorporated multiple members, with properties of the formation varying significantly dependent on location. Primarily, the unit was dominated by silts and clays, with some coarsening of the unit observed in the higher lying NE and NW exposures of the formation. As shown in Table 1 however, various compositions of both silt, clay and minor sand were documented during this study in the field area.

6.2.1.1 Offset bedding within the Walton Sub-group

Dominated by lighter white and grey colours, the unit exhibited distinctive iron and mica staining, resulting in formation of easily distinguishable beds. This is best illustrated by Figure 4.16, 4.17 and 4.18 which show images of the Walton Sub-group, and the easily distinguishable beds within the formation. This bedding was paramount to the identification of deformation, as banding within the unit helped clearly establish both the presence and size of offset. Bedding within the Walton Sub-group was most easily recognisable within the SW and SE of the field area, as the exposures were cut cleaner, and were almost exclusively comprised of the

Walton Sub-group. Beds were also recognisable within the NE field area, but due to the height of the NW cutting in the Kay Road field area, were only just visible.

Bedding within the Walton Sub-group is likely associated with the varied and extensive nature of deposition within the formation, and diverse parent materials of the unit; incorporating pumiceous silt from volcanic origins, and sedimentary sands, gravels, silts and clays (Murashev *et al.*, 2012). Deposition of the Walton Sub-group occurred during the Pliocene to the early Pleistocene (5.33 Ma and 2.68 ma), some 2.65 million years. As such, the distinctive bands are observed throughout the unit, with this distinctive bedding attributable to the variable climatic conditions throughout this time period, and consequent weathering that the Walton Sub-group experienced (GNS, 2017d, 2017e).

Vertical offset was significant within the Walton Sub-group, as shown by offset bedding. Offset measured within the formation ranged from a few mm within beds in the NW and NE faces, to more than 3.6 m of major displacement within the SW face. This major offset is best illustrated by Figure 4.10, which shows a 3.6 m offset of the Walton Sub-group in a digital cross section of the SW face. Smaller offset is also shown, with Figure 4.16 illustrating 320 mm of offset within the formation, and Figure 4.19 illustrating multiple, repetitive offset beds (~approximately 0.04 m) within the Walton Sub-group in the SE face.

6.2.1.2 Intrusion Structures within the Walton Sub-group

Deformation within the Walton Sub-group was not limited to offset bedding however. Other evidence indicative of tectonic deformation within the formation was the extensive presence of injection structures. The clearest example of an injection structure is shown in Figure 4.26, Figure 4.27 and Figure 4.28. These figures were observed in secondary study of the Kay Road field site, which occurred once construction of the Waikato Expressway had excavated lower lying units. Although continuous with the lowest units initially observed in the Kay Road field area, deeper cutting of the Walton Sub-group did show slight variation of the formation. Hydro-seeding of the exposed Walton Sub-group had recently occurred prior to field study, however, so the unit exhibited an atypical purple-grey colour

(as shown in the matrix around structures in Figure 4.26, Figure 4.27 and Figure 4.28).

The presence of the observed intrusion structure outlined in Figure 4.26, Figure 4.27 and Figure 4.28, alongside smaller intrusion structures within the NW of the field area supports the idea of tectonic deformation within the Hamilton Basin, as this type of intrusion structure is typically generated as a consequence of seismic forces (Obermeier, 1989; Madabhushi & Haigh, 2012; Quigley *et al.*, 2013; Bastin *et al.*, 2015).

6.2.2 Karapiro Formation

Although the Karapiro Formation falls under the Walton Sub-group, this section addresses the Karapiro Formation exclusively. The Karapiro Formation was somewhat coarser than younger members of the Walton Sub-group found in the field, and was dominated by orange silt and clay with minor sand. Two variations were observed in the field area, a sandy clay (K1) and a silty clay (K2). Both units were slightly plastic, and appeared to have volcanic origins as documented by pumice clasts and the presence of quartz, mica flakes and iron. Generally, these descriptions align with those presented by Kamp and Lowe (1981), who describe the Karapiro Formation as weathered, cross bedded volcanic grits, pumiceous rhyolites and rhyolitic gravelly sands with varied degrees of weathering.

Discussed by Kamp and Lowe (1981), the Karapiro Formation should lie unconformably over the Puketoka Formation. For the most part within the Kay Road field area, this is true, however in the NW face (shown in Figure 4.8), the Karapiro formation can be seen lying unconformably over weathered tephra variation 2 (WT2), and adjacent to the younger Kauroa Beds. Atypical distribution of the unit suggests that the Karapiro Formation was deposited, prior to the extensive deformation that occurred within the Kay Road field area.

Similarly, Figure 4.9 shows two variations of the Karapiro Formation within the NE of the Kay Road field area. In this image, the unit K2 is found lying unconformably on top of older members of the Walton Sub-group, and K1 found in line with the relatively up-lift Walton Sub-group (silt variations found in eastern and western extent of the NE face). It appears that normal faulting has resulted in the Karapiro

Formation being down-thrown, relative to the older silt members Walton Sub-group, as the Walton Sub-group is found on either side of the unit along two identified fault planes. The most logical reason for this displacement is that substantial tectonic deformation of the Kay Road field area has occurred, resulting in significant normal faulting and subsequent down-throw of units within the field area.

6.3 Kauroa Ash Formation

The Kauroa Ash Formation was found in both the NW and NE faces within the Kay Road field area, and presented as a golden, clayey-silt. The unit was extremely weathered, aligning with descriptions made by Kamp and Lowe (1981). Within the Kay Road field area, the Kauroa Ash Formation exhibited extensive deformation, presenting as a series of tilted, rotated, and uplifted blocks in the NW of the field area, and as tilted, offset repetitive beds in the NE of the field area. This irregular distribution is best shown by Figure 4.8 and Figure 4.9, which show the deformed unit.

It is clear that the Kauroa Ash Formation is incredibly deformed in the NW of the Kay Road field area. Determining the method of deformation however is difficult, due to the irregular properties of the unit. In the NE of the field area, however, the Kauroa Ash Formation exhibits behaviour associated with normal faulting, whereby the unit has been split in two, and the southern block has been down-thrown relative to the northern block. This is a similar trend to the normal faulting observed within the Walton Sub-group, whereby down-throw of the southernmost blocks is apparent.

The key difference between displacement of the Kauroa Ash Formation in the NW of the field area when compared to the NE of the field area is the scale. Displacement of the Kauroa Ash Formation in the NW of the field was significantly larger, with displacement varying from the smallest 2.41 m of down-throw to the largest 8.5 m of down-throw (Figure 4.44). This is compared to the 3.04 m of displacement observed in the NE of the field area (Figure 4.43).

This displacement shows that the Kauroa Ash Formation has been subject to significant tectonic deformation. Although the Kay Road area is largely thought to

have been influenced by normal faulting, some relative uplift of the Kauroa Ash Formation is present, suggesting that the region may have also been subject to crustal compression and reverse faulting, alongside the extensive normal faulting observed within the region. This reverse faulting likely represents relatively localised re-arrangement of blocks associated with normal fault movement.

6.4 Hamilton Ash Formation and Tephra units

Many tephra units were found within the NE and NW of the field area, with colour being the primary differentiating property between variations observed. These Tephra units appeared to align with characteristics associated with older members of the Hamilton Ash Series, outlined by Kamp and Lowe (1981).

Within the field area, tephra units are clearly seen blanketing the older Kauroa Ash Formation, and other units within the field area. Comments on the status of deformation within the older members of the Hamilton Ash Formation is difficult however, due to a lack of features within them allowing for identification of offset. Consequently, deducing whether or not deformation has occurred within the unit is difficult.

6.4.1 Rangitawa Tephra

The Rangitawa Tephra was found overlying units near the top of the profile in the NW and NE of the Kay Road field area. The unit is 0.35 Ma, and exhibited clay like properties. A light brownish grey colour, the unit contained micaceous flakes, a key characteristic of the Rangitawa Tephra (Lowe *et al.*, 2001). Pumiceous material was also found within the unit. Descriptions of the Rangitawa Tephra outlined within Table 4.1 tend to parallel those widely published and accepted regarding the Rangitawa Tephra and its formation (Kamp & Lowe, 1981; Lowe *et al.*, 2001; Matthews *et al.*, 2012).

A widely accepted marker bed, and often used for dating purposes, the Rangitawa Tephra was found extensively throughout the higher lying NE and NW face of the Kay Road field area. No evidence of deformation of the Rangitawa Tephra was found within the Kay Road field area. Consequently, the unit forms an ideal marker bed helping to frame the timescale of deformation within the Kay Road field area.

6.5 Orientation of faults

Faulting within the Kay Road field area was extensive, and it was quickly established that the Kay Road field area was a fault zone, as opposed to a single fault plane. To help characterise the Kay Road field area, these faults were measured, and presented as stereonets in Figure 4.12 and Figure 4.14. These stereonets enable us to best understand structural trends observed within the field area, alongside observing the general mean of faulting within the field areas.

6.5.1 NW face fault orientation

Measurements of structural information within the NW of the Kay Road field area shows that faults generally trend along a N/S plane as shown by Figure 4.12. This plane is consistent with the general direction of a ridgeline running thorough the Hamilton Basin that is thought to have offset the Waikato River (Figure 6.11).

One outlier was observed in dip direction of faulting within the NW of the Kay Road field area, however. Whilst the majority of measured faults were running along a N/W plane, one fault was measured with a dip direction of 074° (NNW/SSE). While it is possible that this measurement may be incorrect, faults are known to bend as they propagate (Suppe, 1983). A fault running against the general trends of other faults observed in the field area does also help explain such chaotic deformation within the field area.

6.5.2 NE face fault orientation

When presented in a stereonet (Figure 4.14), two sets of faults are identified. The first, trends at 021° (NNE), the second trends at 343° (NNW). These faults are consistent with the overall N/S strike of those measured on the NW face, and all faults are consistent with the strike of a ridgeline running through the Hamilton Basin, which propagates between N and NE general directions.

An image presenting the strike of faults observed within the NE of the field area is presented in Figure 6.2. These averaged planes show a similar trend to conjugate faults, as presented by Thatcher and Hill (1991).

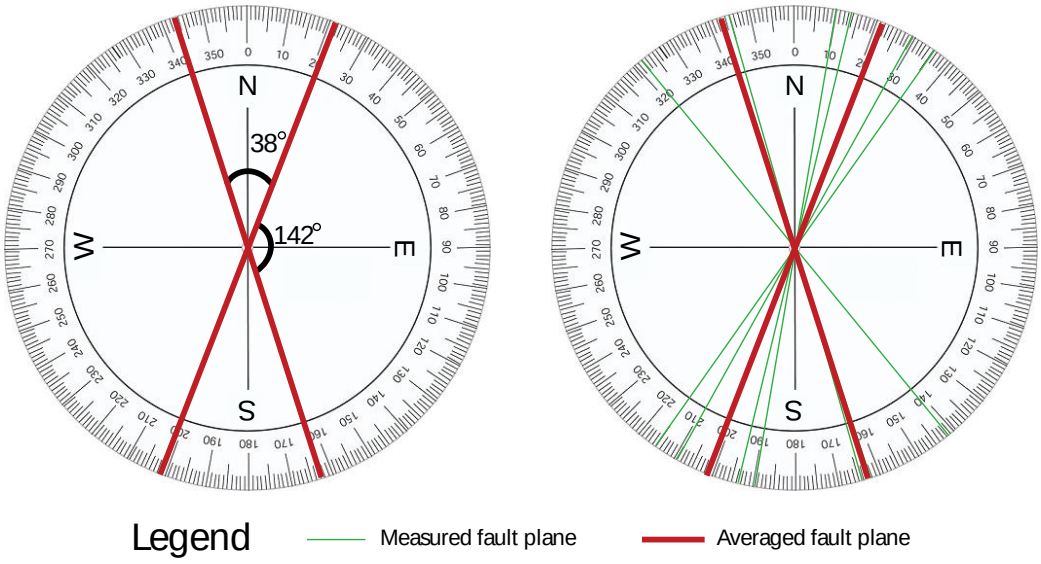

Figure 6.2 - Images showing fault planes measured in the NE face.

An image presenting various types of conjugate faults is shown below in Figure 6.3.

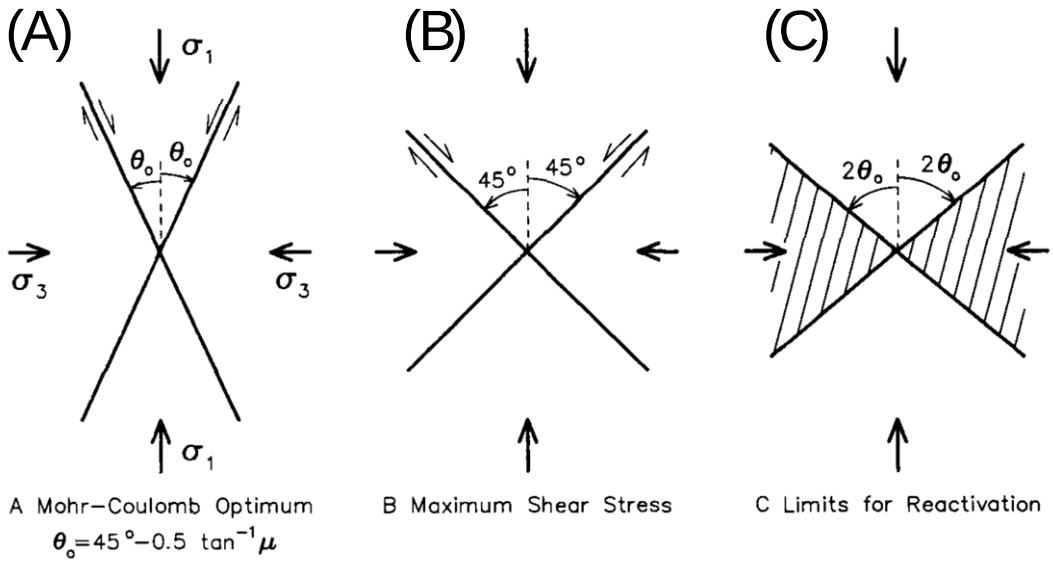

Figure 6.3 - Types of conjugate faults, as presented by Thatcher and Hill (1991).

When comparisons are made between Figure 6.2 and Figure 6.3, similarities between the faults observed in the NE field area, and those presented by Thatcher and Hill (1991) exist. Orense *et al.* (2012) suggest that pumiceous sands such as those found within the Karapiro and Puketoka Formations have friction angles of approximately 42 - 44°. Using the lower bound of 42° in the equation presented by Thatcher and Hill (1991) in Figure 6.3 (A), an estimate of θ_o of 24° is made, inkeeping with the measured value of 19°. As Orense *et al.* (2012) were using fresh

pumiceous sands, some weathering of the Karapiro Formation and Puketoka Formation is likely to have reduced the friction angle. We cannot confirm that faults observed in the Kay Road field area are conjugate faults, however, as we do not know the stress orientations causing the faults.

6.6 Structural Features within the Kay Road field area

The Kay Road field area has many recognised faults, resulting in chaotic deformation within the field area. Such extensive faulting however does generate multiple structural features. Many of the deformation signatures noted within the Kay Road field align with phenomena associated with crustal extension.

Distribution of geology within the area, alongside many structural features present, thus suggest that the Kay Road field area is a structural formation known as a graben. Graben are a geologic phenomenon whereby a depressed block of the Earth's crust is bordered by parallel faults (Lensen, 1958). Ultimately, the phenomenon forms valley like features with distinct escarpments on either side, caused by displacement of land downwards. Graben are typically produced in normal faulting, whereby relative displacement of the hanging wall is downward, while that of the footwall is upwards. When major faulting is only recognised along one side of the boundaries, the phenomenon is known as a half graben (Encyclopædia Britannica, 1998). The most easily recognisable graben is in the NE of the field area (Figure 4.9), and was approximately 40 m wide by 20 m high.

The Kay Road field area appears to be bordered by numerous faults. This is clearest in the southern portion of the field area, where clear boundaries between the Walton Sub-group and displaced members of the Kauroa Ash Formation and Hamilton Ash series are observed in both the SE and SW of the field (Figure 4.8 and Figure 4.9). Observation of these figures does illustrate some over thickening of the Kauroa Ash Formation and overlying paleosol and weathered tephra units, whereby beds considerably thicker than the 1 – 2 m suggested in literature review were observed. This suggests that faulting occurred, allowing displacement of the Kauroa Ash Formation into recognised grabens, and accumulation of overlying paleosol and weathered tephra units to occur, possibly mass wasting or surface

wash features. This can help shape the timeframe of faulting observed in the Kay Road field area.

From observation of the Kay Road field area, I suggest that the majority of displacement observed has been through means of normal faulting. This is documented by the down-thrown of younger units within the Walton Sub-group (Karapiro Formation), alongside displacement of the Kauroa Ash Formation. Consequent geologic formations appear to share characteristics similar to a graben. Figure 4.9 best illustrates this phenomenon, whereby normal faulting has generated a depression that has been infilled by the Kauroa Ash Formation, and units WT1, WT2, K1 and K2 units.

Normal faulting involves downward displacement of one block relative to another. Bordering the NE face within the Kay Road field area are somewhat parallel faults. These faults are normal in nature, that show apparent downward displacement of the Kauroa Ash Formation and Hamilton Ash series, which appear to have infilled a basin-like feature. This has resulted in a smaller scale graben. The presence of this deformation feature, alongside the overarching geology of the Kay Road field area corroborates hypothesis that deformation is present within the Hamilton Basin.

6.7 Deformation Features within Kay Road Field Area

Many signatures indicative of deformation were observed within the Kay Road field area. These are outlined within the following subsections.

6.7.1 Intrusion Structures

The presence of intrusion structures within geology of the Kay Road field area supports hypothesis suggesting that tectonic deformation is present within the Hamilton Basin, as the many of these structures are exclusively induced by tectonic deformation. Many intrusion structures were found within the Kay Road field area, cross cutting the Walton Sub-group and younger units. Identified intrusion structures within the field area included sand dikes and multiple liquefaction structures.

Liquefaction is a phenomenon that involves loosely packed, cohesionless, fine grained, saturated soils acting as fluids momentarily (Allen, 1982; Seed & Idriss, 1982; Kleyburg, 2015). The process can be broadly categorised into two categories; with the first, flow (static) liquefaction occurring in strain softening soils where the initial void ratio is higher than its steady or critical state, and the second type of liquefaction, cyclic loading, occurring when an oscillation force is applied and material is subject to both tension and compression. Typically, flow liquefaction is induced by either monotonic or cyclic loading where a material is subject to increased tension or compression. Cyclic liquefaction occurs in soils that experience shear reversal, whereby effective stresses reach values of zero or near zero. Both flow liquefaction and cyclic liquefaction can be induced by earthquake forces (Kleyburg, 2015). An image of an inferred liquefaction feature is observed in Figure 4.25.

Characteristics of injection structures within the Kay Road field area did vary somewhat from typical liquefaction structures. Primarily, this variation is due to the sheer size of the structure shown in Figure 4.26, Figure 4.27 and Figure 4.28. Although this feature could not be directly traced across the field area as gravel had been put down due to construction of the Waikato Expressway, it is inferred that this structure was continuous. This structure, shown in Figure 4.26, Figure 4.27 and Figure 4.28, is significantly larger than typical structure, spanning more than 9 m vertically within both the west and east of the field area. The structure is thought to have been continuous horizontally throughout the field. The feature is thought to have propagated into younger members of the Walton Sub-group, but due to the steep gradient of the cut face, the Walton Sub-group was unable to be cleaned and this cannot be confirmed. If the structure was continuous, it would also span over 37 m from west to east. Although size limits are undefined for intrusion structures, it would appear that this structure is significantly larger than those reported by Reddy *et al.* (2009), who report structures in their study ranging between 2 – 7 m. For size reasons, amongst lithological reasons, I suggest that the formation may be a sand dike, that has been subject to repeated deformation.

Sand dikes are a result of liquefaction at depth (USGS, 2017b). The phenomenon are induced through the upwelling of pressure through host sediments. An image

of a suspected sand dike found within the Kay Road field area is shown in Figures 4.23, 4.26, 4.27 and 4.28.

Sand blows are associated with tectonic deformation, and largely influenced by the local geologic setting in both development and surface expression of sand blows (Obermeier, 1989; Obermeier *et al.*, 1990). Although this does make drawing comparisons with other sand blows difficult, it would appear that some similarities between Figure 6.4 and the injectite found within the Kay Road field area, and published literature do exist. Consequently, it is implied that the matrix of the injectite is a sand blow that has been cross cut in the Kay Road field area, similar to that presented below Figure 6.4 (Sims & Garvin, 1995).

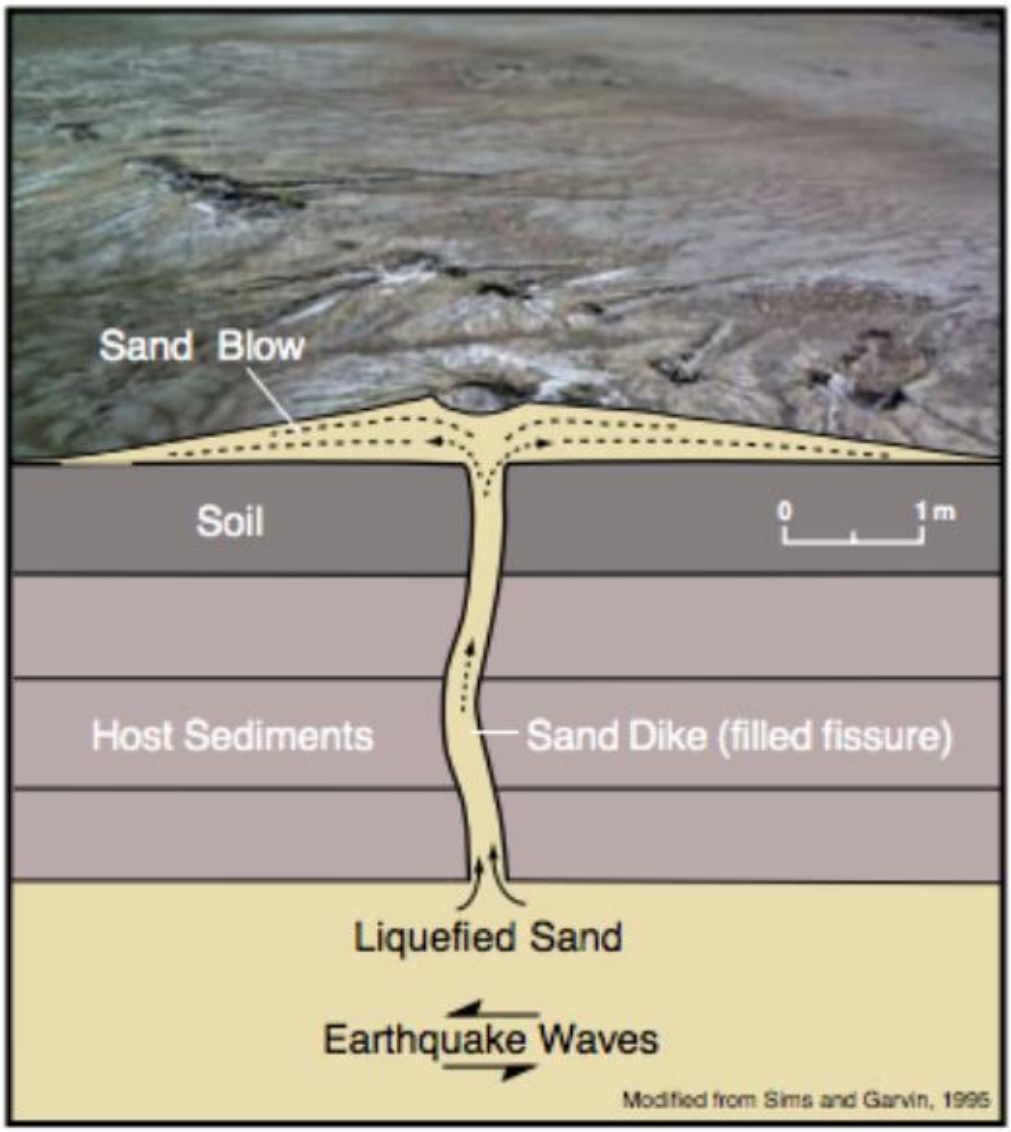

Figure 6.4 - Image of a cross section of a sand dyke, superimposed onto a photograph of a sand blow. Image taken from Sims and Garvin, 1995.

Observed in Figure 4.26, Figure 4.27 and Figure 4.28, are clear boundaries are able to be drawn between an inner sand channel, and an outer silt matrix. As such, it is hypothesized that injection of sand may have occurred within an already weakened silt channel; possibly the result of an injectite within an injectite (sand blow within a liquefaction structure). This similar to ideas proposed by Bastin *et al.* (2015) and Quigley *et al.* (2013), who suggest that pre-existing zones of weakness in the near surface (such as high permeability fracture zones) exert a first order control on sediment distribution, by providing more efficient paths for liquefied material to move through vertically.

As intrusion structures were found extensively throughout the Kay Road field site, I deduce that tectonic deformation must have occurred. Primarily, these structures were found within the older units of the Walton Sub-group, in particular the Puketoka and Karapiro Formations. No evidence of intrusion structures was found within, or in units younger than the Rangitawa Tephra unit, supporting the hypothesis that deformation processes occurred sometime older than 0.35 ka.

6.7.2 Soft sediment deformation

Another phenomenon observed within the field area was the shallowing of faults, as they displaced younger units within the field. This is best shown by Figure 4.9, which shows steeply dipping normal faulting within the Walton Sub-group that shallows out as it propagates through K2, K1, WT2, WT1 and the Kauroa Ash Formation. A significant change in measured dip of the fault plane, which shallowed from 68° to 24°, as noted by measurements 23 and 26 in Appendices J.

Soft sediment deformation structures can form during or shortly after deposition. Often, these structures are associated with pore water pressure changes, most likely induced by fluid escape during fluidization and liquefaction, however they can also be induced by hydrodynamic instabilities in sediments, caused by compaction, slumping or other fluctuations induced by waves, groundwater or movement. Widespread deformation in horizontal sedimentary layers is most commonly linked to pore pressure build up during earthquakes (Rossetti, 1999).

Evidence of this inferred soft sediment deformation is best shown by the irregular boundaries between The Walton Sub-group and Karapiro formation, particularly

in Figure 4.9. Typically, we expect to see sharp or gradational boundaries, however wavy boundaries are what is observed in the NW and NE of the field area. This is shown by *2 in Figure 4.9. which illustrates irregular unit boundaries within the Walton Sub-group and Karapiro formations in the south of the NW face.

The presence of soft sediment deformation could explain the chaotic distribution of units within the Kay Road field area, particularly in the geological models of the NE field area (Figure 4.36 through Figure 4.42). As shown in these images, some geologic boundaries shown in these images are not gradational nor sharp, instead smeared; a phenomenon associated with soft sediment deformation. These smeared boundaries within the Kay Road field area could be indicative of a slide plane, as opposed to tectonic deformation; a phenomenon which could have occurred during the formation of graben during normal faulting.

6.8 Deformation assessment of Kay Road field area

The Kay Road field area not only exhibits complex geology indicative of significant deformation, it also contains multiple structures which are almost exclusively induced through tectonic deformation. Thus, I deduce that the region has been subject to deformation. This is a hypothesis that has been confirmed by the offset beds, irregular geological distribution of units, tilting, uplift and rotation of units, alongside the presence of intrusion structures such injection structures (liquefaction and sand blow features), apparent fault planes and unconformities between geologic beds.

Deciphering faulting mechanisms responsible for creating the current geology of the Kay Road field area has not been easy. From observation of data presented in Chapter 4, it would appear that Kay Road has largely been subject to extensional forces, leading to normal faulting (Şengör, 1987; Leeder & Jackson, 1993). This is corroborated by trends observed in all four of the faces studied, where evidence of normal faulting is observed through relative down-throw of units, alongside the presence of graben-like formations found throughout the Kay Road field area.

The Kay Road field area appears to have been subject to normal faulting, a process associated with crustal extension. This has resulted in an extensive presence of steeply dipping normal faults, generally trending along a N/S plane. Associated

with this normal faulting is the relative down-throw of multiple units, with the field area showing that the southernmost portion of the Kay Road field area has been down-thrown. Processes of normal faulting within the field area have resulted in an extensive presence of deformation signatures within geological units; These include, but are not limited to graben features found within the field are (up to 15.3 m of vertical displacement), offset of geologic beds, rotated, displaced geologic units, and an extensive presence of intrusion structures (including liquefaction structures and sand dikes). Observation of these intrusion structures suggests that repeated deformation has occurred within the Kay Road field area, as shown by the clear boundaries between sand and silt units shown in Figure 4.26, Figure 4.27 and Figure 4.28 . These deformation signatures appear to be restricted to a period older than 0.35 ka, as this is the base age of the undisturbed Rangitawa Tephra unit found within the field area.

Recent faulting is a phenomenon defined by GNS as movement that has occurred within the previous 125 000 years. Although we do not know the exact timing of deformation within the Kay Road field site, we recognize that the Kay Road field area is not an active fault zone (GNS, 2017f).

6.9 Comparison to Literature

As limited information regarding faulting within the Hamilton Basin exists, comparisons between global fault zones and the Kay Road field site have had to be made. Most striking in the study of literature is the similarities that occur between the Kay Road field area and the Zanjan – Kavin fault zone in central Iraq (Toori & Seyitoğlu, 2014). The Zanjan – Kavin fault zone is a normal fault zone, and similarly exhibits disrupted repetitive bedding, like that observed within the Kauroa Ash Formation in the Kay Road field area in Figure 4.8 and Figure 4.9. An image of the Zanjan - Kavin fault is shown below in Figure 6.5.

Figure 6.5 - Normal faulting within Neogene sediments between Zanjan and Ardabil, Iran. Image taken from van der Boon (2013). As shown in this image, a steeply dipping normal fault is observed, with associated low angle faults pictured to the right of the image.

As shown in Figure 6.6, similarities between faulting observed in Figure 6.5 and the Kay Road field area exist. Primarily, this is through observation of units that have been subject to normal faulting, then tilted, down-thrown, and repeated throughout the face. This phenomenon is comparable to the distribution of the Kauroa Ash Formation in Figure 4.8 and Figure 4.9, alongside Figure 6.6 which focuses on this deformation.

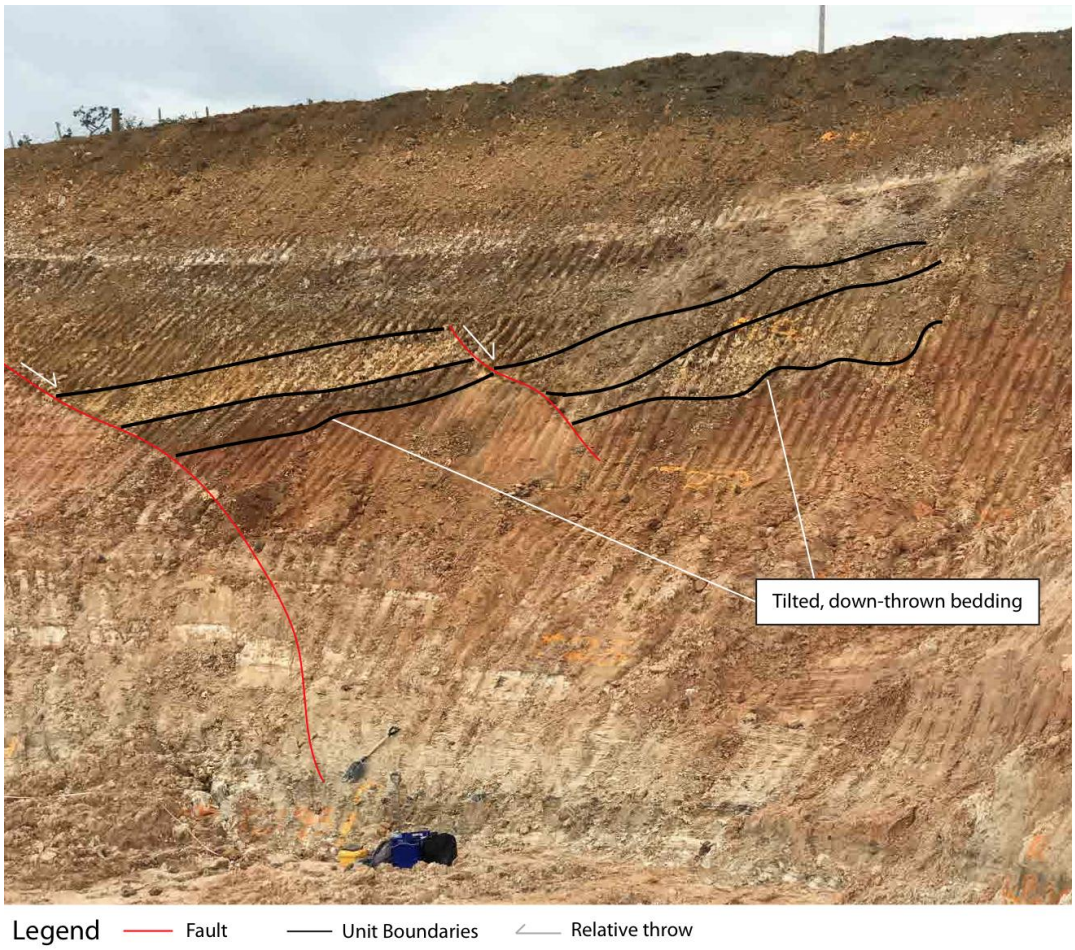

Figure 6.6 - Schematic of the NE face that illustrates tilting and down-throw of bedding, induced by normal faulting.

As normal faulting was extensive throughout the Kay Road field area, and is responsible for the deformation observed in the Zanjan – Kavin fault zone shown in Figure 6.5, we suggest that similar means of deformation are responsible for the displacement of the Kauroa Ash Formation observed at Kay Road. It would appear however that the Kauroa Ash Formation, alongside other units found within the Kay Road field area do appear more chaotic in nature, as shown by geology within the wider NW and NE face. Thus, I infer that more than one process may have influenced the current landscape at Kay Road.

Similar between the two field sites is the presence of a main steeply dipping normal fault, with surrounding, shallower faults cross cutting the main fault. This is shown in the Kay Road field area, with steep faulting offsetting the Kauroa Ash Formation above, and shallower faulting observed in the Walton Sub-group. Key differences between the two field sites are, however, the properties of materials

found within the fault zones. The Zanjan – Kavin fault zone is comprised of mainly older, Neogene sediments from volcanic origins (van der Boon, 2013). It is thought that these sediments are significantly more lithified than the Kay Road field area, compared to the younger, fluvial sediments observed within the Kay Road fault area. The differences in the coherency of faulted units also help explain why fault planes and offset in the Zanjan – Kavin fault zone is more apparent than that observed within the Kay Road fault area.

6.10 Osborne Road discussion

Tectonic deformation is a phenomenon which will often leave distinctive scars within a landscape. As summarised by Burbank and Anderson (2011), evidence of faulting within a landscape is broad, and can include vary significantly in type, size and distribution. Common phenomenon associated with deformation include linear valleys, linear ridgelines, scarps, offset or linear drainage, shutter ridges, beheaded streams, sag ponds and fault traces. Many of these phenomenon are summarised below in Figure 6.7, which illustrates common geomorphic signatures that can be found within a landscape, associated with tectonic deformation.

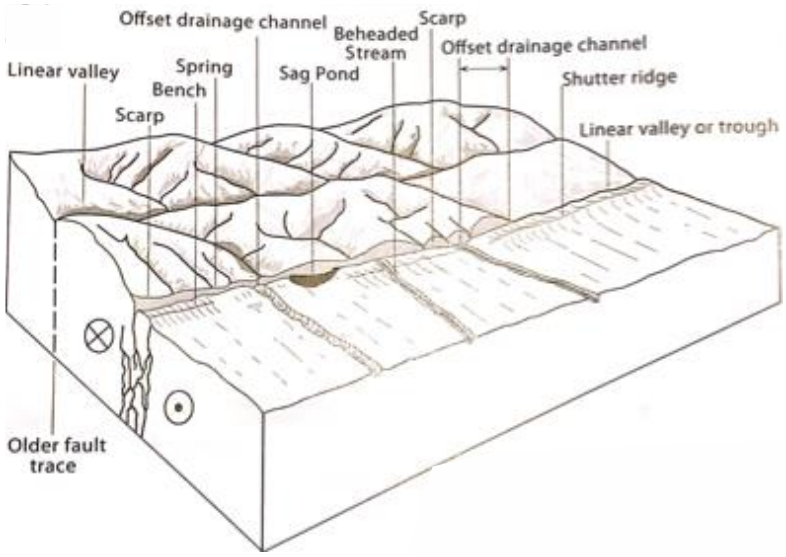

Figure 6.7 - Image illustrating geomorphic signatures of landscapes associated with tectonic deformation. Image taken from Burbank & Anderson (2011).

The initial hypothesis that faulting is present at the Osborne Road field site was first made by Moon and de Lange (2017), after study of LiDAR information showed a linear ridge running through the Hamilton Basin, which was associated with diversion of the Waikato River, and parallel drainage networks within the north of

Hamilton. This evidence is presented in Figure 2.11, alongside Figure 6.14. Consequently, this investigation was commissioned, and the Osborne Road site was identified as a key region of interest.

6.11 Geomorphic evidence

Immediately apparent within the Osborne Road field area following a site walkover was a break in slope within the eastern margin of the field. This scarp ran through the full extent of the field area, approximately parallel to Osborne Road. This break in slope is best shown by a 2 m rounded concave slope break which dominates the east of the image in Figure 5.3, Figure 5.4 and Figure 5.5, and is also shown in Figure 6.6. To the east of this break in slope, elevation of the Osborne Road field area averages 39 m ASL, with the west of the slope lying lower at an average elevation of 37 m ASL.

The formation of a scarp is a process often associated with uplift of the hanging wall during reverse faulting, resulting in collapse of uplifted material when a reverse fault penetrates the ground surface. This phenomenon is recognised as a fault roll over zone. Often resulting in a concave slope break; this is a phenomenon that is clearly observed in the Osborne Road field area. A schematic illustrating a fault roll over zone, and the consequence reverse faulting can have on geomorphology of an effected landscape is shown in Figure 6.8, which shows a collapsed fault roll over zone that has resulted in a rounded concave break in slope. This image has similar geomorphology to that outlined in the geomorphic maps of the Osborne Road field area (Figure 5.3, Figure 5.4 and Figure 5.5), and

an annotated image of the Osborne Road field area and distinct geomorphic slope break presented in Figure 6.9.

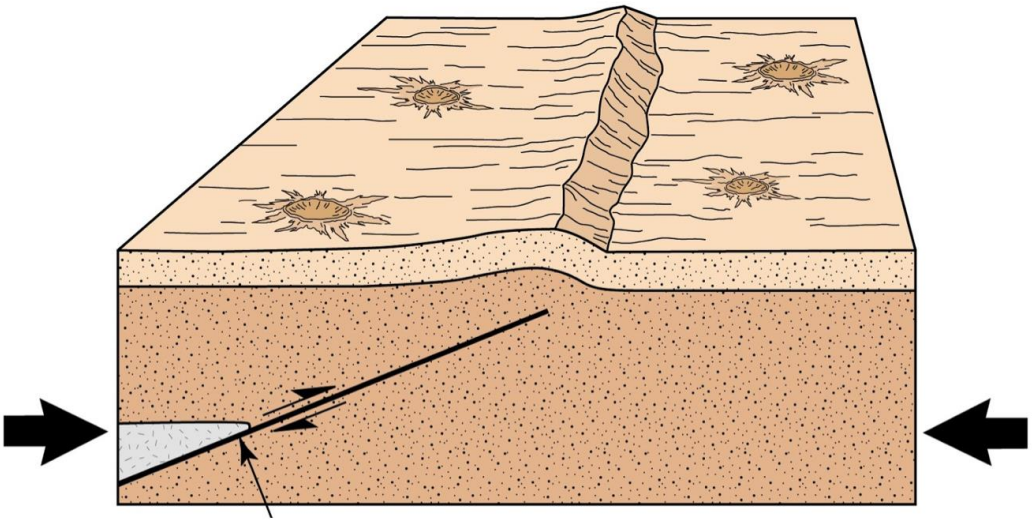

Figure 6.8 - Image illustrating a reverse fault and the consequent ridgeline that can form within a fault roll over zone. Image taken from Khattak (2017).

An annotated schematic of the Osborne Road field area (Figure 6.9) illustrates the change in elevation observed within the field area, alongside an average profile illustrating the observed rounded concave slope break.

Figure 6.9 - Annotated schematic of the Osborne Road field area. As shown in this image, the field area is dominated by a rounded concave slope break, with the eastern portion of the Osborne Road field area sitting higher than the western side of the field area.

Although this break in slope is somewhat masked by vegetation, the eastern portion of the field area was notably higher than the western margin in the field area.

6.11.1 Soil distribution

Secondary evidence supporting the idea of deformation through reverse faulting within the Osborne Road field area is shown by soil auger sampling. Irregular soil distribution was shown in the field area, with the east of the field area showing soil units that tended to coarsen downwards, with silt transitioning to sandy silt before turning into medium sand. Conversely, the western side of the field area was dominated by a much higher content of finer grained materials, including silt and silty sand. An image illustrating the distribution of units is shown below in Figure 6.10, which clearly illustrates concentrations of various materials within the Osborne Road field area.

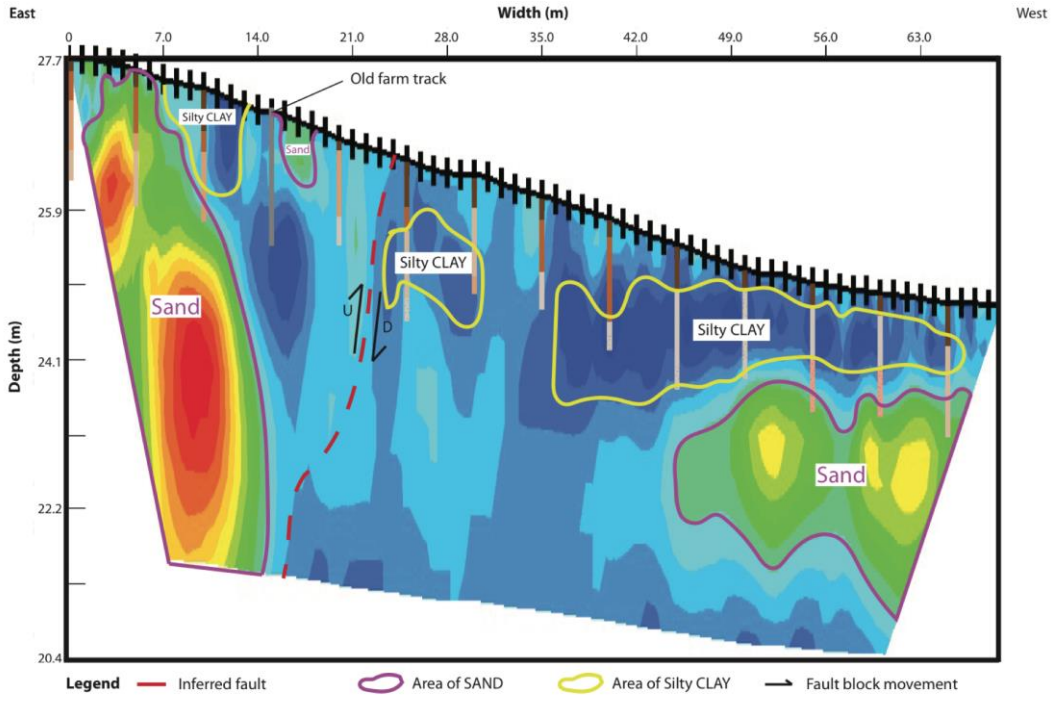

Figure 6.10 - Annotated image illustrating the distribution of units within the Osborne Road field area. As shown in the image, the east of the field area is dominated by sand, which is exposed at a near surface level. Conversely, sand in the west of the field area is deeper within the profile, with silty clay near surface level.

Shown in Figure 6.10 is the inferred fault plane with up-thrown and down-thrown blocks annotated onto the image. Soil auger samples are also shown in this image by vertical bars extending downwards from surface topography. A legend illustrating the units used in these soil auger samples is shown below in Figure 6.11.

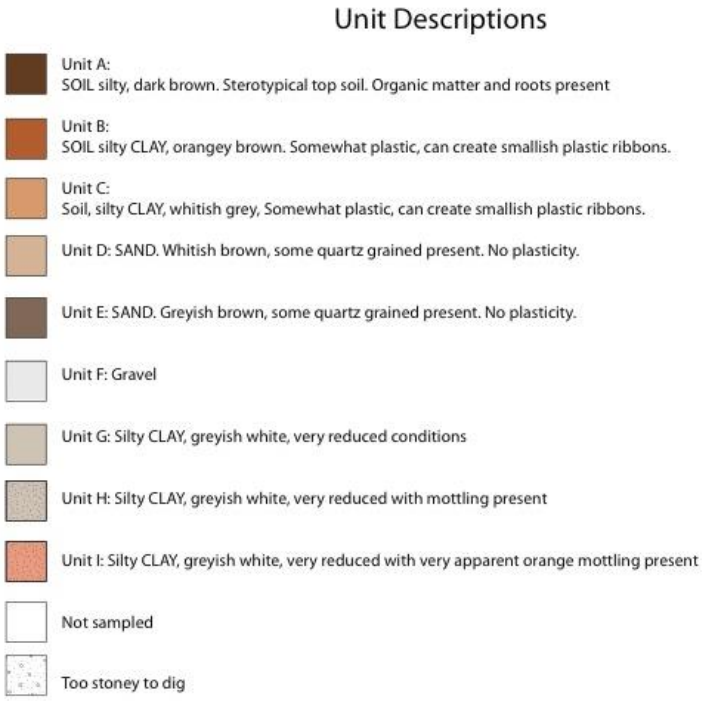

Figure 6.11 - Legend of soil units described in Figure 6.10 and Figure 6.12.

The varied soil characteristics observed in the field area are thought to be associated with reverse faulting, alongside the aforementioned fault roll zone. An image showing inferred movement of the Osborne Road field area is shown below in Figure 6.12. Shown in this image is the inferred process of deformation, with uplift occurring first, followed by mixing of units in the fault roll over zone. These are shown by 1 and 2, annotated onto the left of Figure 6.12

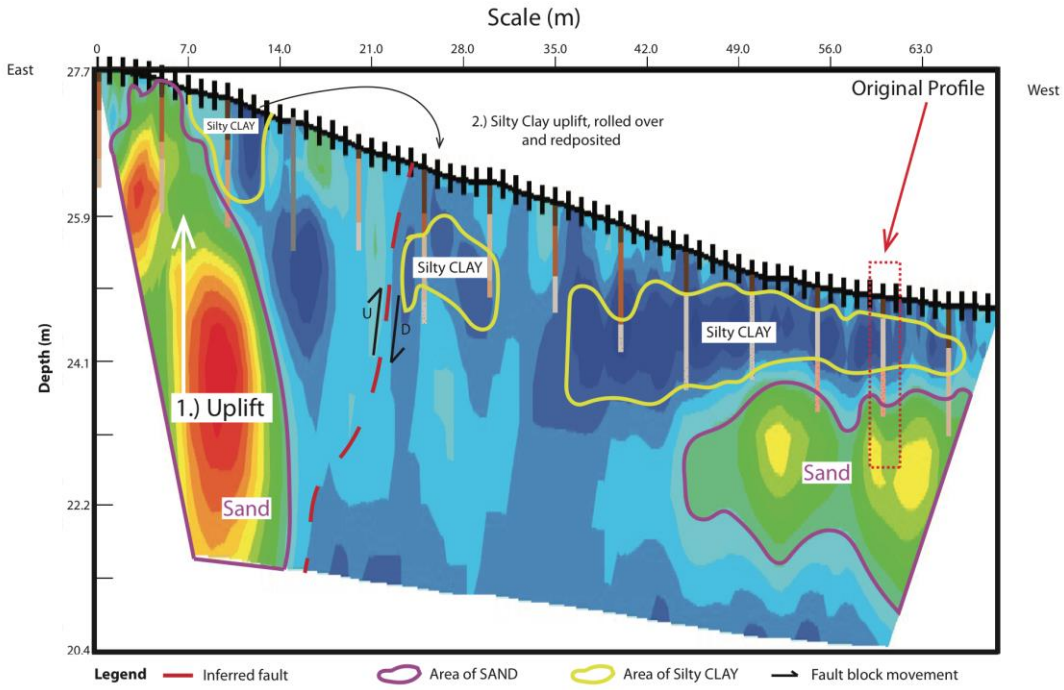

Figure 6.12 - Annotated image combining soil electrical resistivity and soil auger sampling data. Also shown are the inferred consequences of reverse faulting within the Osborne Road field area.

As shown in Figure 6.12, it is hypothesized that reverse faulting is partially responsible for the irregular distribution of soil found within the Osborne Road field area. It is hypothesized that originally the eastern margin of the field area had similar soil distribution to that currently found in the west of the field area (silty clay overlying sand). When subject to reverse faulting however, it is thought that these lower lying sandy units were uplift to near surface. Consequently, the overlying silty clay units are thought to have been toppled in the fault roll over zone, resulting in the irregular distribution of units to the west of the slope break running through the field area.

6.11.2 Reverse faulting

Reverse faulting is when the hanging-wall block moves up and over the footwall block. (Grasemann *et al.*, 2005; Gorse *et al.*, 2012; USGS, 2017c). A simple block diagram illustrating movement of a reverse fault is shown in Figure 6.13.

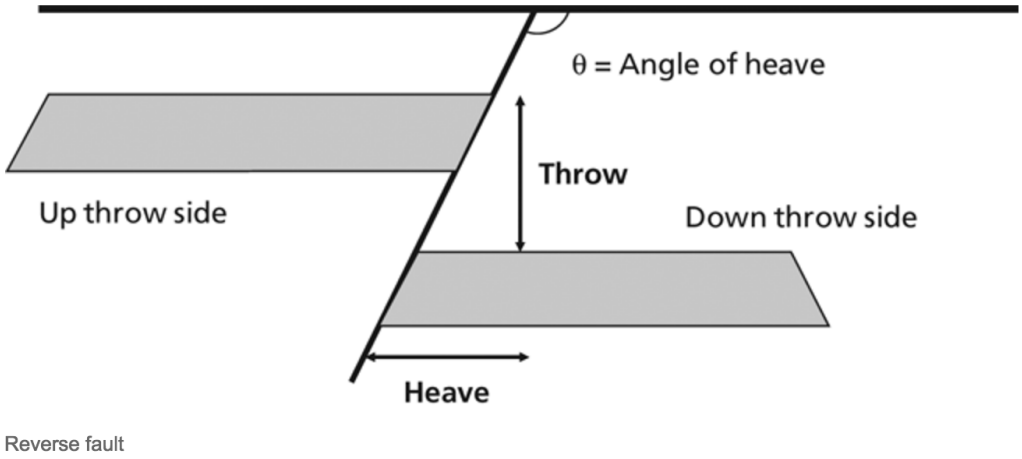

Figure 6.13 - Simple diagram showing the dynamics of a reverse fault. Image courtesy of Gorse, Johnston & Pritchard (2012).

Reverse faulting is a phenomenon associated with forces resulting in crustal compression (GNS, 2017a). Consequently, I infer that the Osborne Road field area has been subject to local crustal compression, resulting in the inferred normal fault presented in this investigation. This local compression is likely associated with larger extensional block movements on normal faults, as shown in Figure 2.8.

The Hinuera formation has a base age of 0.126 Ma, with most recent deposits estimated to be *c.* 16 ka (Selby & Lowe, 1992; Manville & Wilson, 2004; Lowe, 2010; GNS, 2017b). As the Osborne Road field area has displaced the Hinuera Formation, and the surface is thought to have been influenced by these deformation processes, it is hypothesized that recent movement has occurred within the Hamilton Basin. This Movement cannot definitively be confirmed however, due to the non-invasive techniques used in this investigation.

As such, further research to definitively establish faulting is encouraged at the Osborne Road field site.

6.12 Implications for the Hamilton Basin

The presence of deformation signatures within the Hamilton Basin has many consequences. Overall, this investigation, alongside those undertaken by McKay (2017); Moon and de Lange (2017), Spinardi (2017) and Kleyburg (2015), have generated a much needed update regarding the Hamilton Basin, and have presented significant evidence that does support theories that tectonic deformation has occurred within the Hamilton Basin.

Evidence supporting the idea that tectonic deformation is present is best summarised by Figure 6.14, which illustrates both the field sites studied in this investigation, alongside the major ridgelines that were used to assist in identification of these field sites. Figure 6.14 also illustrates recent evidence presented by Moon and de Lange (2017) and (Spinardi *et al.*, 2017 (In Press)), including areas of degradation and aggradation within the Waikato River, alongside highlight areas with linear drainage patterns present and regions of diversion within the Waikato River channel.

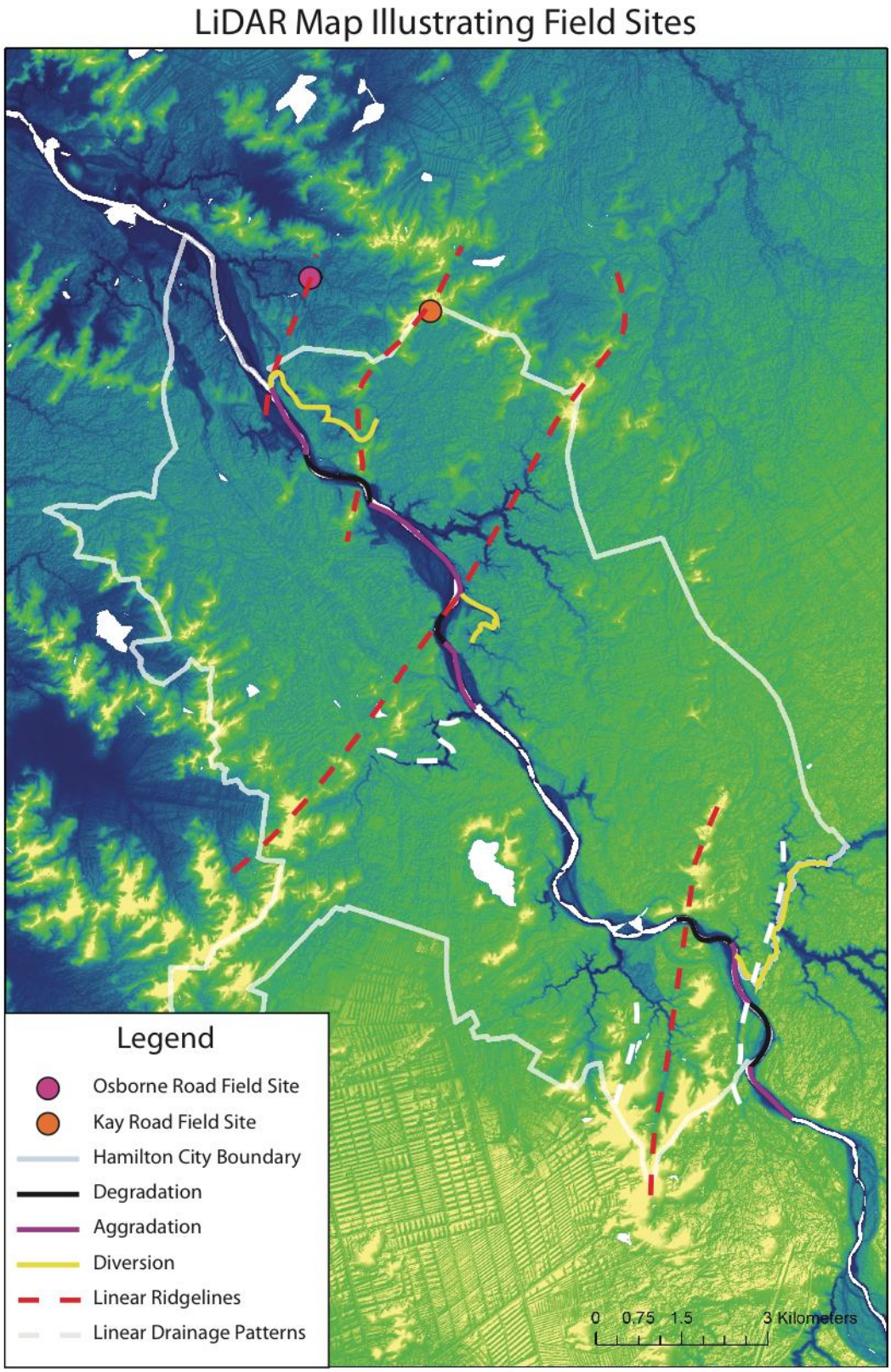

Figure 6.14 – LiDAR Map illustrating most recent phenomenon identified regarding tectonic deformation within the Hamilton Basin. Map adapted from Spinardi *et al.* (2017 (In Press)), and Moon and de Lange (2017).

Although no definitive evidence has been identified in this investigation that can declare the presence of recent faults within the Hamilton Basin, I suggest that

strong evidence is present that suggests deformation has occurred within recent Hinuera Formation sediments, which are dated at *c.* 16 ka by Lowe (2000). I also suggest that significantly more deformation has occurred within the Hamilton Basin, a phenomenon that previously has not been recognised by previous literature.

The presence of inferred movement within the Hinuera Formation in the Hamilton Basin suggests that the low NSHM rating made by Stirling *et al.* (2012), may in fact be incorrect. To fully corroborate these claims, however, definitive evidence needs to be identified and presented. Investigation at Osborne Road has been thus been a successful scoping study however, whereby sufficient evidence was obtained supporting a deformation hypothesis. Providing preliminary evidence, this investigation has now established where the most likely faulting is within the Osborne Road field area, and to a greater extent the Hamilton Basin. Ultimately, this would increase chances of the identifying faulting, should a subsequent paleoseismic investigation occur, and research into structural deformation within the Hamilton Basin continue.

6.13 Summary

Signatures of deformation, associated with tectonic processes are found extensively throughout the two field areas studied in this investigation.

At Kay Road, significant evidence is present indicating that the region has been subject to extensive normal faulting. Cumulatively, some -2.93 m of displacement (down-throw) was observed within the field west of field area, with significant displacement of units, and multiple intrusion structures identified. This deformation at the Kay Road region, however, is thought to be confined to a time period older than 350,000 ka; the age of the Rangitawa tephra. This is inferred as the Rangitawa Tephra unit is found undistributed, blanketing deformation throughout the entirety of the Kay Road field area. Consequently, we do not recognise the Kay Road field area as a region of recent deformation. Deformation within the Kay Road field area is more extensive than previously recognised, and has most likely been induced by normal faulting related to crustal extension.

Conversely, the Osborne Road field area is thought to be a region subject to reverse faulting, associated with compression forces. Unlike the Kay Road field area, the Osborne Road is thought to consist of a single displacement event, as opposed to chaotic faulting with multiple fault planes. Movement at the Osborne Road field area is thought to be more recent than Kay Road, with evidence suggesting that the recent, near surface Hinuera Formation has been displaced. As the Hinuera Formation was deposited between c. 16 ka and 0.126 Ma, it is hypothesized that movement within the Osborne Road field area is recent.

The presence of recent movement within the Hamilton Basin would not only contradict Hamilton City's low national seismic hazard rating, but it would also contradict previous, widely accepted literature regarding the Hamilton Basin. Although preliminary, this investigation is thought to be the first of many which attempt to fill the knowledge gap that exists regarding deformation within the Hamilton Basin.

As no common type of deformation is found between the two studied field sites, I suggest that the Hamilton Basin has been subject to a number of different complex, deformation processes. These include both normal and reverse faulting, alongside associated deformation processes including liquefaction.

Chapter 7

Conclusion

7.1 Chapter outline

This chapter summarises findings regarding investigation of tectonic deformation within the Hamilton Basin. Conclusions are first drawn regarding the Kay Road field site, followed by the Osborne Road field site. Key findings are presented and summarised, and conclusions assessing the discovery and validity of new information regarding the Hamilton Basin are drawn. Recommendations regarding this investigation are also made.

7.2 Kay Road fault zone

Some 7.41 m of total down-throw was observed within the western margin of the Kay Road field area. This total throw was observed and measured during investigation of extensive deformation within geological units at the Kay Road field area. This deformation of geology was not only obvious, but it was extensive; suggesting that the Kay Road field area was a fault zone, as opposed to a single fault plane. Deformation within the field area was significant and included the uplift, tilting, rotation, and displacement of geologic units within the field. This displacement varied significantly in size, with few mm of offset found within the Walton Sub-group, through to > 8 m offset observed within the Kauroa Ash Formation. Within the Kay Road field area, evidence of soft sediment deformation and liquefaction were also found, shown by the presence of various intrusion structures, including a suspected sand dike, injection structures, and liquefaction structures. These liquefaction structures ranged between 55 mm and > 14 m length. Evidence indicative of repeated deformation within these structures was observed, suggesting that deformation history of the Kay Road field area is complex.

Establishing the sequence of deformation within the Kay Road Field Area is difficult, due to the extensive presence of chaotic deformation. Observation of structural features within the field area infer that the Kay Road field area is a

region that has been subject to extensional forces, thus producing a series of steeply dipping normal faults, and down-throwing the southern portion of the Kay Road field area. Consequently, graben like structures are observed.

Although processes of deformation at the Kay Road field site are not entirely understood, we do recognise that deformation within the Kay Road field area is confined to a time period older than deposition of the Rangitawa Tephra (0.35 Ma), as the Rangitawa Tephra is found undisturbed, blanketing deformation features within the field area. Consequently, the Kay Road fault zone is not classified as a region of active faulting, and will not influence the assessment of seismic hazard for the Hamilton Basin. Significant evidence of faulting was present within the field area however, supporting hypothesis that tectonic deformation is present within the Hamilton Basin.

7.3 Osborne Road field area

Evidence suggesting that faulting has occurred within the Osborne Road field area is extensive, and was first noted by Moon and de Lange (2017). First discovered by study of LiDAR data, a linear ridgeline was recognised that was associated with diversion of the Waikato River. This ridgeline was also associated with a large concave slope break recognised in the field area, indicative of reverse faulting and associated fault roll over processes. This ridgeline contained approximately 2 m of vertical displacement, running through the easternmost portion of the field area, parallel to Osborne Road. Study of soil distribution within the Osborne Road field was then undertaken, focusing on soil distribution near the inferred fault. Studied through soil auger sampling along a transect running across the ridgeline, and then by both 2D and 3D soil electrical resistivity surveys, results showed a distinctive transformation in the distribution of soil within the Osborne Road field area. To the east of this ridgeline, coarser sandy material was found, converse to the west of the ridgeline, where finer grained silty clay material was present. A zone of soil with mixed properties was found also found; a phenomenon associated with a fault roll over zone, confirming initial hypothesis that reverse faulting is present within the Osborne Road field area.

As youngest deposits within the Hinuera Formation are dated a c. 16ka, we suggest that Osborne Road faulting may be classified as a recent movement. However, due to the non-invasive nature of this investigation, we can only infer that this faulting is present. Consequently, further investigations at the Osborne Road field site are encouraged.

7.4 Current Understanding of the Hamilton Basin

This investigation suggests that tectonic deformation is far more extensive within the Hamilton Basin than previously recognised. Significant evidence of deformation was found at the Kay Road field site, however, this deformation is not classed as active, as no sign of movement within the previous 100 000 ka was found. As such, the Kay Road field site does not discredit Hamilton City's low NSHM rating.

Evidence suggestive of deformation within the previous 100 000 ka was found within the Osborne Road field area. Due to the non-invasive nature of investigation methods used, however, this cannot be confirmed. Consequently, it is strongly recommended that further research, through means of paleoseismic trenching be undertaken at the Kay Road field site. Further investigation could better establish the presence of faulting within the field area, and establish whether or not recent movement has occurred and possibly establish return periods for movement. Consequently, this could inform a re-assessment of Hamilton City's seismic risk.

7.5 Recommendations and limitations

This section details recommendations and limitations of investigations undertaken at the Osborne and Kay Road field site. Recommendations are also made regarding further research into the Hamilton Basin.

7.5.1 Osborne Road

During soil sampling at Osborne Road, climatic conditions were somewhat undesirable. This meant saturation of the ground within the field site, meaning that soil auger holes could not reach the desired depth before saturation and collapse of soil auger holes occurred. Consequently, soil descriptions were somewhat limited, only scratching the surface of the Osborne Road field area.

To best combat these limitations, it is my recommendation that a trench be opened at the Osborne Road field site; not only would this enable investigations to occur at greater depth, it could also be scheduled to occur at a time of year where climatic conditions may be better suited. Alongside this, the opening of a trench and associated paleoseismic investigation would enable a perspective into deformation that could not be achieved through soil auger sampling and soil electrical resistivity surveys alone. Trenching of the Osborne Road field area could also corroborate hypothesis that recent movement has occurred within the Hamilton Basin, building on work undertaken by Kleyburg (2015); McKay (2017); Moon and de Lange (2017); Spinardi (2017).

7.5.2 Kay Road

Investigation of the Kay Road field area had limitations. The demanding timeframe and nature of work on the Waikato Expressway proved difficult in this investigation, ultimately being the largest limiting factor. Consequently, the nature of the investigation was somewhat rushed, and it is possible that detail may have been lost as a result. It is my recommendation that physical detailing of a face be conducted in an environment that is not rushed for time, giving one enough time to not only double and triple check measurements, descriptions and sketches, but take more. This is particularly true as significant detail will be lost once the Waikato Expressway is completed, and the Kay Road field site becomes a major transport route.

Similarly, I would recommend that more structural information be obtained during the detailing period, particularly regarding bedding orientation and distribution. Lack of measurements goes hand in hand with time constraints; however, the rushed nature of this investigation meant no time could be wasted, and the investigation process had to be as efficient and streamlined as possible. Consequently, fewer measurements were taken than one would like, which has led to some dissatisfaction regarding geologic modelling to represent the Kay Road field area. More structural information would have improved geologic modelling, helping to better establish the movements involved in the Kay Road field site.

7.5.3 Overall recommendations

The Hamilton Basin has long been associated with a low seismic hazard risk, with little evidence recognised to support the idea that deformation is present within the Hamilton Basin. Recent investigations however show that faulting within the Hamilton Basin is far more extensive than previously thought, with multiple signatures associated with tectonic deformation found within the Basin (Kleyburg, 2015; McKay, 2017; Moon & de Lange, 2017; Spinardi, 2017).

Consequently, investigation of deformation within the Hamilton Basin has ramped up. These investigations have proven useful, however, significant knowledge gaps still exist regarding deformation within the basin. Whilst we now understand that deformation is present within the basin, the timing, extent and characteristics of this deformation are still not fully understood.

It is recommended that further extensive study investigate the extent of deformation within the Hamilton Bain. This could include physical trenching of the Osborne Road field site, alongside further detailing and study of the two ridgelines studied in this investigation. It is recommended that this study occur in a different region of the Hamilton Basin, however, as this investigation was largely confined to the northern portion of Hamilton City. The study of ridgelines in alternative locations could help characterize faulting within the wider Hamilton Basin, and improve the overall understanding of deformation within the Hamilton Basin.

References

Allaby, M. (2013). *A dictionary of geology and earth sciences*. Oxford University Press.

Allen, J. R. L. (1982). *Sedimentary structures, their character and physical basis*. (Vol. 1). Elsevier.

Barnett, J. A., Mortimer, J., Rippon, J. H., Walsh, J. J., & Watterson, J. (1987). Displacement geometry in the volume containing a single normal fault. *AAPG Bulletin, 71*(8), 925-937.

Bastin, S. H., Quigley, M. C., & Bassett, K. (2015). Paleoliquefaction in Christchurch, New Zealand. *Geological Society of America Bulletin, 127*(9-10), 1348-1365.

Berra, F., & Felletti, F. (2011). Syndepositional tectonics recorded by soft-sediment deformation and liquefaction structures (continental Lower Permian sediments, Southern Alps, Northern Italy): Stratigraphic significance. *Sedimentary Geology, 235*(3), 249-263.

Burbank, D. W., & Anderson, R. S. (2011). *Tectonic geomorphology*. John Wiley & Sons.

de Lange, P. J., & Lowe, D. J. (1990). History of vertical displacement of Kerepehi Fault at Kopouatai bog, Hauraki Lowlands, New Zealand, since c. 10 700 years ago.

Edbrooke, S. W. (2005). *Geology of the Waikato Area*. Lower Hutt, N.Z: Institute of Geological & Nuclear Sciences.

Encyclopaedia Britannica. (2017). *Strike-slip fault*. Retrieved September 6, 2017, from https://www.britannica.com/science/strike-slip-fault.

Encyclopædia Britannica. (1998). *Horst and Graben*. Retrieved September 10, 2017, from https://www.britannica.com/science/horst.

Ferrari, D. M., & Guiseppi, A. R. (2009). *Geomorphology and Plate Tectonics*. Nova Science Publishers.

GNS. (2017a). *Different types of Faults*. Retrieved September 11, 2017, from https://www.gns.cri.nz/Home/Learning/Science-Topics/Earthquakes/Earthquakes-and-Faults/Different-types-of-Faults.

GNS. (2017b). *New Zealand Stratigraphic Lexicon - Hinuera Formation*. Retrieved 23 August, 2017, from http://data.gns.cri.nz/stratlex/view.jsp?id=1063.

GNS. (2017c). *New Zealand Stratigraphic Lexicon - Karapiro Formation*. Retrieved 25 August, 2017, from http://data.gns.cri.nz/stratlex/view.jsp?id=1297.

GNS. (2017d). *New Zealand Stratigraphic Lexicon - Puketoka Formation*. Retrieved 21 August, 2017, from http://data.gns.cri.nz/stratlex/view.jsp?id=2612.

GNS. (2017e). *New Zealand Stratigraphic Lexicon - Walton Subgroup*. Retrieved 21 August, 2017, from http://data.gns.cri.nz/stratlex/view.jsp?id=3692.

GNS. (2017f). When is a Fault "Active".

Gorse, C., Johnston, D., & Pritchard, M. (Compiler) (2012). *reverse fault*: Oxford University Press.

Grasemann, B., Martel, S., & Passchier, C. (2005). Reverse and normal drag along a fault. *Journal of Structural Geology, 27*(6), 999-1010.

Hazreek, Z., Rosli, S., Chitral, W., Fauziah, A., Azhar, A., Aziman, M., & Ismail, B. (2015) Soil identification using field electrical resistivity method. In *Journal of Physics: Conference Series* (Vol. 622, pp. 012030): IOP Publishing.

Houghton, B., & Cuthbertson, A. (1989). Sheet T14 BD—Kaimai. *Geological map of New Zealand, 1*(50), 000.

Huggett, R. (2007). *Fundamentals of geomorphology*. Routledge.

Hume, T. M. (1972). *The Petrology of the Hinuera Formation.* thesis, The University of Waikato.

Hume, T. M., Sherwood, A. M., & Nelson, C. S. (1975). Alluvial sedimentology of the upper pleistocene hinuera formation, hamilton basin, New Zealand. *Journal of the Royal Society of New Zealand, 5*(4), 421-462.

Kamp, P. J. J., & Lowe, D. J. (1981) Quaternary stratigraphy, landscape, and soils of the Hamilton Basin. In R. M. Briggs (Ed.), *Geological Society of New Zealand 1981 Conference, Hamilton* (pp. 14 - 28).

Kear, D. (1961). Stratigraphy of Pokeno District, Auckland. *New Zealand Journal of Geology and Geophysics, 4*(2), 148-164.

Kear, D. (1967). Economic geology of the Waikato.

Kear, D., Schofield, J. C., & Couper, R. (1978). *Geology of the Ngaruawahia subdivision*. New Zealand, Dept. of Scientific and Industrial Research.

Kearey, P., Brooks, M., & Hill, I. (2013). *An introduction to geophysical exploration*. John Wiley & Sons.

Khattak, O. (2017). *The Birth and growth of a fault*. Retrieved September 5, 2017, from http://geologylearn.blogspot.co.nz/2015/07/the-birth-and-growth-of-fault.html.

Kleyburg, M. A. (2015). *Paleoliquefaction in Late Pleistocene alluvial sediments in the Hauraki and Hamilton basins.* Masters thesis, University of Waikato, Hamilton, New Zealand.

Kohn, B. P., Pillans, B., & McGlone, M. S. (1992). Zircon fission track age for middle Pleistocene Rangitawa Tephra, New Zealand: stratigraphic and paleoclimatic significance. *Palaeogeography, Palaeoclimatology, Palaeoecology, 95*(1), 73-94.

Leeder, M., & Jackson, J. (1993). The interaction between normal faulting and drainage in active extensional basins, with examples from the western United States and central Greece. *Basin research, 5*(2), 79-102.

Lensen, G. J. (1958). A Method of Graben and Horst Formation. *The Journal of Geology, 66*(5), 579-587.

Lowe, D. J. (2000). Upbuilding pedogenesis in multisequal tephra-derived soils in the Waikato region.

Lowe, D. J. (2010). Introduction to the landscapes and soils of the Hamilton Basin.

Lowe, D. J., Tippett, J. M., Kamp, P. J., Liddell, I. J., Briggs, R. M., & Horrocks, J. L. (2001). Ages on weathered Plio-Pleistocene tephra sequences, western north Island, New Zealand.

Madabhushi, G. S. P., & Haigh, S. K. (2012). How Well Do We Understand Earthquake Induced Liquefaction? *Indian Geotechnical Journal, 42*(3), 150-160.

Manville, V., & Wilson, C. J. (2004). The 26.5 ka Oruanui eruption, New Zealand: A review of the roles of volcanism and climate in the post-eruptive sedimentary response. *New Zealand Journal of Geology and Geophysics, 47*(3), 525-547.

Marshak, S. (2011). *Earth: Portrait of a Planet: Fourth International Student Edition*. WW Norton & Company.

Matthews, N. E., Smith, V. C., Costa, A., Durant, A. J., Pyle, D. M., & Pearce, N. J. (2012). Ultra-distal tephra deposits from super-eruptions: examples from Toba, Indonesia and Taupo Volcanic Zone, New Zealand. *Quaternary International, 258*, 54-79.

McCraw, J. (2011). *The wandering river: landforms and geological history of the Hamilton Basin*. (Vol. no. 16.;no. 16;). Lower, Hutt, N.Z.: Geoscience Society of New Zealand.

McCraw, J. D. (1967). The surface features and soil pattern of the Hamilton basin.

McGlone, M. S., Nelson, C. S., & Hume, T. M. (1978). Palynology, age and environmental significance of some peat beds in the Upper Pleistocene

Hinuera Formation, South Auckland, New Zealand. *Journal of the Royal Society of New Zealand, 8*(4), 385-393.

McKay, A. (2017). *Evaluationg soil and landscape models to predict liquefaction susceptibility in the Hinuera Formation, Hamitlon Basin (In Progress).* MSc thesis, The University of Waikato, Hamilton, New Zealand.

Moon, V. G., & de Lange, W. P. (2017). *Final Report on EQC Potential shallow seismic sources in the Hamilton Basin.* Retrieved September 6, from.

Murashev, A., Keepa, C., & Hayes, G. (2012). *Earthquake geotechnical engineering issues assocaited with design of Waikato Expressway.* Opus International Consultants Ltd, Wellington, New Zealand. https://www.nzsee.org.nz/db/2012/Paper031.pdf.

Nelson, C. S., Mildenhall, D. C., Todd, A. J., & Pocknall, D. T. (1988). Subsurface stratigraphy, paleoenvironments, palynology, and depositional history of the late Neogene Tauranga Group at Ohinewai, Lower Waikato Lowland, South Auckland, New Zealand. *New Zealand Journal of Geology and Geophysics, 31*(1), 21-40.

NZGS. (2017). *Field description of soil and rock - field sheet*. Retrieved January 11, 2017, from http://www.nzgs.org/library/field-description-of-soil-and-rock-field-sheet/.

Obermeier, S. F. (1989). *The New Madrid earthquakes; An engineering-geologic interpretation of relict liquefaction features.*

Obermeier, S. F., Jacobson, R. B., Smoot, J. P., Weems, R. E., Gohn, G. S., Powars, D. S., & Monroe, J. E. (1990). Earthquake-induced liquefaction features in the coastal setting of South Carolina and in the fluvial setting of the New Madrid Seismic Zone. *United States Geological Survey, Professional Paper; (USA)*, Medium: X; Size: Pages: 1-44.

Orense, R., Pender, M., & O'Sullivan, A. (2012). *Liquefaction characteristics of pumice sands*. Earthquake Commission.

Owen, G., & Moretti, M. (2011). Identifying triggers for liquefaction-induced soft-sediment deformation in sands. *Sedimentary Geology, 235*(3), 141-147.

Persaud, M., Villamor, P., Berryman, K., Ries, W., Cousins, J., Litchfield, N., & Alloway, B. (2016). The Kerepehi Fault, Hauraki Rift, North Island, New Zealand: active fault characterisation and hazard. *New Zealand Journal of Geology and Geophysics, 59*(1), 117-135.

Pillans, B., Alloway, B., Naish, T., Westgate, J., Abbott, S., & Palmer, A. (2005). Silicic tephras in Pleistocene shallow-marine sediments of Wanganui Basin, New Zealand. *Journal of the Royal Society of New Zealand, 35*(1-2), 43-90.

Quigley, M. C., Bastin, S., & Bradley, B. A. (2013). Recurrent liquefaction in Christchurch, New Zealand, during the Canterbury earthquake sequence. *Geology, 41*(4), 419-422.

Reddy, D. V., Nagabhushanam, P., Kumar, D., Sukhija, B. S., Thomas, P. J., Pandey, A. K., Sahoo, R. N., Ravi Prasad, G. V., & Datta, K. (2009). The great 1950 Assam Earthquake revisited: Field evidences of liquefaction and search for paleoseismic events. *Tectonophysics, 474*(3), 463-472.

Rossetti, D. D. F. (1999). Soft-sediment deformation structures in late Albian to Cenomanian deposits, São Luís Basin, northern Brazil: evidence for palaeoseismicity. *Sedimentology, 46*(6), 1065-1081.

Samouëlian, A., Cousin, I., Tabbagh, A., Bruand, A., & Richard, G. (2005). Electrical resistivity survey in soil science: a review. *Soil and Tillage Research, 83*(2), 173-193.

Seed, H. B., & Idriss, I. M. (1982). *Ground motions and soil liquefaction during earthquakes*. (Vol. 5). Earthquake Engineering Research Institute.

Selby, M. J., & Lowe, D. J. (1992). The middle Waikato Basin and hills. In. Landforms of New Zealand: Second Edition: The University of Waikato.

Şengör, A. (1987). Cross-faults and differential stretching of hanging walls in regions of low-angle normal faulting: examples from western Turkey. *Geological Society, London, Special Publications, 28*(1), 575-589.

Sims, J. D. (1975). Determining earthquake recurrence intervals from deformational structures in young lacustrine sediments. *Tectonophysics, 29*(1-4), 141-152.

Sims, J. D., & Garvin, C. D. (1995). Recurrent liquefaction induced by the 1989 Loma Prieta earthquake and 1990 and 1991 aftershocks: implications for paleoseismicity studies. *Bulletin of the Seismological Society of America, 85*(1), 51-65.

Skempton, A. (1966) Some observations on tectonic shear zones. In *1st ISRM Congress*: International Society for Rock Mechanics.

Spinardi, F. (2017). *Preliminary evaluation of tectonic geomorphological signals in the Hamilton Basin (In Progress).* MSc thesis, The University of Waikato, Hamilton, New Zealand.

Spinardi, F., Campbell, B., Moon, D. V., Pittari, A., Fox, B. R. S., & de Lange, W. P. (2017 (In Press)). Unravelling Fault Structures of the Hamilton Basin. *Proc. 20th NZGS Geotechnical Symposium*.

Stirling, M., McVerry, G., Gerstenberger, M., Litchfield, N., Van Dissen, R., Berryman, K., Barnes, P., Wallace, L., Villamor, P., & Langridge, R. (2012).

National seismic hazard model for New Zealand: 2010 update. *Bulletin of the Seismological Society of America, 102*(4), 1514-1542.

Stirling, M. W., Mc Verry, G. H., & Berryman, K. R. (2002). A new seismic hazard model for New Zealand. *Bulletin of the Seismological Society of America, 92*(5), 1878-1903.

Suppe, J. (1983). Geometry and kinematics of fault-bend folding. *American Journal of science, 283*(7), 684-721.

Thatcher, W., & Hill, D. P. (1991). Fault orientations in extensional and conjugate strike-slip environments and their implications. *Geology, 19*(11), 1116-1120.

Toori, M., & Seyitoğlu, G. (2014). Neotectonics of the Zanjan-Kazvin area, Central Iran: Left lateral strike-slip induced restraining stepovers. *Turkish Journal of Earth Sciences, 23*(3), 260-276.

USGS. (2017a). *Earthquake Glosary*. Retrieved September 6, 2017, from https://earthquake.usgs.gov/learn/glossary/?term=strike-slip.

USGS. (2017b). *Earthquake Glossary - Sand Boils*. Earthquake Glossay. Retrieved September 10, 2017, from https://earthquake.usgs.gov/learn/glossary/?term=sand%20boil.

USGS. (2017c). *Visual Glossary - Faults and Earthquakes*. Retrieved September 6, 2017, from https://geomaps.wr.usgs.gov/parks/deform/gfaults.html.

van der Boon, A. (2013). *Alborz/Talesh Mountains of Iran*. 2017, from http://www.travelinggeologist.com/2013/12/alborztalesh-mountains-of-iran-annique-van-der-boon/.

Ward, W. (1967). Volcanic ash beds of the lower Waikato basin, North Island, New Zealand. *New Zealand journal of geology and geophysics, 10*(4), 1109-1135.

Yeats, R. S., Sieh, K. E., Allen, C. R., & Geist, E. (1997). *The geology of earthquakes*. (Vol. 568). Oxford university press New York.